
ANALYSIS OF THE RIEMANN ZETA FUNCTION

A PREPRINT

Kirill V. Kapitonets
 BAUMAN MSTU, GRADUATE 1990
 MCC EuroChem
 Moscow
 Russian Federation
 kkapitonets@live.com

January 14, 2022

ABSTRACT

The paper uses a feature of calculating the Riemann Zeta function in the critical strip, where its approximate value is determined by partial sums of the Dirichlet series, which it is given.

These expressions are called the first and second approximate equation of the Riemann Zeta function. The representation of the terms of the Dirichlet series by vectors allows us when analyzing the polyline formed by these vectors:

- 1) explain the geometric meaning of the generalized summation of the Dirichlet series in the critical strip;
- 2) obtain formula for calculating the Riemann Zeta function;
- 3) obtain the functional equation of the Riemann Zeta function based on the geometric properties of vectors forming the polyline;
- 4) explain the geometric meaning of the second approximate equation of the Riemann Zeta function;
- 5) obtain the vector equation of non-trivial zeros of the Riemann Zeta function;
- 6) determine why the Riemann Zeta function has non-trivial zeros on the critical line;
- 7) understand why the Riemann Zeta function cannot have non-trivial zeros in the critical strip other than the critical line.

The main result of the paper is a definition of possible ways of the confirmation of the Riemann hypothesis based on the properties of the vector system of the second approximate equation of the Riemann Zeta function.

Keywords the Riemann Zeta function, non-trivial zeros of the Riemann Zeta function, second approximate functional equation of the Riemann Zeta function

1 Introduction

A more detailed title of the paper can be formulated as follows:

Geometric analysis of expressions that determine a value of the Riemann zeta function in the critical strip.

However, this name will not fully reflect the content of the paper. It is necessary to refer to the sequence of problems. The starting point of the analysis of the Riemann zeta function was the question:

Why the Riemann zeta function has non-trivial zeros.

A superficial study of the question led to the idea of geometric analysis of the Dirichlet series.

Preliminary geometric analysis allowed to obtain the following results:

- 1) definition of an expression for calculating a value of the Riemann zeta function in the critical strip;

- 2) derivation of the functional equation of the Riemann zeta function based on the geometric properties of vectors;
- 3) explanation of the geometric meaning of the second approximate equation of the Riemann zeta function.

The most important result of the preliminary geometric analysis was the question why the Riemann zeta function cannot have non-trivial zeros in the critical strip except the critical line.

Therefore, the extended title of the paper is follows:

Geometric analysis of the expressions defining a value of the Riemann zeta function in the critical strip with the aim of answering the question of why the Riemann zeta function cannot have non-trivial zeros in the critical strip, except for the critical line.

At once, it is necessary to define the upper limit of the paper. Although that the paper explores the main question of the Riemann hypothesis, we are not talking about its proof.

The results of the geometric analysis of the expressions defining a value of the Riemann zeta function in the critical strip is the definition of the possible ways of the confirmation of the Riemann hypothesis based on the results of this analysis.

In addition, if we are talking about the boundaries, then we will mark the lower limit of the paper. We will not use the latest advances in the theory of the Riemann zeta function and improve anyone's result (we will state our position on this later).

We turn to the origins of the theory of the Riemann zeta function and base on the very first results obtained by Riemann, Hardy, Littlewood and Titchmarsh, as well as by Adamar and Valle Poussin.

In addition, of course, we cannot do without the official definition of the Riemann hypothesis:

The Riemann zeta function is the function of the complex variable s , defined in the half-plane $\text{Re}(s) > 1$ by the absolutely convergent series:

$$\zeta(s) = \sum_{n=1}^{\infty} \frac{1}{n^s}; \quad (1)$$

and in the whole complex plane C by analytic continuation. As shown by Riemann, $\zeta(s)$ extends to C as a meromorphic function with only a simple pole at $s=1$, with residue 1, and satisfies the functional equation:

$$\pi^{-s/2} \Gamma\left(\frac{s}{2}\right) \zeta(s) = \pi^{-(1-s)/2} \Gamma\left(\frac{1-s}{2}\right) \zeta(1-s); \quad (2)$$

Thus, in terms of the function $\zeta(s)$, we can state Riemann hypothesis: The non-trivial zeros of $\zeta(s)$ have real part equal to $1/2$.

We define two important concepts of the Riemann zeta function theory: the critical strip and the critical line.

Both concepts relate to the region where non-trivial zeros of the Riemann zeta function are located.

Adamar and Valle-Poussin independently in the course of the proof of the theorem about the distribution of prime numbers, which is based on the behavior of non-trivial zeros of the Riemann zeta function, showed that all non-trivial zeros Riemann zeta function is located in a narrow strip $0 < \text{Re}(s) < 1$. In the theory of the Riemann zeta function, this strip is called *critical strip*.

The line $\text{Re}(s) = 1/2$ referred to in the Riemann hypothesis is called *critical line*.

It is known that the Dirichlet series (1), which defines the Riemann zeta function, diverges in the critical strip, therefore, to perform an analytical continuation of the Riemann zeta function, *the method of generalized summation* of divergent series, in particular the generalized Euler-Maclaurin summation formula is used.

We should note that the generalized Euler-Maclaurin summation formula is used in the case where the partial sums of a divergent series are suitable for computing the generalized sum of this divergent series.

From the theory of generalized summation of divergent series [6], it is known that any method of generalized summation, if it yields any result, yields the same result with other methods of generalized summation.

On the one hand, this fact confirms the uniqueness of the analytical continuation of the function of a complex variable, and on the other hand, apparently, the principle of analytical continuation extends in the form of a generalized summation to the functions of a real variable, which are defined in divergent series.

Now we can formulate the principles of geometric analysis of expressions that define a value of the Riemann zeta function in the critical strip:

- 1) a complex number can be represented geometrically using points or vectors on the plane;

- 2) the terms of the Dirichlet series, which defines the Riemann zeta function, are complex numbers;
- 3) a value of the Riemann zeta function in the region of analytic continuation can be represented by any method of generalized summation of divergent series.

What exactly is the geometric analysis of values of the Riemann zeta function, we will see when we construct a polyline, which form a vector corresponding to the terms of the Dirichlet series, which defines the Riemann zeta function.

All results in the paper are obtained empirically by calculations with a given precision (15 significant digits).

2 Representation of the Riemann zeta function value by a vector system

This section presents detailed results of geometric analysis of expressions that determine a value of the Riemann zeta function in the critical strip.

The possibility of such an analysis is due to two important facts:

- 1) representation of complex numbers by vectors;
- 2) using of methods of generalized summation of divergent series.

2.1 Representation of the partial sum of the Dirichlet series by a vector system

Each term of the Dirichlet series (1), which defines the Riemann zeta function, is a complex number $x_n + iy_n$, hence it can be represented by the vector $X_n = (x_n, y_n)$.

To obtain the coordinates of the vector $X_n(s)$, $s = \sigma + it$, we first present the expression n^{-s} in the exponential form of a complex number, and then, using the Euler formula, in the trigonometric form of a complex number:

$$X_n(s) = \frac{1}{n^s} = \frac{1}{n^\sigma} e^{-it \log(n)} = \frac{1}{n^\sigma} (\cos(t \log(n)) - i \sin(t \log(n))); \quad (3)$$

Then the coordinates of the vector $X_n(s)$ can be calculated by formulas:

$$x_n(s) = \frac{1}{n^\sigma} \cos(t \log(n)); y_n(s) = -\frac{1}{n^\sigma} \sin(t \log(n)); \quad (4)$$

Using the rules of analytical geometry, we can obtain the coordinates corresponding to the partial sum $s_m(s)$ of the Dirichlet series (1):

$$s_m(s)_x = \sum_{n=1}^m x_n(s); s_m(s)_y = \sum_{n=1}^m y_n(s); \quad (5)$$

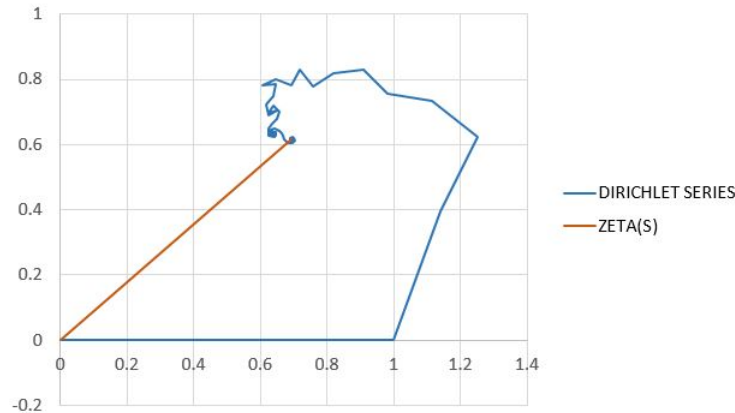


Figure 1: Polyline, $s = 1.25 + 279.229250928i$

We construct a polyline corresponding to partial sums of $s_m(s)$. Select a value *in the convergence region* of the Dirichlet series (1), for example, $s = 1.25 + 279.229250928i$.

We also display the vector $(0.69444570272324, 0.61658346971775)$, which corresponds to a value of the Riemann zeta function at $s = 1.25 + 279.229250928i$.

We will display the first $m = 90$ vectors (later we will explain why we chose such a number) so that the vectors follow in ascending order of their numbers (fig. 1).

Now we change a value of the real part $s = 0.75 + 279.229250928i$ and move to the region where the Dirichlet series (1) *diverges*.

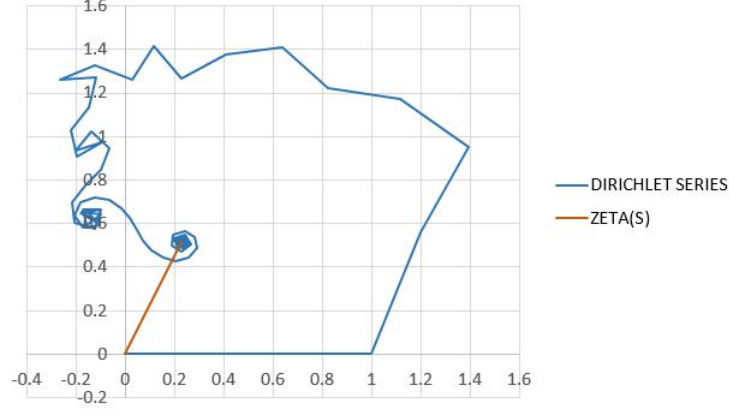


Figure 2: Polyline, $s = 0.75 + 279.229250928i$

We also display the vector $(0.22903651233853, 0.51572970834588)$, which corresponds to a value of the Riemann zeta function at $s = 0.75 + 279.229250928i$.

We observe (fig. 2) an increase of size of the polyline, but the qualitative behavior of the graph does not change. *The polyline twists around a point corresponding to a value of the Riemann zeta function.*

To see what exactly is the difference, we need to consider the behavior of vectors with smaller numbers, for example, in the range $m = (300, 310)$ with relation to vectors with large numbers, for example, in the range $m = (500, 510)$.

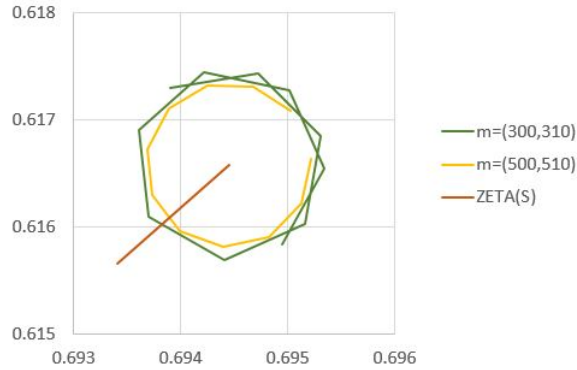


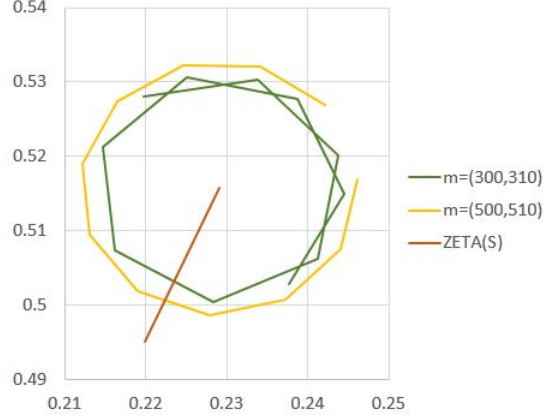
Figure 3: Part of polyline, $s = 1.25 + 279.229250928i$

We see (fig. 3) that when $\sigma = 1.25$ the polyline is a *converging* spiral, as the radius of the spiral in the range of $m = (300, 310)$ is greater than the radius of the spiral in the range of $m = (500, 510)$.

Unlike the first case, when $\sigma = 0.75$ we see (fig. 4) that a polyline is a *divergent* spiral, since the radius of the spiral in the range $m = (300, 310)$ is less than the radius of the spiral in the range $m = (500, 510)$.

But regardless of whether the spiral converges or diverges, in both cases we see that the center of the spiral corresponds to the point corresponding to a value of the Riemann zeta function (we will later show that it is indeed).

This fact can be considered a geometric explanation of the method of generalized summation:

Figure 4: Part of polyline, $s = 0.75 + 279.229250928i$

The coordinates of the partial sums $s_m(s)_x$ and $s_m(s)_y$ of the Dirichlet series (1) vary with relation to some middle values of x and y , which we take as a value of the Riemann zeta function, only in one case the coordinates of the partial sums converge infinitely to these values, and in the other case they diverge infinitely with relation to these values.

2.2 Properties of vector system of the partial sums of the Dirichlet series – the Riemann spiral

In order not to use in the further analysis of the long definitions of the vector system, which we are going to study in detail, we introduce the following definition:

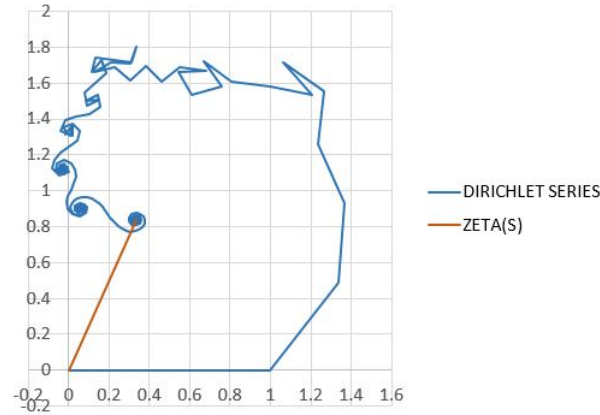
The Riemann spiral is a polyline formed by vectors corresponding to the terms of the Dirichlet series (1) defining the Riemann zeta function, in ascending order of their numbers.

A preliminary analysis of *Riemann spiral* showed that vectors arranged in ascending order of their numbers form a converging or divergent spiral with a center at a point corresponding to a value of the Riemann zeta function.

We also see (fig. 2) that the Riemann spiral has several more centers where the vectors first form a converging spiral and then a diverging spiral.

Comparing (fig. 1) and (fig. 2) we see that the number of such centers does not depend on the real part of a complex number.

While comparing (fig. 2) and (fig. 5), we see that the number of such centers increases when the imaginary part of a complex number increases.

Figure 5: The Riemann spiral, $s = 0.75 + 959.459168807i$

We can explain this behavior of Riemann spiral vectors if we return to the exponential form (3) of the record of terms of the Dirichlet series (1).

The paradox of the Riemann spiral is that with unlimited growth of the function $t \log(n)$, the absolute angles $\varphi_n(t)$ of its vectors behave in a pseudo-random way (fig. 6), because we can recognize angles only in the range $[0, 2\pi]$.

$$\varphi_n(t) = t \log(n) \bmod 2\pi; \quad (6)$$

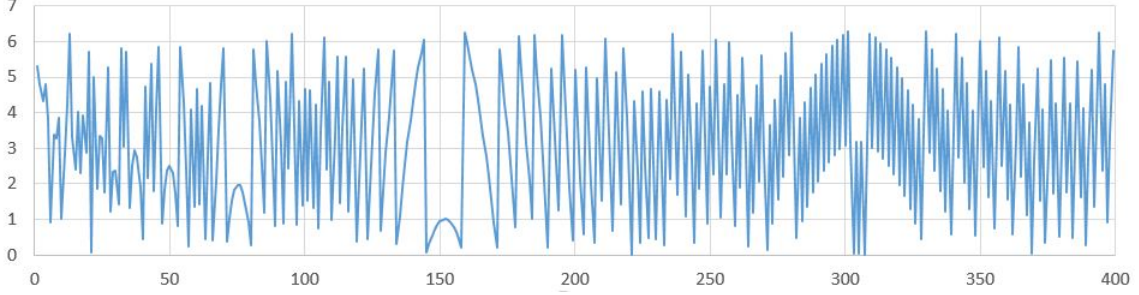


Figure 6: Absolute angles $\varphi_n(t)$ of vectors of the Riemann spiral, rad, $s = 0.75 + 959.459168807i$

The angles between the vectors $\Delta\varphi_n(t)$, if they are measured not as visible angles between segments, but as angles between directions, permanently grow (fig. 7) to a value 2π , then they sharply decrease to a value 0 and again grow to a value 2π .

$$\Delta\varphi_n(t) = \varphi_n(t) - \varphi_{n-1}(t); \quad (7)$$

On the last part this growth is *asymptotic*, i.e. no matter how large the vector number n is, a value $\log(n)$ will never be equal to a value $\log(n+1)$.

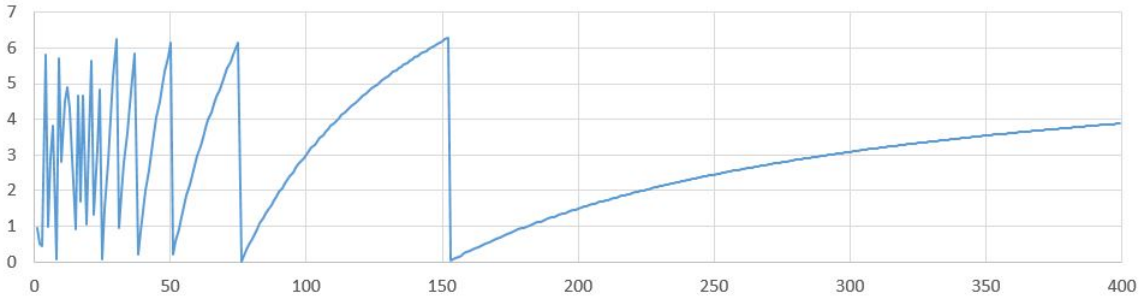


Figure 7: Relative angles $\Delta\varphi_n(t)$ of vectors of the Riemann spiral, rad, $s = 0.75 + 959.459168807i$

In consequence of the revealed properties of the Riemann spiral vectors, we observe two types of singular points:

- 1) *reverse points* where the visible twisting of the vectors is replaced by untwisting, these points are multiples of $(2k-1)\pi$;
- 2) *inflection points*, in which the visible untwisting of the vectors is replaced by twisting, these points are multiples of $2k\pi$;

Now we can explain why for a value of $s = 1.25 + 279.229250928i$ we took 90 vectors to construct the Riemann spiral:

$$279.229250928/\pi = 88.881431082; \quad (8)$$

Therefore, the first reverse point is between the 88th and 89th vectors, we just rounded the number of vectors to a multiple.

This is the number of vectors we must use to build the Riemann spiral in order to vectors fully twisted around the point corresponding to a value of the Riemann zeta function.

In addition, we can determine the number of reverse points m , as we remember, this number determines the range in which (fig. 7) the periodic monotonous increase of angles between the Riemann spiral vectors is observed, moreover this number plays an important role (as we will see later) in the representation of the Riemann zeta function values by the vector system.

We can determine the number of reverse points m from the condition that between two reverse points there is at least one vector:

$$\frac{t}{(2m-1)\pi} - \frac{t}{(2m+1)\pi} = 1; \quad (9)$$

From this equation we find:

$$m = \sqrt{\frac{t}{2\pi} + \frac{1}{4}}; \quad (10)$$

At the end of the consideration of the static parameters of the Riemann spiral, we perform an analysis of its radius of curvature:

$$r_n = \frac{|X_n| \cos(\Delta\varphi_n)}{\sqrt{1 - \cos(\Delta\varphi_n)^2}}; \quad (11)$$

where

$$\cos(\Delta\varphi_n) = \frac{(X_n, X_{n-1})}{|X_n||X_{n-1}|}; \quad (12)$$

$$|X_n| = \sqrt{x_n^2 + y_n^2}; \quad (13)$$

$$(X_n, X_{n-1}) = x_n x_{n-1} + y_n y_{n-1}; \quad (14)$$

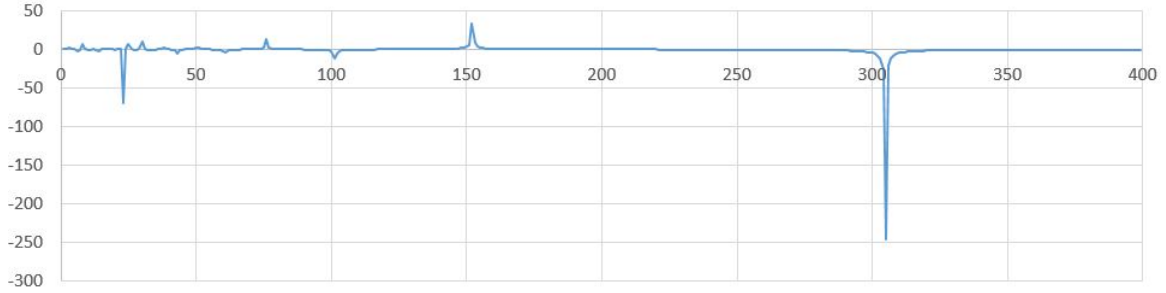


Figure 8: Curvature radius of the Riemann spiral, $s = 0.75 + 959.459168807i$

We see (fig. 8) that the Riemann spiral has an *alternating sign* of radius of curvature. This is the only spiral that has this property.

The maximum negative value of the radius of curvature takes at the reverse point, and the maximum positive is at the inflection point.

2.3 Derivation of an empirical expression for the Riemann zeta function

We study in detail the behavior of Riemann spiral vectors after the first reverse point:

$$m = \frac{t}{\pi};$$

As we know, the Riemann spiral vectors in the critical strip form a divergent spiral (fig. 4).

Consider the Riemann spiral after the first reverse point on the left boundary of the critical strip (Fig. 9) i.e. when $\sigma = 0$.

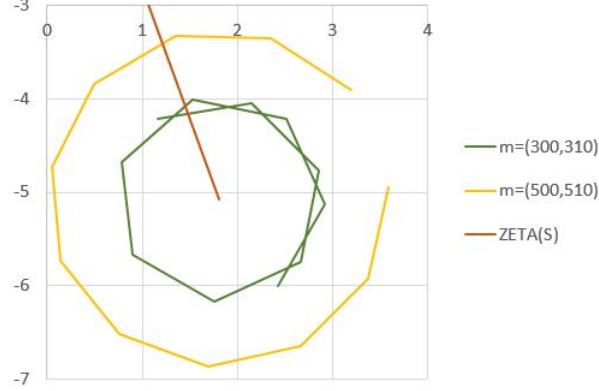


Figure 9: Part of polyline, $s = 0 + 279.229250928i$

We see that the size of the polyline has increased in comparison with (fig. 4), but the behavior of the vectors has not changed, as their numbers increase, the vectors tend to form a regular polygon and the quantity of edges grows with the growth of vector numbers.

And as we understand, as a result of the vectors tend to form a circle of the greater radius, than the greater the number of vectors, and the center of the circle tends to the center of the spiral, consequently, to the point, which corresponds to a value of the Riemann zeta function.

In analytic number theory, this fact¹ is known as the first approximate equation of the Riemann zeta function:

$$\zeta(s) = \sum_{n \leq x} \frac{1}{n^s} - \frac{x^{1-s}}{1-s} + \mathcal{O}(x^{-\sigma}); \sigma > 0; |t| < 2\pi x/C; C > 1 \quad (15)$$

As we know, Hardy and Littlewood obtained this approximate equation based on the generalized Euler-Maclaurin summation method.

It is known from the theory of generalized summation of divergent series [6] that we can apply *any other method* of generalized summation (if it gives any value) and get the same result.

We use the Riemann spiral to determine another method of generalized summation.

Consider the first 30 vectors of the Riemann spiral after the first reverse point (fig. 10), here the vectors form a star-shaped polygon, with the point that corresponds to a value of the Riemann zeta function at the center of this polygon, as in the case of a divergent spiral (fig. 4).

Connect the middle of the segments formed by vectors and get 29 segments (fig. 11).

We see that the star-shaped polygon has decreased in size, and the point that corresponds to a value of the Riemann zeta function is again at the center of this polygon.

We will repeat the operation of reducing the polygon (fig. 12) until there is one segment left.

Calculations show that when calculating the coordinates of vectors with an accuracy of 15 characters, the coordinates of the middle of this segment with an accuracy of not less than 13 digits match a value of the zeta function of Riemann, for example, at point $0.75 + 279.229250928i$ the exact value of [22] equals $0.22903651233853 + 0.51572970834588i$, and in the calculation of midpoints of the segments we get a value $0.22903651233856 + 0.51572970834589i$.

To calculate values of the Riemann zeta function, a reduced formula can be obtained by the described method. Write sequentially the expressions to calculate the midpoints of the segments and substitute successively the obtained formulas one another:

$$a_i = \frac{x_i + x_{i+1}}{2}; \quad (16)$$

¹The first is the correspondence to the graph of partial sums of the Dirichlet series considered by Erickson in his paper [13]

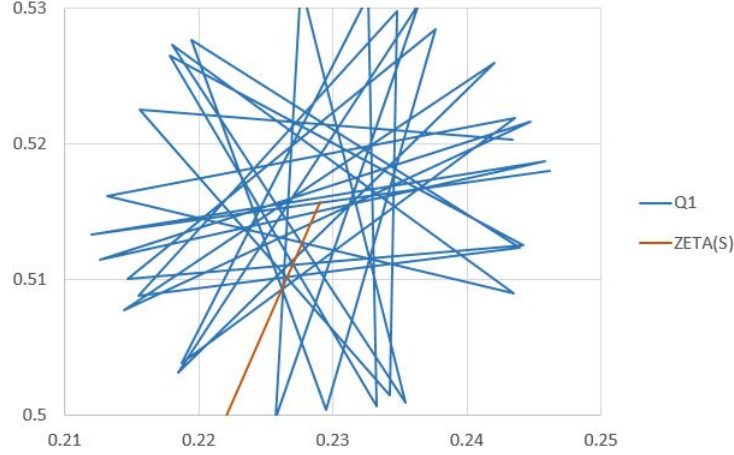


Figure 10: First 30 vectors after the first reverse point, $s = 0.75 + 279.229250928i$

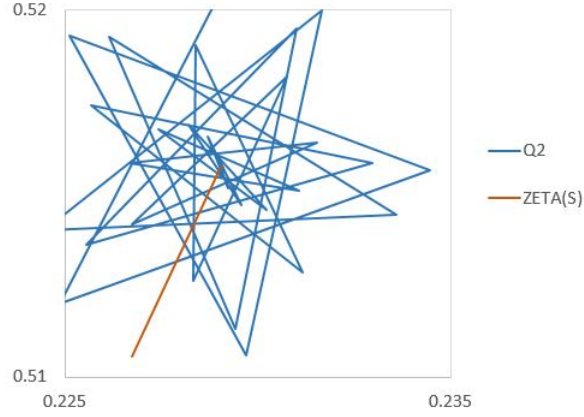


Figure 11: The first step of generalized summation, $s = 0.75 + 279.229250928i$

$$b_i = \frac{a_i + a_{i+1}}{2} = \frac{x_i + 2x_{i+1} + x_{i+2}}{4}; \quad (17)$$

$$c_i = \frac{b_i + b_{i+1}}{2} = \frac{x_i + 3x_{i+1} + 3x_{i+2} + x_{i+3}}{8}; \quad (18)$$

$$d_i = \frac{c_i + c_{i+1}}{2} = \frac{x_i + 4x_{i+1} + 6x_{i+2} + 4x_{i+3} + x_{i+4}}{16}; \quad (19)$$

We write the same formulas for the coordinates y_k .

In the numerator of each formula (16-19) we see the sum of vectors multiplied by binomial coefficients, which correspond to the degree of Newton's binomial, equal to the number of vectors minus one, and in the denominator the degree of two, equal to the number of vectors minus one.

Now we can write down the abbreviated formula:

$$s_x = \frac{1}{2^m} \sum_{k=0}^m \binom{k}{m} x_k; s_y = \frac{1}{2^m} \sum_{k=0}^m \binom{k}{m} y_k; \quad (20)$$

where x_k and y_k are coordinates of partial sums (5) of Dirichlet series.

We obtained the formula of the generalized Cesaro summation method (C, k) [6].

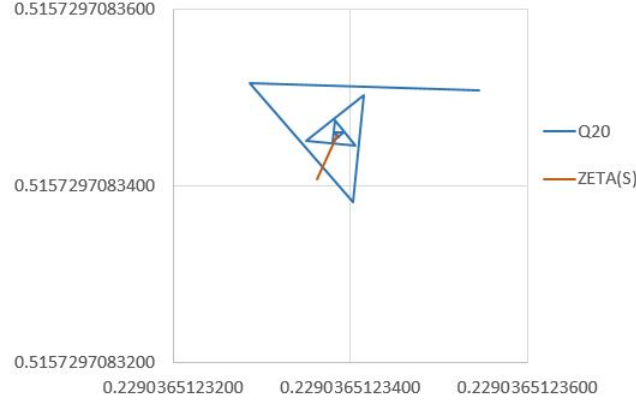


Figure 12: The twentieth step of generalized summation, $s = 0.75 + 279.229250928i$

It should be noted that to calculate the coordinates of the center of the star-shaped polygon when a value of the imaginary part of the complex number is equal to 279.229250928, we use 30 vectors after the first reverse point, while starting with a value of the imaginary part of a complex number equal to 1000, it is enough to use only 10 vectors after the first reverse point.

We obtained a result that applies not only to the Riemann zeta function, but also to all functions of a complex variable that have an analytic continuation.

A result that relates not only to the analytic continuation of the Riemann zeta function, but to the analytic continuation as the essence of any function of a complex variable.

A result that refers to any function and any physical process where such functions are applied, and hence a result that defines the essence of that physical process.

Euler's intuitive belief² that a divergent series can be matched with a certain value [11], has evolved into the fundamental theory³ of generalized summation of divergent series, which Hardy systematically laid out in his book [6].

The essence of our conclusions is as follows:

1) When it comes to analytical continuation of some function of a complex variable, it automatically means that there are at least two regions of definition of this function:

- a) the region where the series by which this function is defined converges;
- b) the region where the same series diverges.

Actually, the question of analytical continuation arises because there is an region where the series that defines the function of a complex variable diverges.

Thus, the analytical continuation of any function of a complex variable is inseparably linked to the fact that there is a divergent series.

We can say that this is the very essence of the analytical continuation.

2) Analytical continuation is possible only if there is some method of generalized summation that will give a result, i.e. some value other than infinity.

This value will be a value of the function, in the region where the series by which this function is defined diverges.

3) The most important thing in this question is that the series by which the function is defined must behave asymptotically in the region where this series infinitely converges and in the region where it infinitely diverges.

And then we come to an important point:

²These inconveniences and apparent contradictions can be avoided if we give the word „sum“ a meaning different from the usual. Let us say that the sum of any infinite series is a finite expression from which the series can be derived.

³It is impossible to state Euler's principle accurately without clear ideas about functions of a complex variable and analytic continuation.

The function of a complex variable, if it has an analytical continuation (and therefore is given by a series that converges in one region and diverges in another, i.e. has no limit of partial sums of this series) is determined by the asymptotic law of behavior of the series by which this function is given and it is no matter whether this series converges or diverges, a value of this function will be the asymptotic value with relation to which this series converges or diverges.

Analytical continuation is possible only if the series with which the function is given has asymptotic behavior, i.e. its values oscillate with relation to the asymptote, which is a value of the function.

In the case of a function of a complex variable, there are two such asymptotes, and in the case of a function of a real variable, such an asymptote is one.

If the Riemann zeta function is given asymptotic values, then it also has *asymptotic value of zero*, hence it may seem that the Riemann hypothesis cannot be proved.

As we will show later, a value of the Riemann zeta function can be given by a finite vector system, the sum of which gives *the exact value of zero* if these vectors form a polygon.

In this regard, we can conclude that the Riemann hypothesis can be confirmed only if such a finite vector system exists and only using the properties of the vectors of this system.

One can disagree with the conclusion that it is possible to confirm the Riemann hypothesis using a finite vector system, but we will go this way, because the chosen method of geometric analysis of the Riemann zeta function allows us to penetrate into the essence of the phenomenon.

2.4 Derivation of an empirical expression for the functional equation of the Riemann zeta function

We already know one dynamic property of the Riemann spiral, which is that the number of reverse points increases with the growth of the imaginary part of a complex number.

We will study *the reverse points* and *inflection points*, which, as we will see later, are not just special points of the Riemann spiral, they are its essential points that define the essence of the Riemann spiral and the Riemann zeta function.

We will use our empirical formula for calculating a value of the Riemann zeta function, which corresponds to the Cesaro generalized summation method.

As we saw (fig. 5), the Riemann spiral vectors at any reverse point where the Riemann spiral has a negative radius of curvature, up to the reverse point form a converging spiral, and after the reverse point form a divergent spiral.

This fact allows us to apply the formula for calculating a value of the Riemann zeta function at any reverse point, because this formula allows us to calculate the coordinates of any center of the divergent spiral, which form the Riemann spiral vectors.

For the convenience of further presentation, we introduce the following definition:

Middle vector of the Riemann spiral is a directed segment connecting two adjacent centers of the Riemann spiral, drawn in the direction from the center with a smaller number to the center with a larger number (fig. 13) when numbering from the center corresponding to value of the Riemann zeta function.

To identify modulus of middle vectors of the Riemann spiral first using the formula (20) we define the coordinates of the centers of the Riemann spiral.

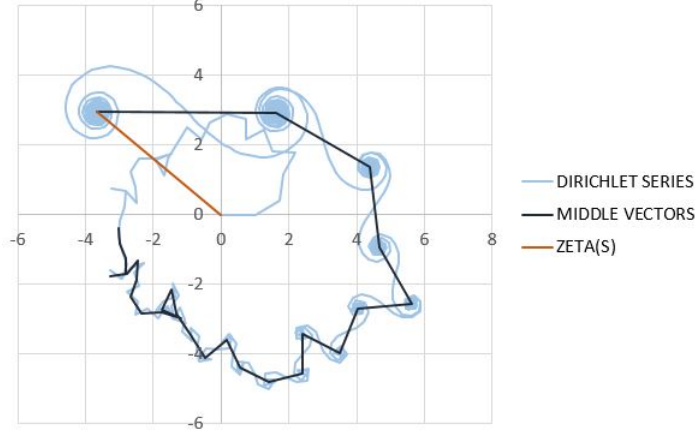
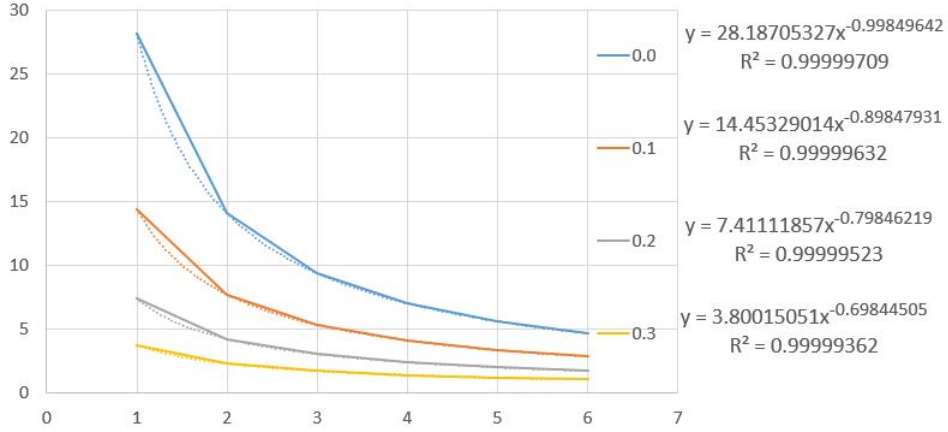
To calculate the coordinates of the first center of the Riemann spiral (a value of the Riemann zeta function) we will use 30 vectors, to calculate the coordinates of the second center - 20 vectors.

To increase the accuracy, we can choose a different number of vectors for each center of the Riemann spiral, but since we choose a sufficiently large value of the imaginary part of a complex number and a sufficiently small number of vectors, it will be enough to use 5 vectors to calculate the coordinates starting from the third center of the Riemann spiral.

Then, using the formula to determine the distance between two points, we find the modulus of the middle vectors:

$$|Y_n| = \sqrt{(x_{n+1} - x_n)^2 + (y_{n+1} - y_n)^2}; \quad (21)$$

We calculate the modulus of the first six middle vectors of the Riemann spiral for values of the real part in the range from 0 to 1 in increments of 0.1 and a fixed value of the imaginary part of a complex number - 5000 and then we approximate the dependence of the modulus of the middle vector of the Riemann spiral on its sequence number (fig. 14).

Figure 13: The middle vectors of the Riemann spiral , $s = 0.25 + 5002.981i$ Figure 14: The dependence of the modulus of the middle vector from the sequence number, $Re(s) = (0.0, 0.1, 0.2, 0.3)$, $Im(s) = 5000$

The best method of approximation of dependence of the modulus of the middle vector from the sequence number (fig. 14, where $x = n$) for different values of the real part of a complex number (and the fixed imaginary part of a complex number) is a power function

$$|Y_n| = An^B; \quad (22)$$

It should be noted that the accuracy of the approximation increases or with a decrease in the number of vectors (fig. 15), or by increasing a value of the imaginary part of a complex number (fig. 16), this fact indicates the *asymptotic* dependence of the obtained expressions.

Now approximate the dependence of the coefficients A and B on a value of the real part of a complex number.

We start with the coefficient B , because at this stage we will complete its analysis, and for the analysis of the coefficient A additional calculations will be required.

The coefficient B has a linear dependence (fig. 17, where $x = \sigma$) from a value of the real part of a complex number. Therefore, taking into account the identified asymptotic dependence, we can rewrite the expression (22) for the modulus of the middle vectors of the Riemann spiral:

$$|Y_n| = A \frac{1}{n^{1-\sigma}}; \quad (23)$$

The best way to approximate the dependence of the coefficient A (fig. 18, where $x = \sigma$) from a value of the real part of a complex number is the exponent:

$$A = Ce^{D\sigma}; \quad (24)$$

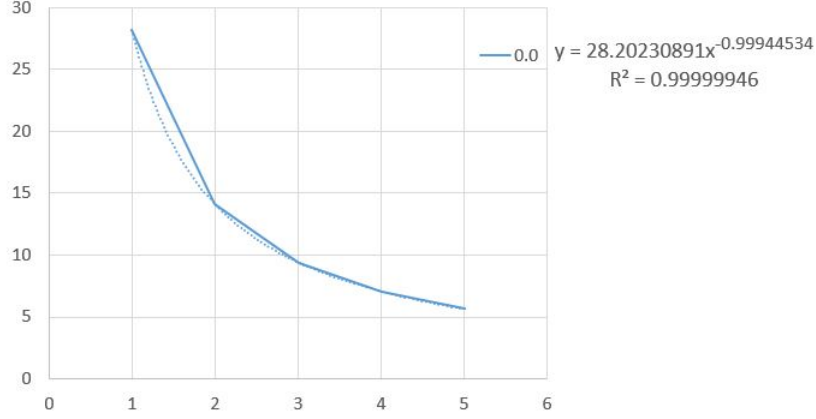


Figure 15: The dependence of the modulus of the middle vector for the five vectors , $s = 0 + 5000i$

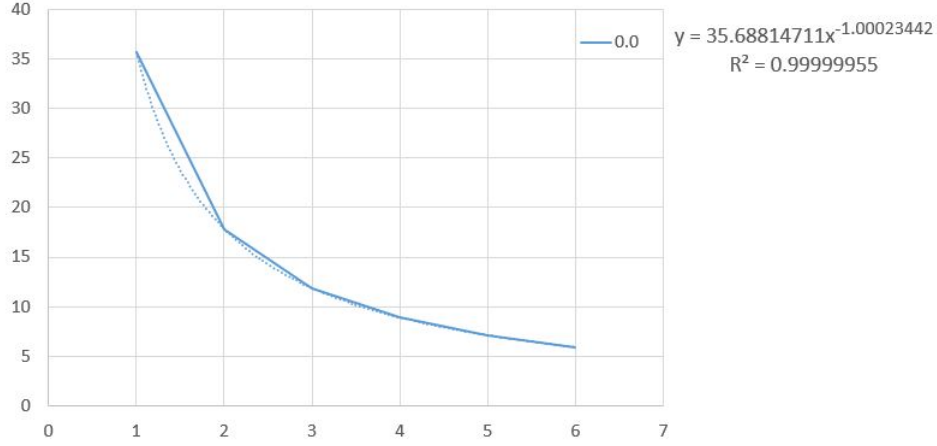


Figure 16: Dependence of the middle vector modulus for a larger value of the imaginary part of a complex number , $s = 0 + 8000i$

We first find the ratio of the coefficients C and D , for this we calculate $\log(C)$:

$$2\log(C) = 6.67772573; \quad (25)$$

Taking into account the revealed asymptotic dependence $2\log(C) = D$, we can rewrite the expression (24) for the coefficient A :

$$A = Ce^{-2\log(C)\sigma} = e^{\log(C)-2\log(C)\sigma} = e^{2\log(C)(\frac{1}{2}-\sigma)} = (C^2)^{\frac{1}{2}-\sigma}; \quad (26)$$

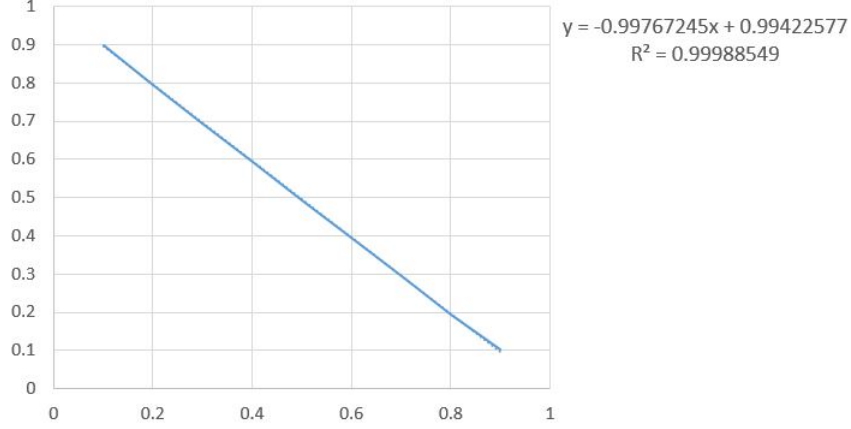
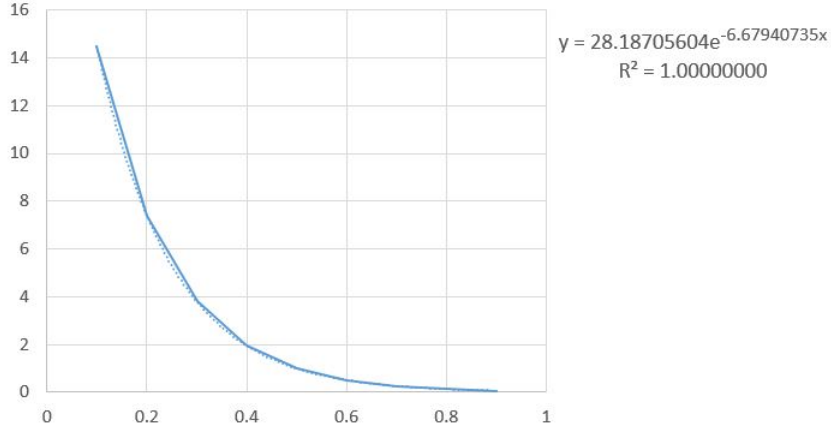
Now, taking into account the identified asymptotic dependence $|Y_n| = A = C$ when $\sigma = 0$, we calculate the modulus of the first middle vector when $\sigma = 0$ for different values of the imaginary part of a complex number in the range from 1000 to 9000 in increments of 1000 and then approximate the dependence of the coefficients C on a value of the imaginary part of a complex number.

The best way to approximate the dependence of the coefficient C (Fig. 19, where $x = t$) from a value of the imaginary part of a complex number is a power function:

$$C = Et^F; \quad (27)$$

Taking into account the revealed asymptotic dependence consider

$$F = \frac{1}{2};$$

Figure 17: Dependence of the coefficient B on the real part of a complex number, $Im(s) = 5000$ Figure 18: Dependence of the coefficient A on the real part of a complex number, $Im(s) = 5000$

then we can write the final expression for the modulus of the middle vectors of the Riemann spiral:

$$|Y_n| = (E^2 t)^{\frac{1}{2}-\sigma} \frac{1}{n^{1-\sigma}}; \quad (28)$$

where $E^2 = 0.159154719364$ some constant, the meaning of which we learn later.

We obtained an asymptotic expression (28) for the modulus of the middle vectors of the Riemann spiral, which becomes, as we found out, more precisely when the imaginary part of a complex number increases.

As a consequence of the asymptotic form of the resulting expression, we can apply it to any middle vector, even if we can no longer calculate its coordinates or the calculated coordinates give an inaccurate value of the middle vector modulus.

Therefore, we can obtain any quantity of middle vectors necessary to construct *the inverse Riemann spiral*.

So we can get an infinite series, which is given by the middle vectors of the Riemann spiral.

By comparing the expression for the modulus of vectors (4) of the Riemann spiral and the expression for the modulus of its middle vectors (28), we can assume that the infinite series formed by the middle vectors of the Riemann spiral sets a value of the Riemann zeta function $\zeta(1-s)$.

So we can assume that values of the Riemann zeta function $\zeta(s)$ and $\zeta(1-s)$ are related through an expression for the middle vectors of the Riemann spiral.

To complete the derivation of the dependence of the Riemann zeta function $\zeta(s)$ and $\zeta(1-s)$, it is necessary to determine the dependence of the angles between the middle vectors of the Riemann spiral and construct an inverse Riemann spiral whose vectors, as we show further, asymptotically twist around the zero of the complex plane.

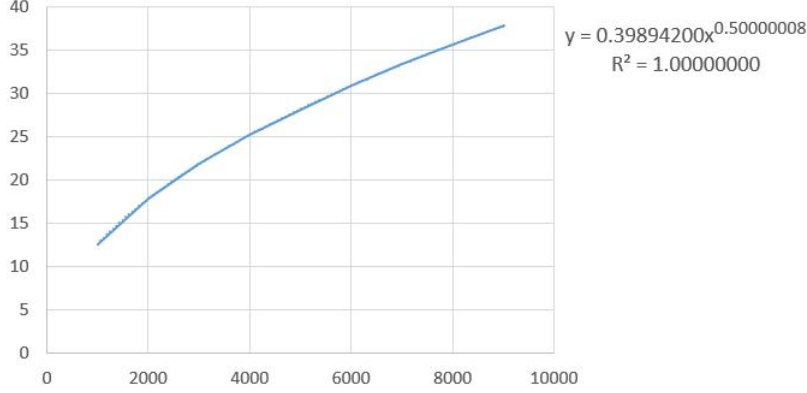


Figure 19: Dependence of the coefficient C on the imaginary part of a complex number, $Re(s) = 0$

If to determine the coordinates of the centers of Riemann spiral, we used the *reverse points*, to determine the angles between middle vectors of the Riemann spiral, we will use *inflection points*. We see (fig. 13) that the inflection points are not only the points at which the visible untwisting of the vectors is replaced by the twisting, but also the points at which the middle vectors intersect the Riemann spiral.

One can show by computing that the angles between the middle vectors and the Riemann spiral at the intersection points are asymptotically equal to $\pi/4$, then the angles between the middle vectors can be equated to the angles between the Riemann spiral vectors at the inflection points.

As we remember, the inflection points are multiples of $2k\pi$, then using the properties of the logarithm, we can find the angle between the first and any other middle vector of the Riemann spiral:

$$\beta_k = \alpha_k - \alpha_1 = t \log\left(\frac{t}{2\pi}\right) - t \log(k) - t \log\left(\frac{t}{2\pi}\right) = -t \log(k); \quad (29)$$

We have obtained an expression that shows that the angles between the first middle vector of the Riemann spiral and any other middle vector are equal in modulus and opposite in sign to the angles between the first vector and corresponding vector of the Riemann spiral, the negative sign shows that the middle vectors have a special kind of symmetry (which we will consider later) with relation to the vectors of value of the Riemann spiral.

Knowing the coordinates of the first middle vector, which we calculated with sufficient accuracy, we can now find the angles and modulus of the remaining middle vectors using the obtained asymptotic expressions and construct the inverse Riemann spiral (Fig. 20).

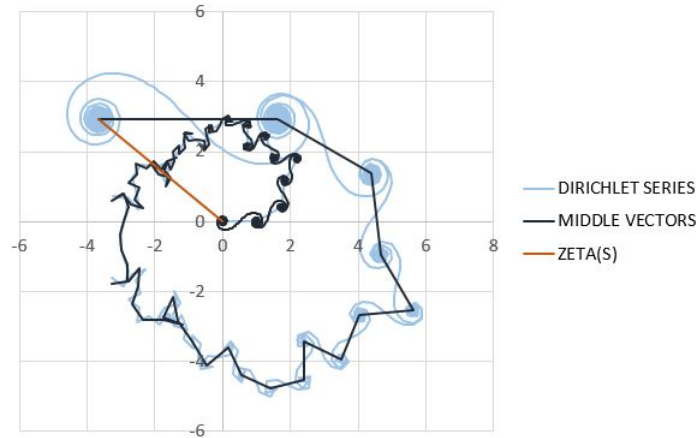


Figure 20: Inverse Riemann spiral, $s = 0.25 + 5002.981i$

Now at $n = k$ we can write the final formula to calculate the coordinates of the middle vectors Y_n :

$$\tilde{x}_n(s) = (E^2 t)^{\frac{1}{2}-\sigma} \frac{1}{n^{1-\sigma}} \cos(\alpha_1 - t \log(n)); \tilde{y}_n(s) = (E^2 t)^{\frac{1}{2}-\sigma} \frac{1}{n^{1-\sigma}} \sin(\alpha_1 - t \log(n)); \quad (30)$$

Using Euler's formula for complex numbers we write the expression for the middle vectors of the Riemann spiral in exponential form:

$$Y_n(s) = (E^2 t)^{\frac{1}{2}-\sigma} \frac{1}{n^{1-\sigma}} e^{-i(\alpha_1 - t \log(n))}; \quad (31)$$

Using the rules of analytical geometry, we can obtain the coordinates of the vector corresponding to the partial sum of $\hat{s}_m(s)$ inverse Riemann spiral:

$$\tilde{s}_m(s)_x = \zeta(s)_x - \sum_{n=1}^m \tilde{x}_n(s); \tilde{s}_m(s)_y = \zeta(s)_y - \sum_{n=1}^m \tilde{y}_n(s); \quad (32)$$

To verify that the obtained expression for the middle vectors of the Riemann spiral defines the relation values of the Riemann zeta function $\zeta(s)$ and $\zeta(1-s)$, consider the middle vectors of the Riemann spiral near the point of zero (fig. 21).

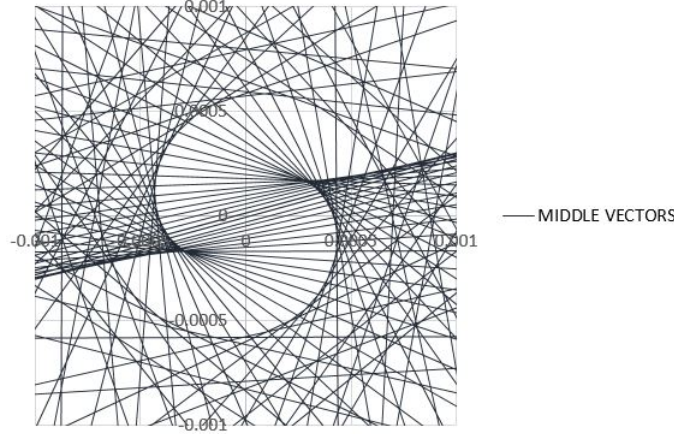


Figure 21: Middle vectors of the inverse Riemann spiral near the point of zero, $s = 0.25 + 5002.981i$

We see that the middle of the vectors twist around the zero point, in the same way as the vectors of the Riemann spiral twist around the point with the coordinates of a value of the Riemann zeta function⁴.

Now we can write the final equation that relates values of the Riemann zeta function $\zeta(s)$ and $\zeta(1-s)$ taking into account the rules of generalized summation of divergent series:

$$\sum_{n=1}^{\infty} \frac{1}{n^s} - (E^2 t)^{\frac{1}{2}-\sigma} e^{-i\alpha_1} \sum_{n=1}^{\infty} \frac{1}{n^{1-s}} = 0; \quad (33)$$

where α_1 is the angle of the first middle vector of the Riemann spiral.

This fact shows the asymptotic form of functional equation and the geometric nature of the Riemann zeta function, based on the significant role of turning points and inflection points of the Riemann spiral, which determine the middle vectors and the inverse Riemann spiral.

We can try to find an asymptotic expression for the angle α_1 of the first middle vector of the Riemann spiral in a geometric way, but this will not significantly improve the result.

We use the results of the analytical theory of numbers to an arithmetic way to find the exact expression for the angle α_1 of the first middle vector of the Riemann spiral and to determine the meaning of the constant $E^2 = 0.159154719364$.

⁴This fact was already considered by the forum Stack Exchange [18], but nobody try to compute the Riemann zeta function with geometric method, which corresponds to the method of generalized summation Cesaro.

2.5 Derivation of empirical expression for CHI function

The functional equation of the Riemann zeta function [9] has several equivalent entries:

$$\zeta(s) = \chi(s)\zeta(1-s); \quad (34)$$

where

$$\chi(s) = \frac{(2\pi)^s}{2\Gamma(s)\cos(\frac{\pi s}{2})} = 2^s \pi^{s-1} \sin(\frac{\pi s}{2}) \Gamma(1-s) = \pi^{s-\frac{1}{2}} \frac{\Gamma(\frac{1-s}{2})}{\Gamma(\frac{s}{2})}; \quad (35)$$

Comparing (33) and (34), we get:

$$\chi(s) = (E^2 t)^{\frac{1}{2}-\sigma} e^{-i\alpha_1}; \quad (36)$$

We find the same expression in Titchmarsh [9]:

in any fixed strip $\alpha \leq \sigma \leq \beta$, when $t \rightarrow \infty$:

$$\chi(s) = \left(\frac{2\pi}{t}\right)^{(\sigma+it-\frac{1}{2})} e^{i(t+\frac{\pi}{4})} \left\{1 + \mathcal{O}\left(\frac{1}{t}\right)\right\}; \quad (37)$$

We write the expression (37) in the exponential form of a complex number:

$$\chi(s) = \left(\frac{t}{2\pi}\right)^{(\frac{1}{2}-\sigma)} e^{-i(t(\log \frac{t}{2\pi}-1)-\frac{\pi}{4}+\tau(s))}; \quad (38)$$

where

$$\tau(s) = \mathcal{O}\left(\frac{1}{t}\right); \quad (39)$$

By matching (36) and (38), we obtain the angle of the first middle vector of the Riemann spiral:

$$\alpha_1 = t(\log \frac{t}{2\pi} - 1) - \frac{\pi}{4} + \tau(s); \quad (40)$$

And define the meaning of the constant $E^2 = 0.159154719364$:

$$E^2 = \frac{1}{2\pi} = 0.159154943091; \quad (41)$$

Now we can write the asymptotic equation (33) in its final form:

$$\sum_{n=1}^{\infty} \frac{1}{n^s} - \left(\frac{t}{2\pi}\right)^{\frac{1}{2}-\sigma} e^{-i\alpha_1} \sum_{n=1}^{\infty} \frac{1}{n^{1-s}} = 0; \quad (42)$$

We will find the empirical expression for remainder term $\tau(s)$ of the CHI function, which defines the ratio of the modulus and the argument of the exact $\chi(s)$ and the approximate $\tilde{\chi}(s)$ value of the CHI function:

$$\tau(s) = \Delta\varphi_{\chi} + \log\left(\frac{|\chi(s)|}{|\tilde{\chi}(s)|}\right)i; \quad (43)$$

where

$$\Delta\varphi_{\chi} = \text{Arg}(\chi(s)) - \text{Arg}(\tilde{\chi}(s)); \quad (44)$$

The exact values⁵ CHI functions we find from the functional equation of the Riemann zeta function, substituting the exact values of the Riemann zeta function:

$$\chi(s) = \frac{\zeta(s)}{\zeta(1-s)}; \quad (45)$$

Approximate values of the CHI function we find from the expression (38), dropping the function $\tau(s)$.

$$\tilde{\chi}(s) = \left(\frac{t}{2\pi}\right)^{(\frac{1}{2}-\sigma)} e^{-i(t(\log \frac{t}{2\pi}-1)-\frac{\pi}{4})}; \quad (46)$$

⁵The exact value will be understood as a value obtained with a given accuracy.

The calculation of values of the Riemann zeta function is currently available in different mathematical packages. To calculate the exact values of the Riemann zeta function we will use the Internet service [22].

We will use 15 significant digits, because this accuracy is enough to analyze the CHI function.

We will calculate values of the Riemann zeta function in the numerator (45) for values of the real part of a complex number in the range from 0 to 1 in increments of 0.1 and values of the imaginary part of a complex number in the range from 1000 to 9000 in increments of 1000. Note that the range of values of the real part of the a complex number contains $2m+1$ value, which are related by the following relation:

$$1 - \sigma_{k+1} = \sigma_{2m-k+1}; \quad (47)$$

where k varies between 0 and $2m$, hence, for $k=m$:

$$\sigma_{m+1} = 0.5; \quad (48)$$

We use, on the one hand, the property of the Riemann zeta function as a function of a complex variable:

$$\overline{\zeta(1 - \sigma + it)} = \zeta(\overline{1 - \sigma + it}) = \zeta(1 - \sigma - it) = \zeta(1 - s); \quad (49)$$

From other side:

$$\overline{\zeta(1 - \sigma + it)} = \text{Re}(\zeta(1 - \sigma + it)) - \text{Im}(\zeta(1 - \sigma + it))i; \quad (50)$$

Equate (49) and (50):

$$\zeta(1 - s) = \zeta(1 - \sigma - it) = \text{Re}(\zeta(1 - \sigma + it)) - \text{Im}(\zeta(1 - \sigma + it))i; \quad (51)$$

Now we use the relation (47):

$$\zeta(1 - s_{k+1}) = \text{Re}(\zeta(\sigma_{2m-k+1} + it)) - \text{Im}(\zeta(\sigma_{2m-k+1} + it))i = \text{Re}(\zeta(s_{2m-k+1}) - \text{Im}(s_{2m-k+1})i); \quad (52)$$

We use the resulting formula to compute the Riemann zeta function in the denominator (45) based on values computed for the numerator. Then we get an expression for CHI function:

$$\chi(s_{k+1}) = \frac{(\text{Re}(\zeta(s_{k+1})) + \text{Im}(\zeta(s_{k+1}))i)(\text{Re}(\zeta(s_{2m-k+1})) + \text{Im}(\zeta(s_{2m-k+1}))i)}{\text{Re}(\zeta(s_{2m-k+1}))^2 + \text{Im}(\zeta(s_{2m-k+1}))^2}; \quad (53)$$

We will open brackets and write separate expressions for the real part of the CHI function:

$$\text{Re}(\chi(s_{k+1})) = \frac{\text{Re}(\zeta(s_{k+1}))\text{Re}(\zeta(s_{2m-k+1})) - \text{Im}(\zeta(s_{k+1}))\text{Im}(\zeta(s_{2m-k+1}))}{\text{Re}(\zeta(s_{2m-k+1}))^2 + \text{Im}(\zeta(s_{2m-k+1}))^2}; \quad (54)$$

and for imaginary:

$$\text{Im}(\chi(s_{k+1})) = \frac{\text{Re}(\zeta(s_{k+1}))\text{Im}(\zeta(s_{2m-k+1})) + \text{Im}(\zeta(s_{k+1}))\text{Re}(\zeta(s_{2m-k+1}))}{\text{Re}(\zeta(s_{2m-k+1}))^2 + \text{Im}(\zeta(s_{2m-k+1}))^2}; \quad (55)$$

We will consider this to be the exact value of CHI function, because we can calculate it with a given accuracy.

Now write the expression for the real part of the approximate value of the CHI function:

$$\text{Re}(\tilde{\chi}(s_{k+1})) = \left(\frac{2\pi}{t}\right)^{(\sigma - \frac{1}{2})} \cos(t(\log(\frac{2\pi}{t}) + 1) + \frac{\pi}{4}); \quad (56)$$

and for imaginary:

$$\text{Im}(\tilde{\chi}(s_{k+1})) = \left(\frac{2\pi}{t}\right)^{(\sigma - \frac{1}{2})} \sin(t(\log(\frac{2\pi}{t}) + 1) + \frac{\pi}{4}); \quad (57)$$

Calculate the modulus for the exact $|\chi(s)|$ value of CHI function:

$$|\chi(s)| = \sqrt{\text{Re}(\chi(s))^2 + \text{Im}(\chi(s))^2}; \quad (58)$$

and for the approximate $|\tilde{\chi}(s)|$ value of CHI function:

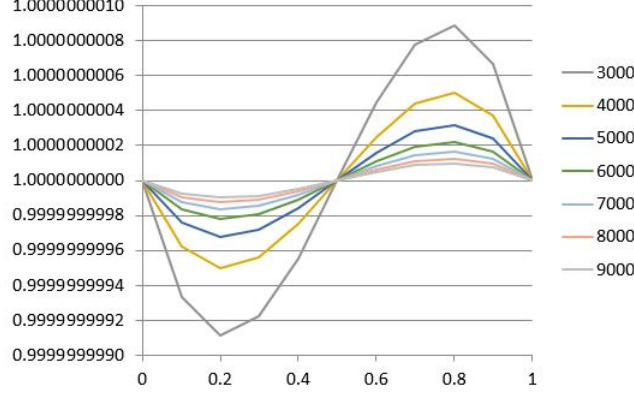


Figure 22: The ratio of the exact $|\chi(s)|$ and approximate $|\tilde{\chi}(s)|$ module of the CHI function

$$|\tilde{\chi}(s)| = \sqrt{\text{Re}(\tilde{\chi}(s))^2 + \text{Im}(\tilde{\chi}(s))^2}; \quad (59)$$

and the angle between the exact $\chi(s)$ and approximate $\tilde{\chi}(s)$ value of CHI function:

$$\Delta\varphi_\chi = \text{Arg}(\chi(s)) - \text{Arg}(\tilde{\chi}(s)) = \arccos\left(\frac{\text{Re}(\chi(s))}{|\chi(s)|}\right) - \arccos\left(\frac{\text{Re}(\tilde{\chi}(s))}{|\tilde{\chi}(s)|}\right); \quad (60)$$

We construct graphs of the ratio of the modulus of the exact $|\chi(s)|$ and approximate $|\tilde{\chi}(s)|$ values of the CHI function of the real part of a complex number of numbers (fig. 22).

The graph shows (fig. 22) that the ratio of the modulus of the exact $|\chi(s)|$ and approximate $|\tilde{\chi}(s)|$ values CHI functions can be taken as 1, therefore, we can say that:

$$\tau(s) = \Delta\varphi_\chi; \quad (61)$$

We construct graphs of the dependence of $\Delta\varphi_\chi$ on the real part of a complex number (fig. 23) and from the imaginary part of a complex number (fig. 24).

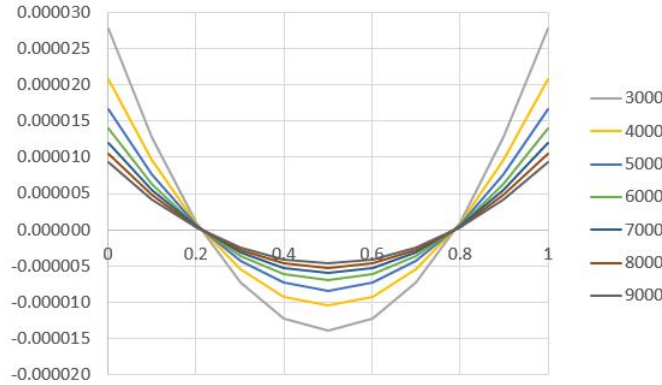


Figure 23: The angle $\Delta\varphi_\chi$ between the exact $\chi(s)$ and approximate $\tilde{\chi}(s)$ value of the CHI function (on the real part)

$\tau(s)$ provided (61) is the argument of remainder term of the CHI function, hence it is a combination of the arguments of remainder terms of the product $\Gamma(s) \cos(\pi s/2)$ in (35).

The argument of the remainder term $\mu(s)$ of the gamma function can be obtained from an expression we can find in Titchmarsh [9]:

$$\log(\Gamma(\sigma + it)) = (\sigma + it - \frac{1}{2}) \log it - it + \frac{1}{2} \log 2\pi + \mu(s); \quad (62)$$

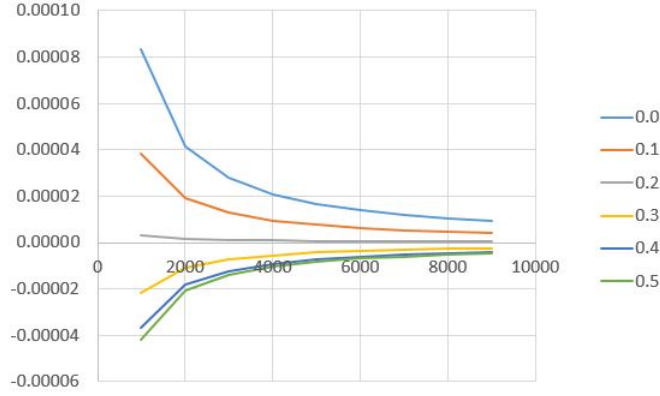


Figure 24: The angle $\Delta\varphi_\chi$ between the exact $\chi(s)$ and approximate $\tilde{\chi}(s)$ value of the CHI function (on the imaginary part)

The most significant researches of remainder term of the gamma function can be found in the paper of Riemann [5] and Gabcke [8], they independently and in different ways obtain an expression for the argument of the remainder term of the gamma function when $\sigma = 1/2$.

We use the expression explicitly written by Gabcke [8]:

$$\mu(t) = \frac{1}{48t} + \frac{1}{5760t^3} + \frac{1}{80640t^5} + \mathcal{O}(t^{-7}); \quad (63)$$

We construct a graph of the dependence of the argument of the remainder term $\mu(t)$ of the gamma function from the imaginary part of a complex number when $\sigma = 1/2$ (fig. 25). We compare the obtained graph with the graph of

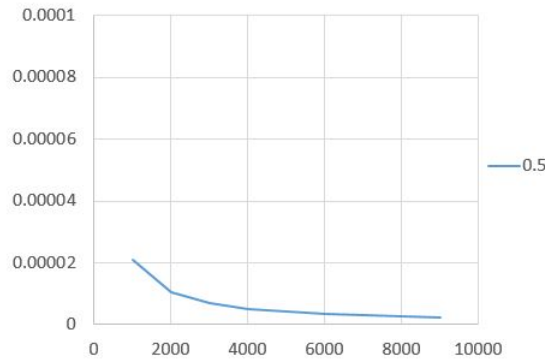


Figure 25: The remainder term of the gamma function, $\sigma = 1/2$

dependence $\Delta\varphi_\chi$ on the imaginary part of a complex number when $\sigma = 1/2$ (fig. 26).

These graphs correspond to each other up to sign and constant value, i.e. the absolute value of the angle between the exact $\chi(s)$ and approximate $\tilde{\chi}(s)$ value of the CHI function is exactly two times greater than a value of the argument of the remainder term of the gamma function when $\sigma = 1/2$.

But a more significant result is obtained by dividing the angle values $\Delta\varphi_\chi$ between the exact $\chi(s)$ and approximate $\tilde{\chi}(s)$ value of the CHI function by a value of the argument of remainder term $\mu(t)$ of the gamma function when $\sigma = 1/2$.

The result of this operation we get the functional dependence $\lambda(\sigma)$ values of the argument of the remainder term $\tau(s)$ of CHI function (with different values of the real part of a complex number) from a value of the argument of the remainder term $\mu(t)$ of the gamma function when $\sigma = 1/2$.

$$\tau(s) = \Delta\varphi_\chi = \lambda(\sigma)\mu(t); \quad (64)$$

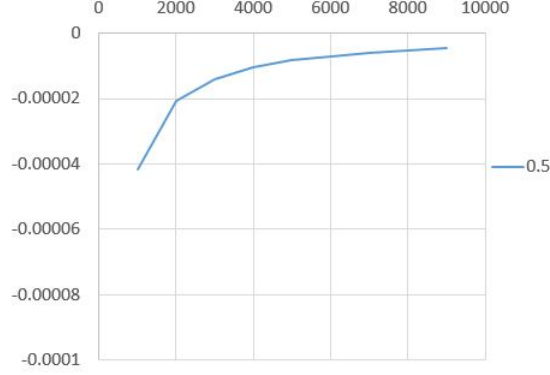


Figure 26: The angle $\Delta\varphi_\chi$ between the exact $\tilde{\chi}(s)$ and approximate $\hat{\chi}(s)$ value of the CHI function, $\sigma = 1/2$

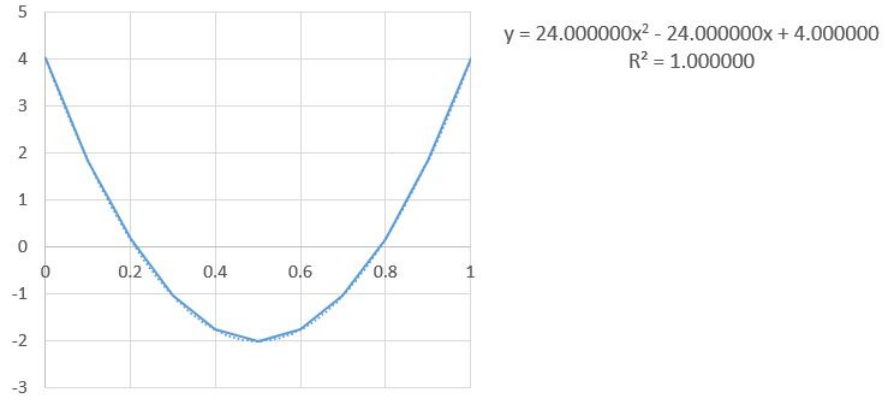


Figure 27: Factor $\lambda(\sigma)$ (from the real part of a complex number)

The coefficient of $\lambda(\sigma)$ shows which number to multiply a value of the argument of the remainder term $\mu(t)$ of the gamma function in the form of the Riemann-Gabcke to get a value of the argument of the remainder term $\tau(s)$ of CHI function.

We will find an explanation for this paradoxical identity in the further study of expressions that determine a value of the Riemann zeta function.

We obtained an exact expression for the angle α_1 of the first middle vector of the Riemann spiral:

$$\alpha_1 = t(\log \frac{t}{2\pi} - 1) - \frac{\pi}{4} + \lambda(\sigma)\mu(t); \quad (65)$$

As well as the exact expression for the CHI function:

$$\chi(s) = \left(\frac{t}{2\pi}\right)^{(\frac{1}{2}-\sigma)} e^{-i(t(\log \frac{t}{2\pi}-1)-\frac{\pi}{4}+\lambda(\sigma)\mu(t))}; \quad (66)$$

Now we can perform the exact construction of the inverse Riemann spiral.

2.6 Representation of the second approximate equation of the Riemann zeta function by a vector system

We write the second approximate equation of the Riemann zeta function [3] in vector form.

$$\zeta(s) = \sum_{n \leq x} \frac{1}{n^s} + \chi(s) \sum_{n \leq y} \frac{1}{n^{1-s}} + \mathcal{O}(x^{-\sigma}) + \mathcal{O}(|t|^{1/2-\sigma} y^{\sigma-1}); \quad (67)$$

$$0 < \sigma < 1; 2\pi xy = |t|; \quad (68)$$

$$\chi(s) = \frac{(2\pi)^s}{2\Gamma(s) \cos(\frac{\pi s}{2})} = 2^s \pi^{s-1} \sin(\frac{\pi s}{2}) \Gamma(1-s); \quad (69)$$

We use the exponential form of a complex number, then, using Euler's formula, go to the trigonometric form of a complex number and get the coordinates of the vectors. Put $x = y$, then for $m = \left\lceil \sqrt{\frac{t}{2\pi}} \right\rceil$ we get:

$$\zeta(s) = \sum_{n=1}^m X_n(s) + \sum_{n=1}^m Y_n(s) + R(s); \quad (70)$$

where

$$X_n(s) = \frac{1}{n^s} = \frac{1}{n^\sigma} e^{-it \log(n)} = \frac{1}{n^\sigma} (\cos(t \log(n)) - i \sin(t \log(n))); \quad (71)$$

$$Y_n(s) = \chi(s) \frac{1}{n^{1-s}} = \chi(s) \frac{1}{n^{1-\sigma}} e^{it \log(n)} = \chi(s) \frac{1}{n^{1-\sigma}} (\cos(t \log(n)) + i \sin(t \log(n))); \quad (72)$$

$R(s)$ - some function of the complex variable, which we will estimate later using the exact values of $\zeta(s)$ and $\chi(s)$.

The vector system (70) determines a value of $\zeta(s)$ at each interval:

$$t \in [2\pi m^2, 2\pi(m+1)^2); m = 1, 2, 3... \quad (73)$$

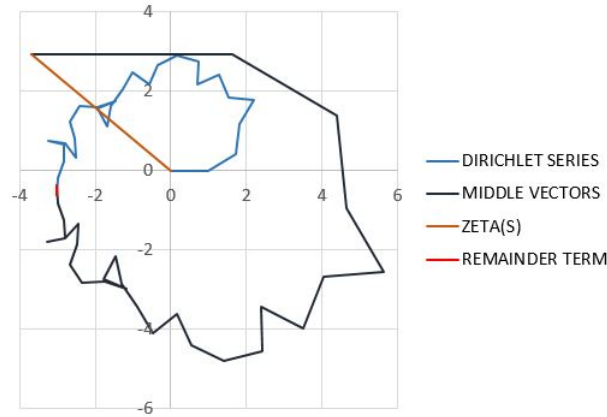


Figure 28: Finite vector system, $s = 0.25 + 5002.981i$

We see that the first sum (70) corresponds to the vectors of the Riemann spiral, and the second is the middle vector of the Riemann spiral.

Thus, we can explain the geometric meaning of the second approximate equation of the Riemann zeta function.

In the analysis of Riemann spiral we received the quantity of reverse points:

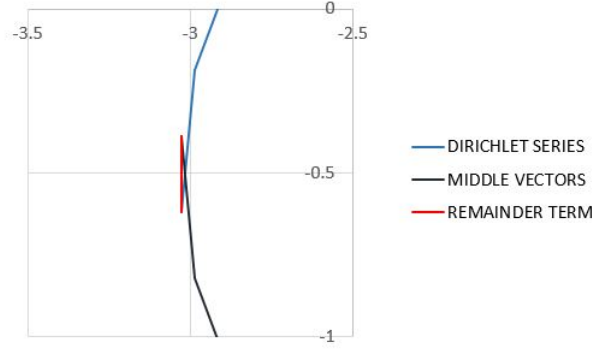
$$m = \sqrt{\frac{t}{2\pi} + \frac{1}{4}}$$

of the conditions that between two reverse points is at least one vector of the Riemann spiral.

If we look at the inverse Riemann spiral (fig. 20), we note that the number of reverse points, which corresponds to one side of the middle vectors of the Riemann spiral, and on the other hand, the vectors of value of the Riemann spiral, which had not yet twist in a convergent and then a divergent spiral.

If we remove the vectors that twist into spirals, we get the vector system of (fig. 28), which corresponds to the second approximate equation of the Riemann zeta function.

We can also explain the geometric meaning of the remainder term of the second approximate equation of the Riemann zeta function.

Figure 29: Gap of vector system, $s = 0.25 + 5002.981i$

As the scale of the picture of the vector system increases (fig. 28), we see a gap between the vectors and the middle vectors of the Riemann spiral (fig. 29), this gap is the remainder term of the second approximate equation of the Riemann zeta function.

2.7 The axis of symmetry of the vector system of the second approximate equation of the Riemann zeta function - conformal symmetry

In the process of geometric derivation of the functional equation of the Riemann zeta function we found that the angles (29) between the first middle vector of the Riemann spiral and any other middle vector are equal in modulus and opposite in sign to the angles between the first vector and appropriate vector of the Riemann spiral.

The same result (71) and (72) we obtained when writing the second approximate equation of the Riemann zeta function in vector form.

We show 1) that the angles between any two middle vectors Y_i and Y_j of the Riemann spiral are equal in modulus and opposite in sign, if we measure the angle from the respective vectors, to the angles between the corresponding vectors X_i and X_j of the Riemann spiral and 2) there is a line that has angles equaled modulus and opposite in sign, if we measure the angle from this line, with any pair of corresponding vectors Y_i and X_i of the Riemann spiral (Lemma 1).

Put in accordance with the first middle vector Y_1 , the two random middle vectors Y_i and Y_j of the Riemann spiral, the vector X_1 and two relevant vectors X_i and X_j of the Riemann spiral the segments A_1A_2 , A_2A_3 , A_3A_4 , $A'_1A'_2$, $A'_2A'_3$ and $A'_3A'_4$ respectively.

Consider (fig. 30) two polyline formed by vertices $A_1A_2A_3A_4$ and $A'_1A'_2A'_3A'_4$ respectively, and oriented arbitrarily. Then edges A_2A_3 and A_3A_4 have angles with the edge A_1A_2 is equal in modulus and opposite in sign to the angles, which have edge $A'_2A'_3$ and $A'_3A'_4$ respectively, with the edge $A'_1A'_2$, if we measure angles from the edges A_1A_2 and $A'_1A'_2$ respectively.

1) We show that the angle between edges A_2A_3 and A_3A_4 is equal in modulus and opposite in sign to the angle between the edges $A'_2A'_3$ and $A'_3A'_4$, if we measure the angle from the corresponding edges, for example, from A_3A_4 and $A'_3A'_4$.

A) Consider first (fig. 30) case when edges A_1A_2 , A_3A_4 and edges $A'_1A'_2$, $A'_3A'_4$ respectively are not parallel to each other.

Continue edges A_1A_2 , A_3A_4 and edges $A'_1A'_2$, $A'_3A'_4$ to the intersection, we obtain the triangles $A_2B_2A_3$ and $A'_2B'_2A'_3$ respectively (fig. 30).

These triangles are congruent by two angles, because the angles $A_1B_2A_4$ and $A'_1B'_2A'_4$ are equal in modulus, as the angle of the edges A_3A_4 and $A'_3A'_4$ with edges A_1A_2 and $A'_1A'_2$ respectively, and the angles $B_2A_2A_3$ and $B'_2A'_2A'_3$ are adjacent angles $A_1A_2A_3$ and $A'_1A'_2A'_3$ respectively which are also equal in modulus, as the angle of the edges A_2A_3 and $A'_2A'_3$ with edges A_1A_2 and $A'_1A'_2$ respectively.

Hence, the angles $A_2A_3A_4$ and $A'_2A'_3A'_4$ are equal in modulus as the angles adjacent to the angles $A_2A_3B_2$ and $A'_2A'_3B'_2$ respectively, which are equal as corresponding angles of congruent triangles.

B) Now consider (fig. 31) case when edges A_1A_2 , A_3A_4 and edges $A'_1A'_2$, $A'_3A'_4$ respectively parallel to each other.

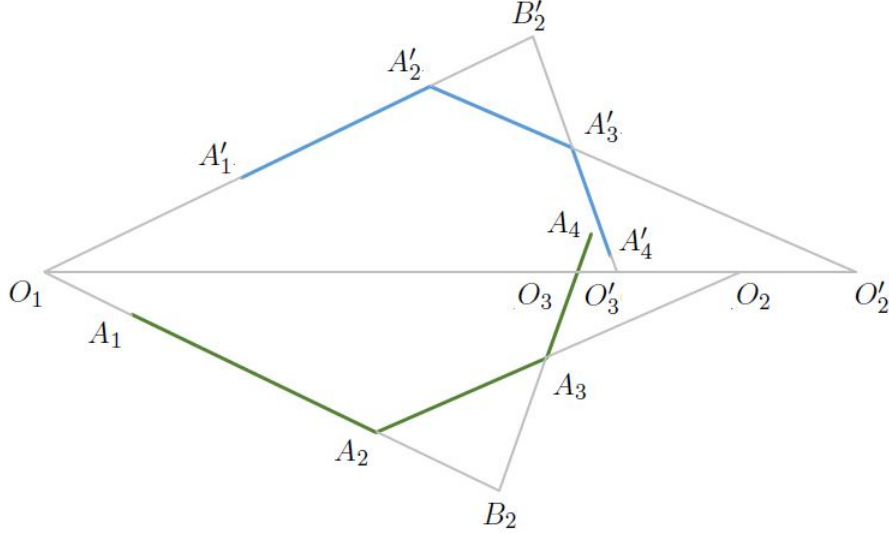


Figure 30: Polylines with equal angles

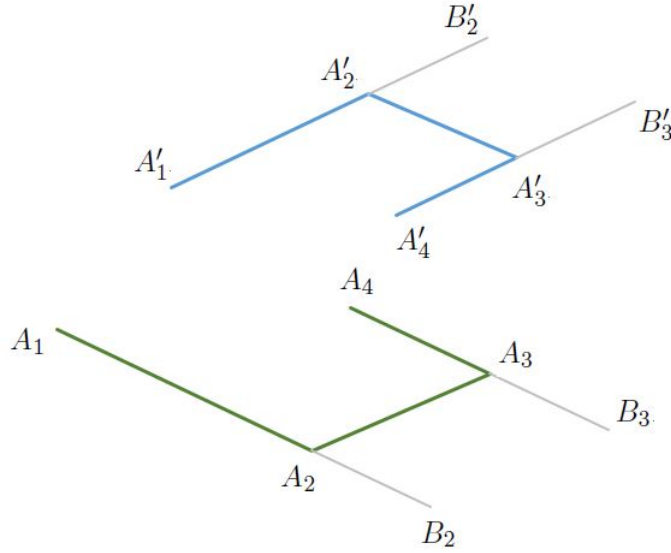


Figure 31: Polylines with equal angles, parallel edges

The continue of edges A_1A_2 , A_3A_4 and edges $A'_1A'_2$, $A'_3A'_4$ respectively do not intersect, because they form parallel lines A_1B_2 , A_4B_3 and $A'_1B'_2$, $A'_4B'_3$ respectively.

Thus edges A_2A_3 and $A'_2A'_3$ are intersecting lines of those parallel lines, respectively.

Hence, the angles $A_2A_3A_4$ and $A'_2A'_3A'_4$ are equal in modulus as corresponding angles at intersecting lines of two parallel lines because the angles $A_1A_2A_3$ and $A'_1A'_2A'_3$ are equal in modulus, as the angle of the edges A_2A_3 and $A'_2A'_3$ with edges A_1A_2 and $A'_1A'_2$ respectively.

If we measure the angle $A_2A_3A_4$ from edge A_3A_4 , it is necessary to count its anti-clockwise, then it has a positive sign.

If we measure the angle $A'_2A'_3A'_4$ from edge $A'_3A'_4$, it is necessary to count its clockwise, then it has a negative sign.

Therefore, the angle between the edges A_2A_3 and A_3A_4 equal in modulus and opposite in sign to the angle between the edges $A'_2A'_3$ and $A'_3A'_4$, if we measure the angle from the edges A_3A_4 and $A'_3A'_4$ respectively.

2) Now we continue edges A_1A_2 and $A'_1A'_2$ to the intersection and divide the angle $A_2O_1A'_2$ into two equal angles, we will get a line O_1O_3 , which has equal in modulus and opposite in sign angles, if we measure the angle from this line, to edges A_1A_2 and $A'_1A'_2$ (fig. 30).

We show that line O_1O_3 also is equal in modulus and opposite in sign to angles, if we measure the angle from this line, with edges A_2A_3 , A_3A_4 and $A'_2A'_3$, $A'_3A'_4$ respectively.

A) Consider first (fig. 30) case when edges A_2A_3 and $A'_2A'_3$ are not parallel to each other (sum of angles $A_2O_1O_3$, $A_1A_2A_3$ and $A'_2O_1O_3$, $A'_1A'_2A'_3$ is not equal to π).

Continue edges A_2A_3 , $A'_2A'_3$ to the intersection with the line O_1O_3 , we get the triangles $O_1A_2O_2$ and $O_1A'_2O'_2$ respectively.

These triangles are congruent by two angles, because the angles $A_2O_1O_3$ and $A'_2O_1O_3$ are equal in modulus by build, and the angles $A_1A_2A_3$ and $A'_1A'_2A'_3$ are equal in modulus, as the angle of the edges A_1A_2 and $A'_1A'_2$ with edges A_2A_3 and $A'_2A'_3$ respectively.

Hence, angles $A_2O_2O_1$ and $A'_2O'_2O_1$ are equal in modulus as the corresponding angles of the congruent triangles.

B) Now consider (fig. 32) case when edges A_2A_3 and $A'_2A'_3$ are parallel to each other (sum of angles $A_2O_1O_3$, $A_1A_2A_3$ and $A'_2O_1O_3$, $A'_1A'_2A'_3$ is equal to π).

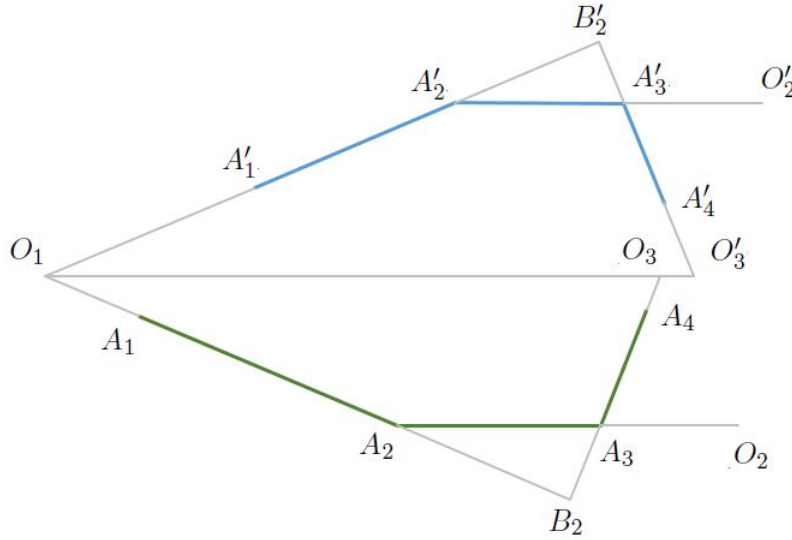


Figure 32: Polyline with equal angles, sum of angles π

In this case, lines O_1A_2 and $O_1A'_2$ are intersecting two parallel lines O_1O_3 , A_2O_2 and O_1O_3 , $A'_2O'_2$ respectively, since the angles $A_2O_1O_3$ and $A'_2O_1O_3$ are equal in modulus by build, and the angles $A_1A_2A_3$ and $A'_1A'_2A'_3$ are equal in modulus as the angle of the edges A_1A_2 and $A'_1A'_2$ with edges A_2A_3 and $A'_2A'_3$ respectively, and the sum of the respective angles at intersecting lines is equal to π .

Therefore, the angles between the line segments A_2A_3 and $A'_2A'_3$ and line O_1O_3 is equal to zero because A_2A_3 and $A'_2A'_3$ are parallel to line O_1O_3 .

Continue edges A_3A_4 , $A'_3A'_4$ to the intersection with the straight line O_1O_3 , get the triangles $O_1B_2O_3$ and $O_1B'_2O'_3$ respectively (fig. 30).

These triangles are congruent by two angles, because the angles $A_2O_1O_3$ and $A'_2O_1O_3$ are equal in modulus by build, and the angles $A_1B_2A_4$ and $A'_1B'_2A'_4$ are equal in modulus, as the angle of the edges A_1A_2 and $A'_1A'_2$ with edges A_3A_4 and $A'_3A'_4$ respectively.

Hence, angles $B_2O_3O_1$ and $B'_2O'_3O_1$ are equal in modulus as the corresponding angles of the congruent triangles.

If we measure the angles $A_2O_2O_1$ and $B_2O_3O_1$ from a line O_1O_3 , they need to count anti-clockwise, then either have a positive sign.

If we measure the angles $A'_2O'_2O_1$ and $B'_2O'_3O_1$ from a line O_1O_3 , they need to count clockwise, then either have a negative sign.

Therefore, line O_1O_3 has equal in modulus and opposite in sign angles, if we measure the angle from this line, with edges A_1A_2 , A_2A_3 , A_3A_4 and $A'_1A'_2$, $A'_2A'_3$, $A'_3A'_4$ respectively. \square

According to the Lemma 1, the vector system of the second approximate equation of the Riemann zeta function has a *special kind of symmetry* when there is a line that has angles equal in modulus and opposite in sign, if we measure its from this line, with any pair of corresponding vectors Y_i and X_i of the Riemann spiral.

It should be noted that this symmetry of angles is kept when $\sigma = 1/2$ when, as we will show later, the vector system of the second approximate equation of the Riemann zeta function has *mirror symmetry*.

To distinguish these two types of symmetry, we give a name to a special kind of symmetry of the vector system of the second approximate equation of the Riemann zeta function by analogy with the conformal transformation in which the angles are kept.

Conformal symmetry - a special kind of symmetry in which there is a line that has equal modulus and opposite sign angles, if we measure the angle from this line, with any pair of corresponding segments.

The angle $\hat{\varphi}_M$ of the axis of mirror symmetry is equal to the angle φ_M of the axis of conformal symmetry

$$\hat{\varphi}_M = \varphi_M = \frac{\text{Arg}(\chi(s))}{2} + \frac{\pi}{2}; \quad (74)$$

In other words, it is the same line if we draw the axis of conformal symmetry at the same distance from the end of the first middle vector Y_1 and from the end of the first vector X_1 of the Riemann spiral.

2.8 Mirror symmetry of the vector system of the second approximate equation of the Riemann zeta function

In 1932 Siegel published notes of Riemann [5] in which Riemann, unlike Hardy and Littlewood, represented the remainder term of the second approximate equation of the Riemann zeta function explicitly:

$$\zeta(s) = \sum_{l=1}^m l^{-s} + \frac{(2\pi)^s}{2\Gamma(s)\cos(\frac{\pi s}{2})} \sum_{l=1}^m l^{s-1} + (-1)^{m-1} \frac{(2\pi)^{\frac{s+1}{2}}}{\Gamma(s)} t^{\frac{s-1}{2}} e^{\frac{\pi i s}{2} - \frac{t i}{2} - \frac{\pi i}{8}} \mathcal{S}; \quad (75)$$

$$\mathcal{S} = \sum_{0 \leq 2r \leq k \leq n-1} \frac{2^{-k} i^{r-k} k!}{r!(k-2r)!} a_k F^{(k-2r)}(\delta) + \mathcal{O}\left(\left(\frac{3n}{t}\right)^{\frac{n}{6}}\right); \quad (76)$$

$$n \leq 2 \cdot 10^{-8} t; m = \left\lceil \sqrt{\frac{t}{2\pi}} \right\rceil; \delta = \sqrt{t} - \left(m + \frac{1}{2}\right) \sqrt{2\pi}; \quad (77)$$

$$F(u) = \frac{\cos(u^2 + \frac{3\pi}{8})}{\cos(\sqrt{2\pi}u)}; \quad (78)$$

We use an approximate expression (62) for the gamma function to write the expression for the remainder term of the second approximate equation of the Riemann zeta function in exponential form.

$$R(s) = (-1)^{m-1} \left(\frac{t}{2\pi}\right)^{-\frac{\sigma}{2}} e^{-i[\frac{t}{2}(\log \frac{t}{2\pi} - 1) - \frac{\pi}{8} + \mu(s)]} \mathcal{S}, \quad (79)$$

Given an estimate for the sum of \mathcal{S} , which can be found, for example, Titchmarsh [9]:

$$\mathcal{S} = \frac{\cos(\delta^2 + \frac{3\pi}{8})}{\cos(\sqrt{2\pi}\delta)} + \mathcal{O}(t^{-\frac{1}{2}}); \quad (80)$$

we can identify the expression for the argument of the remainder term of the second approximate equation of the Riemann zeta function:

$$\text{Arg}(R(s)) = -\left(\frac{t}{2}(\log \frac{t}{2\pi} - 1) - \frac{\pi}{8} + \mu(s)\right); \quad (81)$$

Taking into account the expression (63) for the argument of the remainder term of the gamma function when $\sigma = 1/2$, we obtain an expression for the argument of the remainder term of the second approximate equation of the Riemann zeta function on the critical line.

$$\text{Arg}(\hat{R}(s)) = -\left(\frac{t}{2}(\log \frac{t}{2\pi} - 1) - \frac{\pi}{8} + \mu(t)\right); \quad (82)$$

In the derivation of exact expressions for the CHI function, we found the expression (64), which shows that when $\sigma = 1/2$ value of the argument of remainder term $\tau(s)$ of CHI function is exactly twice the argument of the remainder term $\mu(t)$ of gamma functions (63) in the form of the Riemann-Gabcke.

$$\text{Arg}(\hat{\chi}(s)) = -(t(\log \frac{t}{2\pi} - 1) - \frac{\pi}{4} + 2\mu(t)); \quad (83)$$

Comparing the expression (82) for the argument, the remainder term of the second approximate equation of the Riemann zeta function of and the expression (83) for the argument CHI-function on the critical line, we find a fundamental property of the vector of the remainder term of the second approximate equation of the Riemann zeta function:

$$\text{Arg}(\hat{R}(s)) = \frac{\text{Agr}(\hat{\chi}(s))}{2}; \quad (84)$$

On the critical line, the argument of the remainder term of the second approximate equation of the Riemann zeta function is exactly half the argument of the CHI function.

Comparing (74) and (84) we see that when $\sigma = 1/2$, the vector of the remainder term $\hat{R}(s)$ is perpendicular to the axis of symmetry of the vector system of the second approximate equation of the zeta function of Riemann:

$$\text{Arg}(\hat{R}(s)) = \varphi_L; \quad (85)$$

As we will show later, this fact is fundamental in the existence of non-trivial zeros of the Riemann zeta function on the critical line.

When changing the imaginary part of a complex number, the vectors of the vector system of the second approximate equation of the Riemann zeta function can occupy an any position in the entire range of angles $[0, 2\pi]$, in consequence of which they form a polyline with self-intersections (fig. 28), which complicates the analysis of this vector system.

To obtain the polyline formed by the vectors X_n and the middle vectors of the Riemann spiral Y_n , without self-intersections, the vectors can be ordered by a value of the angle, then they will form a polyline, which has no intersections (fig. 33).

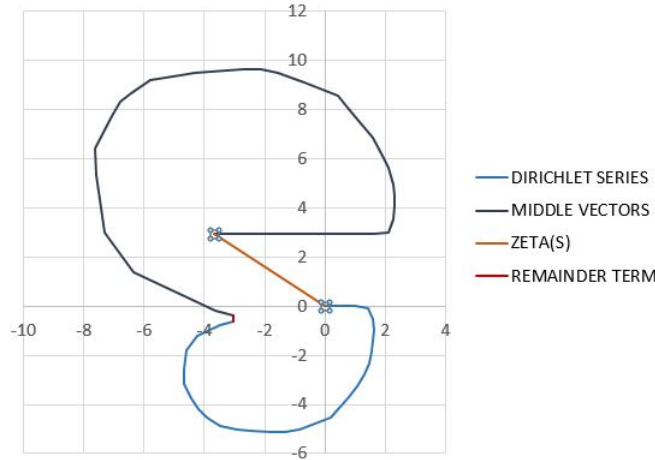


Figure 33: Permutation of vectors of the Riemann spiral vector system, $s = 0.25 + 5002.981i$

We determine the properties of the vector system of the second approximate equation of the Riemann zeta function in the permutation of vectors.

As it is known from analytical geometry, the sum of vectors conforms the permutation law, i.e. it does not change when the vectors are permuted.

Thus, the permutation of the vectors of the vector system of the second approximate equation of the Riemann zeta function does not affect a value of the Riemann zeta function.

Since conformal symmetry, by definition, depends only on angles and does not depend on the actual position of the segments, then the permutation of the vectors of the vector system of the second approximate equation of the Riemann

zeta function, conformal symmetry is kept because the angles between the lines formed by the vectors and axis of symmetry do not change.

While, for mirror symmetry, the permutation of vectors forms a new pair of vertices and it is necessary to determine that they are on the same line perpendicular to the axis of symmetry and at the same distance from the axis of symmetry.

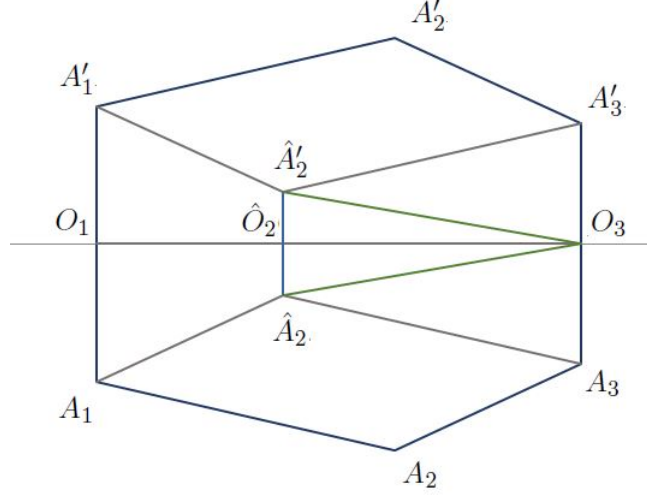


Figure 34: Permutation vectors, new pair of vertices

Consider (fig. 34) symmetrical polygon S_1 formed by the vertices $A_1 A_2 A_3 A'_3 A'_2 A'_1$.

The axis of symmetry $O_1 O_3$ divides segments $A'_1 A_1$, $A'_2 A_2$ and $A'_3 A_3$ into equal segments, because vertices A'_1 and A_1 , A'_2 and A_2 , A'_3 and A_3 is mirror symmetrical relative to the axis of symmetry $O_1 O_3$.

Change the edges $A'_1 A'_2$, $A'_2 A'_3$ and $A_1 A_2$, $A_2 A_3$ of their places, we get two new vertices \hat{A}'_2 and \hat{A}_2 .

We connect vertices \hat{A}'_2 , O_3 and \hat{A}_2 , O_3 , we get the triangles T'_1 and T_1 are formed respectively the vertices of $\hat{A}'_2 A'_3 O_3$ and $\hat{A}_2 A_3 O_3$.

We show that the triangles T'_1 and T_1 are equal.

Parallelograms $A'_1 A'_2 A'_3 \hat{A}'_2$ and $A_1 A_2 A_3 \hat{A}_2$ are equal by build, therefore, angles $A'_2 A'_3 \hat{A}'_2$ and $A_2 A_3 \hat{A}_2$ are equal;

In the source polygon S_1 , the angles $A'_2 A'_3 O_3$ and $A_2 A_3 O_3$ are equal, hence angles $\hat{A}'_2 A'_3 O_3$ and $\hat{A}_2 A_3 O_3$ are equal as the difference of equal angles;

Then the triangles T'_1 and T_2 are equal by the equality of the two edges $\hat{A}'_2 A'_3$, $\hat{A}_2 A_3$ and $A'_3 O_3$, $A_3 O_3$ and the angle between them $\hat{A}'_2 A'_3 O_3$ and $\hat{A}_2 A_3 O_3$;

Connect vertices \hat{A}'_2 and \hat{A}_2 , we get the intersection of \hat{O}_2 segments $\hat{A}'_2 \hat{A}_2$ and the axis of symmetry $O_1 O_3$.

The angles $\hat{A}'_2 O_3 A'_3$ and $\hat{A}_2 O_3 A_3$ are equal as the corresponding angles of equal triangles T'_1 and T_1 , hence angles $\hat{A}'_2 O_3 \hat{O}_2$ and $\hat{A}_2 O_3 \hat{O}_2$ are equal;

Then the triangle $\hat{A}'_2 O_3 \hat{A}_2$ is isosceles and the segment $\hat{O}_2 O_3$ is its height, because the bisector in an equilateral triangle is its height.

Therefore, the vertices \hat{A}'_2 and \hat{A}_2 lie on the line perpendicular to the axis of symmetry $O_1 O_3$ and they have the same distance from the axis of symmetry $O_1 O_3$.

Thus, when the corresponding edges of the symmetric polygon are permuted, the mirror symmetry is kept (Lemma 2). \square

Now we define the property of the vector system of the second approximate equation of the Riemann zeta function when $\sigma = 1/2$.

Consider (fig. 35) polygon, formed by the vertices $A_1A_2A_3A'_3A'_2A'_1$, whose edges $A'_1A'_2$, $A'_2A'_3$ and A_1A_2 , A_2A_3 are equal, have conformal symmetry with relation to the axis of symmetry O_1O_3 and vertices A'_1 and A_1 is mirror symmetrical relative to the axis of symmetry O_1O_3 .

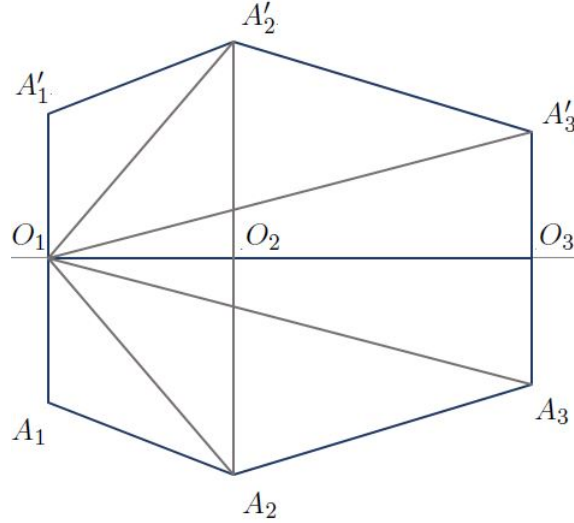


Figure 35: Equal vectors possessing conformal symmetry

We show that the vertices A'_2 , A'_3 and A_2 , A_3 respectively are mirror symmetric about the axis of symmetry O_1O_3 (Lemma 3).

The axis of symmetry O_1O_3 divides the segment A'_1A_1 into equal segments and segment A'_1A_1 is perpendicular to the axis of symmetry O_1O_3 .

The angles $A_1A_2A_3$ and $A'_1A'_2A'_3$ are equal by Lemma 1, since edges A_1A_2 , A_2A_3 and $A'_1A'_2$, $A'_2A'_3$ respectively have conformal symmetry.

Construct segments $O_1A'_2$, $O_1A'_3$ and O_1A_2 , O_1A_3 .

Triangles $O_1A'_1A'_2$ and $O_1A_1A_2$ are equal by the equality of the two sides $O_1A'_1$, $A'_1A'_2$ and O_1A_1 , A_1A_2 respectively and the angle between them $O_1A'_1A'_2$ and $O_1A_1A_2$.

The angles $O_1A'_2A'_3$ and $O_1A_2A_3$ are equal as parts of the equal angles $A'_1A'_2A'_3$ and $A_1A_2A_3$ since angles $A'_1A'_2O_1$ and $A_1A_2O_1$ are equal as the corresponding angles of equal triangles.

Triangles $O_1A'_2A'_3$ and $O_1A_2A_3$ are equal by the equality of the two sides $O_1A'_2$, $A'_2A'_3$ and O_1A_2 , A_2A_3 respectively and the angle between them $O_1A'_2A'_3$ and $O_1A_2A_3$.

The angles $O_3O_1A'_2$ and $O_3O_1A_2$ are equal as parts of the equal angles $A'_1O_1O_3$ and $A_1O_1O_3$ since angles $A'_1O_1A'_2$ and $A_1O_1A_2$ are equal as the corresponding angles of equal triangles.

The angles $O_3O_1A'_3$ and $O_3O_1A_3$ are equal as parts of the equal angles $A'_1O_1O_3$ and $A_1O_1O_3$ since angles $A'_1O_1A'_2$, $A_1O_1A_2$ and $A'_2O_1A'_3$, $A_2O_1A_3$ respectively are equal as the corresponding angles of equal triangles.

Triangles $A'_3O_1A_3$ and $A'_2O_1A_2$ are isosceles and segments O_1O_2 and O_1O_3 are respectively their height, hence the segments O_1O_2 and O_1O_3 divide segments A'_2A_2 and A'_3A_3 into equal parts and segments A'_2A_2 and A'_3A_3 are perpendicular to axis of symmetry O_1O_3 . \square

We construct a polyline formed by the vectors of the second approximate equation of the Riemann zeta function when $\sigma = 1/2$ (fig. 36).

In accordance with (71) and (72) for X_n and Y_n respectively all segments $A'_1A'_2$, $A'_2A'_3$, ..., $A'_{m-2}A'_{m-1}$, $A'_{m-1}A'_m$ and A_1A_2 , A_2A_3 , ..., $A_{m-2}A_{m-1}$, $A_{m-1}A_m$ when $\sigma = 1/2$ are equal.

We draw the axis of symmetry M of the vector system of the second approximate equation of the Riemann zeta function through the middle of the segment formed by the vector $\hat{R}(s)$ of the remainder term when $\sigma = 1/2$.

We obtain two mirror-symmetric vertices A'_m and A_m because when $\sigma = 1/2$ the vector $\hat{R}(s)$ of the remainder term is perpendicular to the axis of symmetry M of the vector system of the second approximate equation of the Riemann zeta function.

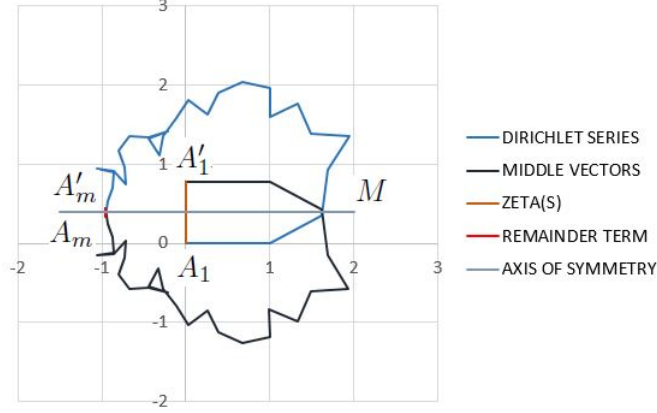


Figure 36: Mirror symmetry of the Riemann spiral vector system, $s = 0.5 + 5002.981i$

According to Lemma 3, the vector system of the second approximate equation of the Riemann zeta function when $\sigma = 1/2$ has mirror symmetry⁶.

Corollary 1. The vector $A'_1 A_1$ corresponds to the vector of a value of the Riemann zeta function when $\sigma = 1/2$, therefore, when $\sigma = 1/2$, the argument of the Riemann zeta function up to the sign corresponds to the direction of the normal L to the axis of symmetry of the vector system of the second approximate equation of the Riemann zeta function.

Corollary 2. Consider the projection of the vector system of the second approximate equation of the Riemann zeta function when $\sigma = 1/2$ on the axis of symmetry M of this vector system (fig. 36).

Segments $A'_1 A_1$ and $A'_m A_m$ is perpendicular to the axis of symmetry of M , hence, their projection on axis of symmetry M equal to zero.

The projections of the vectors X_n and Y_n on the axis of symmetry M are equal in modulus and opposite sign, hence

$$\left(\sum_{n=1}^m X_n\right)_M + \left(\sum_{n=1}^m Y_n\right)_M = 0; \quad (86)$$

Therefore

$$\left(\sum_{n=1}^m X_n\right)_M + \left(\sum_{n=1}^m Y_n\right)_M + \hat{R}(s)_M = 0; \quad (87)$$

and

$$\hat{\zeta}(s)_M = 0; \quad (88)$$

Corollary 3. Consider the projection of the vector system of the second approximate equation of the Riemann zeta function when $\sigma = 1/2$ on the normal L to the axis of symmetry M of this vector system (fig. 36).

According to the rules of vector summation

$$\hat{\zeta}(s) = \hat{\zeta}(s)_L = \left(\sum_{n=1}^m X_n\right)_L + \left(\sum_{n=1}^m Y_n\right)_L + \hat{R}(s)_L; \quad (89)$$

This expression, as we will show later, called the Riemann-Siegel formula, is used to find the non-trivial zeros of the Riemann zeta function on the critical line.

⁶We later show that the mirror symmetry of the vector system of the second approximate equation of the Riemann zeta function is also determined by the argument of the Riemann zeta function when $\sigma = 1/2$.

It should be noted that, while, vector X_1 remains fixed relative to the axes $x = Re(s)$ and $y = Im(s)$, relative to the normal of L to the axis of symmetry and the axis of symmetry M of the vector system of the second approximate equation of the Riemann zeta function vectors X_n and Y_n are rotated, in accordance with (71) and (72) towards each other with equal speeds and the angles of the vector of the remainder term $R(s)$ remains fixed when $\sigma = 1/2$.

This rotation of the vectors X_n and Y_n leads to the cyclic behavior of the projection $\hat{\zeta}(s)_L$ of the Riemann zeta function on the normal L to the axis of symmetry of the vector system of the second approximate equation of the Riemann zeta function on the critical line, i.e. $\hat{\zeta}(s)_L = \zeta(1/2 + it)_L$ alternately takes the maximum positive and maximum negative value, therefore, $\hat{\zeta}(s)_L$ cyclically takes a value of zero.

Projections $\zeta(s)_L$ and $\zeta(s)_M$ of the Riemann zeta function respectively on the normal L to the axis of symmetry and on the axis of symmetry M of the vector system of the second approximate equation of the Riemann zeta function in the critical strip when $\sigma \neq 1/2$ have the same cyclic behavior, i.e. $\zeta(s)_L$ and $\zeta(s)_M$ alternately take the maximum positive and maximum negative value, hence $\zeta(s)_L$ and $\zeta(s)_M$ is cyclically takes a value of zero, and, as we will show later, if $\zeta(s)_L$ or $\zeta(s)_M$ are set to zero for any value of $\sigma + it$, then they take a value of zero for value $1 - \sigma + it$ also.

2.9 Non-trivial zeros of the Riemann zeta function

Using the vector equation of the Riemann zeta function (70), we can obtain the vector equation of the non-trivial zeros of the Riemann zeta function.

$$\sum_{n=1}^m X_n(s) + \sum_{n=1}^m Y_n(s) + R(s) = 0; \quad (90)$$

Denote the sums of vectors X_n and Y_n :

$$L_1 = \sum_{n=1}^m X_n(s); L_2 = \sum_{n=1}^m Y_n(s); \quad (91)$$

The vectors L_1 and L_2 are invariants of the vector system of the second approximate equation of the Riemann zeta function, since they do not depend on the order of the vectors X_n and Y_n , nor on their quantity.

We can now determine the geometric condition of the non-trivial zeros of the Riemann zeta function:

$$L_1 + L_2 + R = 0; \quad (92)$$

This condition means that when the Riemann zeta function takes a value of non-trivial zero when $\sigma = 1/2$, the vectors L_1 , L_2 and R form an *isosceles* triangle, because when $\sigma = 1/2$ $|L_1| = |L_2|$, and when $\sigma \neq 1/2$, if the Riemann zeta function takes a value of non-trivial zero, these vectors must form a triangle of *general form*, because when $\sigma \neq 1/2$ $|L_1| \neq |L_2|$.

According to Hardy's theorem [2], the Riemann zeta function has an infinite number of zeros when $\sigma = 1/2$.

This fact is confirmed by the projection values $\hat{\zeta}(s)_L$ and $\hat{\zeta}(s)_M$ of the Riemann zeta function respectively on the normal L to the axis of symmetry and on the axis of symmetry M of the vector system of the second approximate equation of the Riemann zeta function on the critical line.

The Riemann zeta function takes a value of non-trivial zero when $\sigma = 1/2$ every time when the projection $\hat{\zeta}(s)_L$ takes a value of zero, because the projection $\hat{\zeta}(s)_M$ when $\sigma = 1/2$, according to the mirror symmetry of the vector system of the second approximate equation of the Riemann zeta function on the critical line are equal to zero identically.

Geometric meaning of non-trivial zeros of the Riemann zeta function means that when the Riemann zeta function takes a value of non-trivial zero when $\sigma = 1/2$, the vector system of the second approximate equation of the Riemann zeta function, as a consequence of the mirror symmetry of this vector system on the critical line, in accordance with Lemma 3, forms a symmetric polygon, since the sum of the vectors forming the polygon is equal to zero.

Using the vector system of the second approximate equation of the Riemann zeta function, we can also explain the geometric meaning of the Riemann-Siegel function [5, 8, 9], which is used to compute the non-trivial zeros of the Riemann zeta function on the critical line:

$$Z(t) = e^{\theta i} \zeta\left(\frac{1}{2} + it\right); \quad (93)$$

where

$$e^{\theta i} = \left(\chi\left(\frac{1}{2} + it\right)\right)^{\frac{1}{2}}; \quad (94)$$

According to the rules of multiplication of complex numbers, the Riemann-Siegel function determines the projection $\hat{\zeta}(s)_L$ of the Riemann zeta function on the normal L to the axis of symmetry of the vector system of the second approximate equation of the Riemann zeta function, since

$$\theta = \frac{\text{Arg}(\chi(\frac{1}{2} + it))}{2} = \varphi_L; \quad (95)$$

Which corresponds to the results of our research, i.e. $\hat{\zeta}(s) = \hat{\zeta}(s)_L$, since when $\sigma = 1/2$ in accordance with the mirror symmetry of the vector system of the second approximate equation of the Riemann zeta function on the critical line $\hat{\zeta}(s)_M = 0$.

In conclusion of the research of the vector system of the second approximate equation of the Riemann zeta function, we establish another fundamental fact.

The first middle vector Y_1 of the Riemann spiral rotates relative to the axes $x = \text{Re}(s)$ and $y = \text{Im}(s)$ around a fixed first vector X_1 of the Riemann spiral, and in accordance with the argument of the CHI function (36) does $N(t)$ complete rotations:

$$N(t) = \frac{|\text{Arg}(\chi(s))|}{2\pi}; \quad (96)$$

Later we show that when $\sigma = 1/2$ the first middle vector Y_1 of the Riemann spiral passes through the zero of the complex plane average once for each complete rotation ⁷ since, in accordance with the mirror symmetry of the vector system of the second approximate equation of the Riemann zeta function on the critical line, the end of first middle vector Y_1 makes reciprocating motions along the normal L to the axis of symmetry of this vector system, since this normal passes through the end of the first vector X_1 of the Riemann spiral, which is at the zero of the complex plane.

Thus, we can determine the number of non-trivial zeros of the Riemann zeta function on the critical line (as opposed to the Riemann-von Mangoldt formula, which determines the number of non-trivial zeros of the Riemann zeta function in the critical strip) via the number of complete rotations of the first middle vector Y_1 of the Riemann spiral:

$$N_0(t) = \left\lceil \frac{|\text{Arg}(\chi(s)) - \alpha_2|}{2\pi} \right\rceil + 2; \quad (97)$$

where α_2 argument to the second base point ⁸ of the first middle vector Y_1 of the Riemann spiral.

3 Variants of confirmation of the Riemann hypothesis

Before proceeding to the variants of confirmation of the Riemann hypothesis based on the analysis of the vector system of the second approximate equation of the Riemann zeta function, we consider two traditional approaches.

The authors of the first approach estimate the proportion of non-trivial zeros k and the proportion of simple zeros k^* on the critical line compared to $N(T)$ the number of non-trivial zeros of the Riemann zeta function in the critical strip.

$$k = \lim_{T \rightarrow \infty} \inf \frac{N_0(T)}{N(T)}; \quad (98)$$

$$k^* = \lim_{T \rightarrow \infty} \inf \frac{N_{0s}(T)}{N(T)}; \quad (99)$$

In the critical strip $N(T)$, the number of non-trivial zeros of the Riemann zeta function is determined by the Riemann-von Mangoldt formula [9]:

$$N(T) = \frac{T}{2\pi} (\log \frac{T}{2\pi} - 1) + \frac{7}{8} + S(T) + \mathcal{O}(\frac{1}{T}); \quad (100)$$

$$S(T) = \frac{1}{\pi} \text{Arg}(\zeta(\frac{1}{2} + iT)) = \mathcal{O}(\log T), T \rightarrow \infty; \quad (101)$$

⁷The research of the vector system of the second approximate equation of the Riemann zeta function on the critical line shows that if the first middle vector Y_1 of the Riemann spiral for any complete rotation around the fixed first vector X_1 of the Riemann spiral never passes through the zero of the complex plane, then for another complete rotation it passes through the zero value of the complex plane twice.

⁸base point is a value of a complex variable in which the first middle vector Y_1 occupies the position opposite to the first vector X_1 of the Riemann spiral.

This expression [15] is used to determine the proportion of non-trivial zeros k and the proportion of simple zeros k^* on the critical line:

$$k \geq 1 - \frac{1}{R} \log \left(\frac{1}{T} \int_1^T |V\psi(\sigma_0 + it)|^2 dt \right) + o(1); \quad (102)$$

$$k^* \geq 1 - \frac{1}{R} \log \left(\frac{1}{T} \int_2^T |V\psi(\sigma_0 + it)|^2 dt \right) + o(1); \quad (103)$$

where $V(s)$ is some function whose number of zeros is the same as the number of zeros $\zeta(s)$ in a contour bounded by a rectangle (i. e. not on the critical line):

$$\frac{1}{2} < \sigma < 1; 0 < t < T; \quad (104)$$

$\psi(s)$ some „mollifier“ function that has no zeros and compensates for the change of $|V(s)|$.

R is some positive real number

and

$$\sigma_0 = \frac{1}{2} - \frac{R}{\log T}; \quad (105)$$

In recent papers [15, 16] the function $V(s)$ is used in the form of Levenson [7].

$$V(s) = Q\left(-\frac{1}{\log T} \frac{d}{dt}\right)\zeta(s); \quad (106)$$

where $Q(x)$ is a real polynomial with $Q(0) = 1$ and $Q'(x) = Q'(1 - x)$.

In this approach, the authors use different kinds of polynomials $Q(x)$, „mollifier“ functions $\psi(s)$, as well as different methods of approximation and evaluation of the integral

$$\int_1^T |V\psi(\sigma_0 + it)|^2 dt; \quad (107)$$

In the paper [15] in 2011 it is proved that

$$k \geq .4105; k^* \geq .4058 \quad (108)$$

In the parallel paper [16] also in 2011 it is proved that

$$k \geq .4128; \quad (109)$$

To understand the dynamics of the results in this direction, we compare them with the paper [10] in which in 1989.

$$k \geq .4088; k^* \geq .4013 \quad (110)$$

The complexity of this approach lies in the fact that different methods of approximation of the integral (107) allow to obtain an insufficiently accurate result.

We hope, the authors of [20] in 2019 found a way to accurately determine the number of non-trivial zeros in the critical strip and on the critical line, because they claim to have obtained the result $k = 1$.

The second traditional direction of confirmation of the Riemann hypothesis is connected with direct verification of non-trivial zeros of the Riemann zeta function.

As we have already mentioned, the Riemann-Siegel formula (93) is used for this.

One of the recent papers [12], which besides computing 10^{13} of the first non-trivial zeros of the Riemann zeta function on the critical line offers a statistical analysis of these zeros and an improved approximation method of the Riemann-Siegel formula, was published in 2004.

The complexity of this approach lies in the fact that it is impossible to calculate all the non-trivial zeros of the Riemann zeta function, therefore, by this method of confirmation the Riemann hypothesis it can be refuted rather than confirm.

It should be noted that there is a contradiction between the results of the first and second method of confirmation of the Riemann hypothesis.

The determination of the proportion of non-trivial zeros on the critical line is in no way related to *the specific interval* of the imaginary part of a complex number, the authors of the first approach do not try to show that there is a sufficiently large interval where the Riemann hypothesis is true in accordance with the second method of confirmation the Riemann Hypothesis.

In other words, by determining the proportion of non-trivial zeros of the Riemann zeta function on the critical line, the authors of the first direction of confirmation of the Riemann hypothesis *indirectly indicate that part of the non-trivial zeros of the Riemann zeta function lies not on the critical line at any interval*, i.e. even where these zeros are already verified by the second method.

The site [21] collects some unsuccessful attempts to prove the Riemann hypothesis, some of them are given with a detailed error analysis.

In his presentation, Peter Sarnak [19], in the course of analyzing the different approaches to proving the Riemann hypothesis, mentions that about three papers a week are submitted for consideration annually.

However, the situation with the proof of the Riemann hypothesis remains uncertain and we tend to agree with Pete Clark [14]:

So far as I know, there is no approach to the Riemann Hypothesis which has been fleshed out far enough to get an even moderately skeptical expert to back it, with any odds whatsoever. I think this situation should be contrasted with that of Fermat's Last Theorem [FLT]: a lot of number theorists, had they known in say 1990 that Wiles was working on FLT via Taniyama-Shimura, would have found that plausible and encouraging.

Based on the research results described in the second section of our paper, we propose several new approaches to confirm the Riemann hypothesis based on the properties of the vector system of the second approximate equation of the Riemann zeta function:

- 1) the first method is based on determining the exact number (97) of non-trivial zeros of the Riemann zeta function on the critical line;
- 2) the second method of confirmation of the Riemann hypothesis is based on the analysis of projections $\zeta(s)_L$ and $\zeta(s)_M$ of the Riemann zeta function respectively on the normal L to the axis of symmetry and on the axis of symmetry M of the vector system of the second approximate equation of the Riemann zeta function in the critical strip;
- 3) the third method is based on the vector condition (92) of non-trivial zeros of the Riemann zeta function.

Determining the exact number (97) of non-trivial zeros of the Riemann zeta function on the critical line is based on several facts:

- 1) the vector system of the second approximate equation of the Riemann zeta function when $\sigma = 1/2$ has mirror symmetry (88);
- 2) the vector system of the second approximate equation of the Riemann zeta function rotates around the end of the first vector X_1 of the Riemann spiral (74) in a fixed coordinate system of the complex plane;
- 3) vectors X_n and the middle vectors Y_n of the Riemann spirals rotate in opposite directions (71) and (72) in the moving coordinate system formed by a normal L to the axis of symmetry and axis of symmetry M of the vector system of the second approximate equation of the Riemann zeta function.

The first middle vector Y_1 of the Riemann spiral rotates with the vector system of the second approximate equation of the Riemann zeta function around the end of the first vector X_1 of the Riemann spiral (74) in the fixed coordinate system of the complex plane, so the first middle vector Y_1 of the Riemann spiral, in accordance with (36), periodically passes *base point* where it takes a position opposite to the first vector X_1 of the Riemann spiral:

$$\text{Arg}(\chi(\frac{1}{2} + it_k)) = (2k - 1)\pi; \quad (111)$$

The argument of *the base points* of the first middle vector Y_1 of the Riemann spiral differs from the argument of the Gram points [1] by $\pi/2$:

$$\theta = \frac{\text{Arg}(\chi(\frac{1}{2} + it_n))}{2} = (n - 1)\pi; \quad (112)$$

We consider that the complete rotation of the first middle vector Y_1 of the Riemann spiral is the rotation from any base point to the next base point.

In accordance with the mirror symmetry of the vector system of the second approximate equation of the Riemann zeta function when $\sigma = 1/2$, at the base points the end of the first middle vector Y_1 of the Riemann spiral is on the

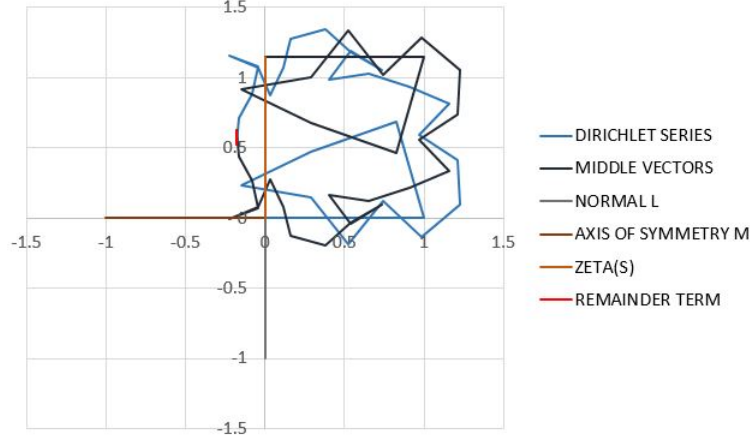


Figure 37: Base point #4520, the first middle vector is above the real axis, $s = 0.5 + 5001.099505i$

imaginary axis of the complex plane, so the vector can occupy one of two positions above (fig. 37) or bottom (fig. 38) of the real axis of the complex plane.

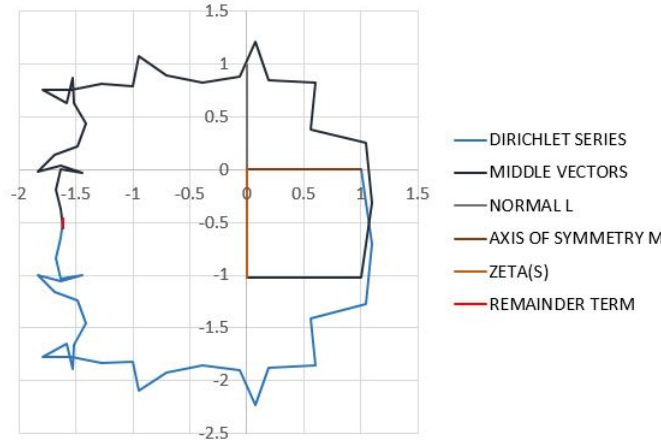


Figure 38: Base point #4525, the first middle vector is below the real axis, $s = 0.5 + 5005.8024855i$

Since the vectors X_n and the middle vectors Y_n of the Riemann spiral rotate in opposite directions (71, 72) in the moving coordinate system formed by the normal L to the axis of symmetry M of the vector system of the second approximate equation of the Riemann zeta function, in the fixed coordinate system of the complex plane, the first middle vector Y_1 of the Riemann spiral, when it is below the real axis of the complex plane, rotates towards the first vector X_1 Riemann Spirals and opposite when the first middle vector Y_1 of the Riemann spiral is on top of the real axis of the complex plane, it rotates away from the first vector X_1 of the Riemann spiral.

If the first middle vector Y_1 of the Riemann spiral at the base point rotates towards the first vector X_1 of the Riemann spiral, then, in accordance with the mirror symmetry of the vector system of the second approximate equation of the Riemann zeta function when $\sigma = 1/2$, until the rotation of the first middle vector Y_1 of the Riemann spiral is completed, the axis of symmetry M of this vector system crosses the zero of the complex plane (fig. 39).

Conversely, if the first middle vector Y_1 of the Riemann spiral at the base point rotates away from the first vector X_1 of the Riemann spiral, then from the beginning of the rotation of the first middle vector Y_1 of the Riemann spiral, the axis of symmetry M of this vector system has already crossed the zero of the complex plane (fig. 40).

In the result of the mirror symmetry of the vector system of the second approximate equation of the Riemann zeta function, when the axis of symmetry M of this vector system crosses the zero of the complex plane, the end of the first middle vector Y_1 of the Riemann spiral also crosses the zero of the complex plane, so the vector system of the second approximate equation of the Riemann zeta function at this point forms a closed polyline.

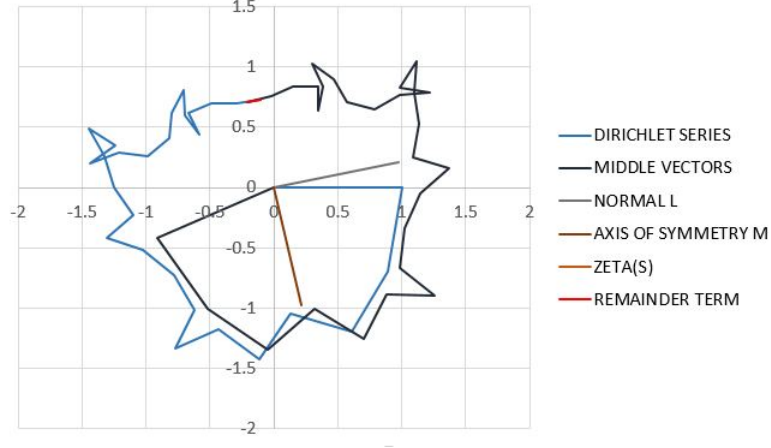


Figure 39: Non-trivial zero of the Riemann zeta function #4525, after the base point, $s = 0.5 + 5006.208381106i$

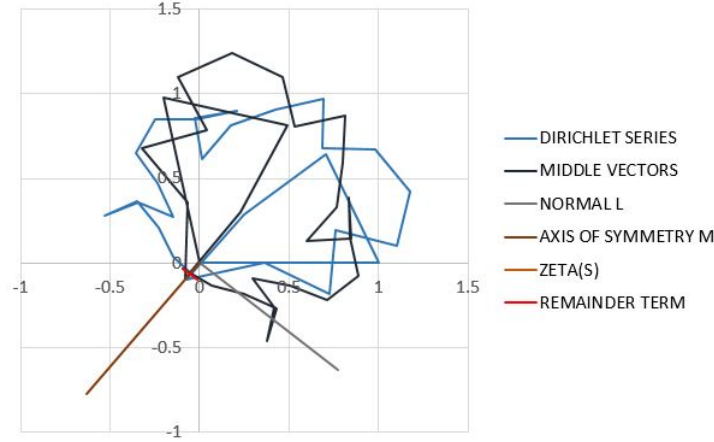


Figure 40: Non-trivial zero of the Riemann zeta function #4520, up to the base point, $s = 0.5 + 5000.834381i$

It is known from analytical geometry that the sum of vectors forming a closed polyline is equal to zero.

Therefore, when the first middle vector Y_1 of the Riemann spiral is at the base point, we can be sure that either before that point or after that point the Riemann zeta function takes a value of non-trivial zero.

This fact allows us to conclude that one non-trivial zero of the Riemann zeta function corresponds to one complete rotation of the first middle Y_1 vector of the Riemann spiral.

In accordance with of different combinations of the location of the first middle vector Y_1 of the Riemann spiral relative to the real axis of the complex plane at adjacent base points, there may be a different number of non-trivial zeros of the Riemann zeta function in the intervals between the base points:

- a) one non-trivial zero if the first middle vector Y_1 of the Riemann spiral occupies the same positions at two serial base points;
- b) two zeros if at the first base point the first middle vector Y_1 of the Riemann spiral is below and at the next base point is above the real axis of the complex plane;
- c) no zero, if, on the contrary, at the first base point the first middle vector Y_1 of the Riemann spiral is above, and at the next base point, is below the real axis of the complex plane.

Denote the types of base points:

a_1 - if the first middle vector Y_1 of the Riemann spiral occupies a position above⁹ the real axis of the complex plane;
 a_2 - if the first middle vector Y_1 of the Riemann spiral occupies the position below the real axis of the complex plane.
 Then we can define a sequence of base points of the same types, which correspond to the first type of interval, which has one non-trivial zero:

$$\begin{aligned} A_1 &= a_1 a_1; \\ A_2 &= a_2 a_2; \end{aligned}$$

and sequence base points with different types, which correspond to the second and third interval type, respectively:

$$\begin{aligned} B &= a_2 a_1; \\ C &= a_1 a_2; \end{aligned}$$

It is obvious that the sequence A_1 and A_2 can't follow each other, because

$$a_1 a_1 a_2 a_2 = A_1 C A_2$$

or

$$a_2 a_2 a_1 a_1 = A_2 B A_1$$

It is also clear that each other can not follow the sequence B , since

$$a_2 a_1 a_2 a_1 = B C$$

and each other can not follow sequence C , since

$$a_1 a_2 a_1 a_2 = C B C$$

Therefore, if at some interval between two base points of the Zeta-function of Riemann has no non-trivial zeros, i.e. is the interval of type C , then at another interval the Zeta-function of Riemann will have two non-trivial zero, it is the interval of type B , since these intervals appear every time when the type of base point changed, such as

$$a_1 a_2 a_1 = C B$$

or more long chain

$$a_1 a_2 a_2 a_2 a_1 a_1 a_1 a_1 a_1 a_2 a_2 a_1 = C A_2 A_2 B A_1 A_1 A_1 C A_2 B$$

Thus, the total number of non-trivial zeros of the Riemann zeta function at critical line always corresponds to the number of base points or the number of complete rotations of the first middle Y_1 vector of the Riemann spiral around the end of the first vector X_1 of the Riemann spiral in the fixed coordinate system of the complex plane.

We used this property to obtain the expression (97) the number of non-trivial zeros of the Riemann zeta function on the critical line through the angle of the first middle vector Y_1 of the Riemann spiral.

We substitute the exact expression (83) argument CHI functions in (97):

$$N_0(T) = \left\lceil \left| \frac{T}{2\pi} \left(\log \frac{T}{2\pi} - 1 \right) - \frac{1}{8} + \frac{2\mu(T) - \alpha_2}{2\pi} \right| \right\rceil + 2; \quad (113)$$

where $\mu(T)$ is the remainder term of the gamma function (63) when $\sigma = 1/2$;

α_2 argument of the CHI function at the second base point.

Comparing the expression for the number of non-trivial zeros in the critical strip (100) and the expression for the number of non-trivial zeros on the critical line (113), we see that these values „match“.

We are in a paradoxical situation where we know the exact number of zeros on the critical line, because $\mu(T) \rightarrow 0$ at $T \rightarrow \infty$ and do not know the exact number of zeros in the critical strip, because in the most optimistic estimate [17]:

$$|S(T)| < 1.998 + 0.17 \log(T); T > e; \quad (114)$$

⁹If the Riemann zeta function can take a value of non-trivial zero at the base point, then the first middle vector Y_1 will occupy the position of the first vector X_1 of the Riemann spiral (we will not consider this state in detail), we assume that this position belongs to the base point type a_1 .

Thus, based on the last estimate (114) of the remainder term of the Riemann-von Mangoldt formula, we can say that „almost all“ non-trivial zeros of the Riemann zeta function lie on the critical line.

It should be noted that for the final solution of the problem by this method it is not enough to show that

$$|S(T)| < \mathcal{O}\left(\frac{\log(T)}{\log \log(T)}\right); T \rightarrow \infty; \quad (115)$$

Although that this result was obtained by Littlewood [4] provided that the Riemann hypothesis is true, since the expression $(2\mu(T) - \alpha_2)/2\pi$ has a limit at $T \rightarrow \infty$, and the expression $\log(T)/\log \log(T)$ has no such limit, although it grows very slowly.

In other words, by comparing the number of non-trivial zeros of the Riemann zeta function in the critical strip and on the critical line, it is almost impossible to confirm the Riemann hypothesis.

Using the method of analyzing the vector system of the second approximate equation of the Riemann zeta function, we can offer a confirmation of the Riemann hypothesis *from the contrary*.

This approach is to show that Riemann zeta functions *cannot have non-trivial zeros* when $\sigma \neq 1/2$.

This problem is solved in different ways by the second and third methods of confirmation of the Riemann hypothesis, based on the properties of the vector system of the second approximate equation of the Riemann zeta function.

We have already considered the dynamics of the first middle vector Y_1 of the Riemann spiral at the base points when $\sigma = 1/2$, now consider the dynamics of the first middle vector Y_1 of the Riemann spiral at the base points when $\sigma \neq 1/2$.

In accordance with (65) base point when $\sigma \neq 1/2$ are in the neighborhood $\epsilon = \mathcal{O}(t^{-1})$ points when $\sigma = 1/2$, i.e. they have practically the same value at $t \rightarrow \infty$.

Therefore, at the base points when $\sigma \neq 1/2$ the first middle vector Y_1 of the Riemann spiral occupies a position opposite to the first vector X_1 of the Riemann spiral, while, in accordance with the violation of the mirror symmetry of the vector system of the second approximate equation of the Riemann zeta function, the end of the first middle vector Y_1 of the Riemann spiral *cannot be* on the imaginary axis of the complex plane.

Therefore, when $\sigma < 1/2$, the end of the first middle vector Y_1 of the Riemann spiral is on the left (fig. 41), when $\sigma > 1/2$ it is on the right (fig. 42) from the imaginary axis of the complex plane, regardless of the position relative to the real axis of the complex plane.

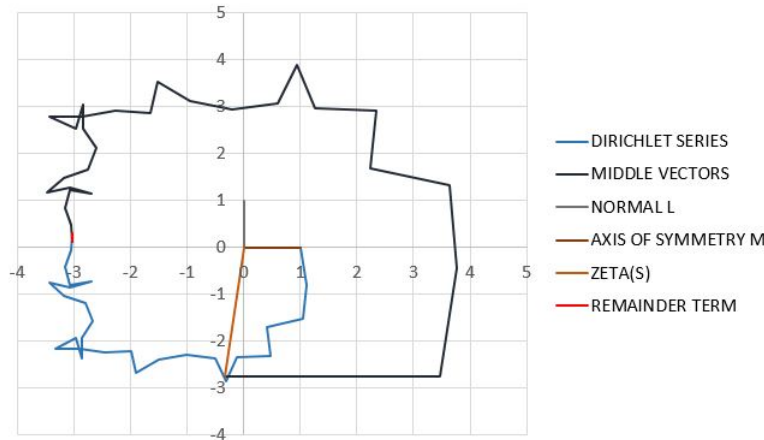


Figure 41: Base point #4525, the first middle vector of the Riemann spiral is on the left, $s = 0.35 + 5005.8024855i$

It is easy to notice that at the base point of the vector values of the Riemann zeta function at values $\sigma + it$ and $1 - \sigma + it$ deviate from the normal L to the axis of symmetry of the vector system of the second approximate equation in different directions at *the same angle* (fig. 43).

This behavior of vectors of values of the Riemann zeta function for values of the complex variable symmetric about the critical line can be easily explained by the arithmetic of arguments of a complex numbers at the base point.

$$\text{Arg}(\zeta(s))_B = \text{Arg}(\chi(s))_B + \text{Arg}(\zeta(1-s))_B \quad (116)$$

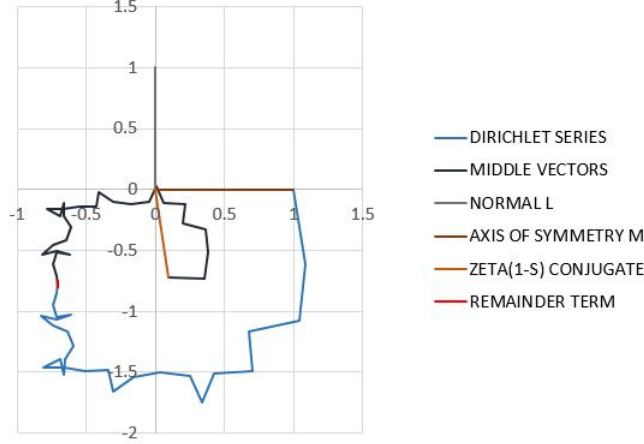


Figure 42: Base point #4525, the first middle vector of the Riemann spiral is on the right, $s = 0.65 + 5005.8024855i$

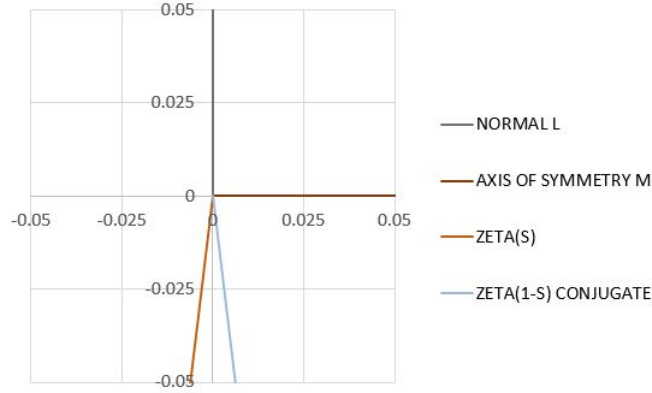


Figure 43: The deviation of the vector of values of the Riemann zeta function in the base point #4525, when $\sigma = 0.35$ and $\sigma = 0.65$

At the base point

$$\text{Arg}(\chi(s))_B = \pi; \quad (117)$$

since

$$\zeta(1 - \sigma + it) = \zeta(\overline{1 - \sigma - it}) = \zeta(\overline{1 - s}) = \overline{\zeta(1 - s)}; \quad (118)$$

$$\text{Arg}(\zeta(1 - s)) = -\text{Arg}(\overline{\zeta(1 - s)}) = -\text{Arg}(\zeta(1 - \sigma + it)); \quad (119)$$

then at the base point

$$\text{Arg}(\zeta(\sigma + it))_B = \pi - \text{Arg}(\zeta(1 - \sigma + it))_B; \quad (120)$$

This ratio of arguments is kept in the moving coordinate system formed by the normal L to the axis of symmetry and the axis of symmetry M of the vector system of the second approximate equation of the Riemann zeta function *for any values* of the complex variable symmetric about the critical line.

$$\text{Arg}(\zeta(\sigma + it)) - \frac{\text{Arg}(\chi(\sigma + it))}{2} = -(\text{Arg}(\zeta(1 - \sigma + it)) - \frac{\text{Arg}(\chi(\sigma + it))}{2}); \quad (121)$$

The vector system of the second approximate equation of the Riemann zeta function rotates relative to the end of the first vector X_1 of the Riemann spiral (74), while, in accordance with (71, 72), each next vector of this vector system rotates relative to the previous vector in the same direction as the entire vector system, therefore, the angle of twist of the vectors *grows monotonically*.

Thus, in accordance with (71, 72) when $\sigma < 1/2$, the angle of twist of vectors *grows faster* than when $\sigma = 1/2$, because the angles between the vectors are equal, but when $\sigma < 1/2$, the modulus of each vector is greater than the modulus of the corresponding vector when $\sigma = 1/2$, so the vector system when $\sigma < 1/2$ is twisted *at a greater angle* than in the case $\sigma = 1/2$.

While, when $\sigma > 1/2$, the angle of twist of vectors *grows slower* than when $\sigma = 1/2$, because the angles between the vectors are equal to, but $\sigma > 1/2$, the modulus of each vector is less than the modulus of the corresponding vector when $\sigma = 1/2$, so the vector system when $\sigma > 1/2$ is twisted *at a smaller angle* than in the case $\sigma = 1/2$.

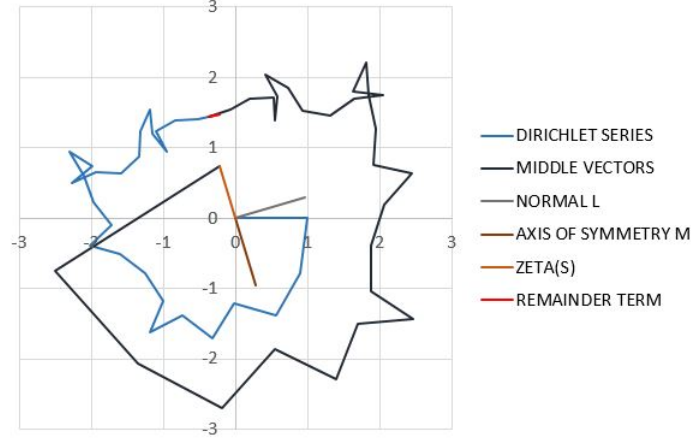


Figure 44: Base point #4525, the vector of values of the Riemann zeta function parallel to the axis of symmetry, $s = 0.35 + 5006.186i$

In accordance with the identified ratio of the arguments (121) and a monotonic increase of the angle of twist of vectors, we can conclude that the vectors of value of the Riemann zeta function, when values of the complex variable are symmetric about the critical line, rotate in the moving coordinate system formed by a normal of L to the axis of symmetry and axis of symmetry M of the vector system of the second approximate equation of the Riemann zeta function in opposite directions with the same speed and therefore at different values of the imaginary part of a complex number has a special positions:

- directed in different sites, along the axis of symmetry M (fig. 44, 45);
- directed in the same site, along the normal L to the axis of symmetry of the vector system of the second approximate equation of the Riemann zeta function (fig. 46, 47).

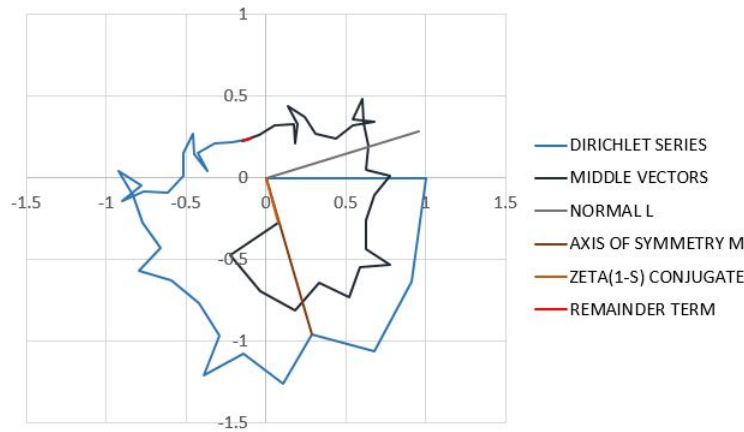


Figure 45: Base point #4525, the vector of values of the Riemann zeta function parallel to the axis of symmetry, $s = 0.65 + 5006.186i$

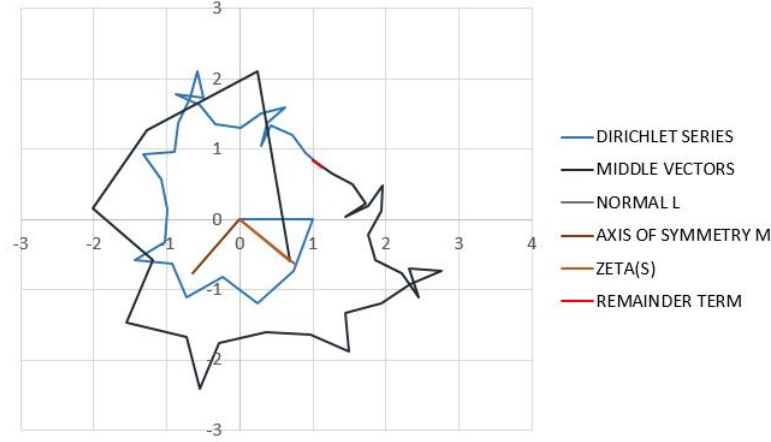


Figure 46: Base point #4525, the vector of values of the Riemann zeta function parallel to the normal to the axis of symmetry, $s = 0.35 + 5006.484i$

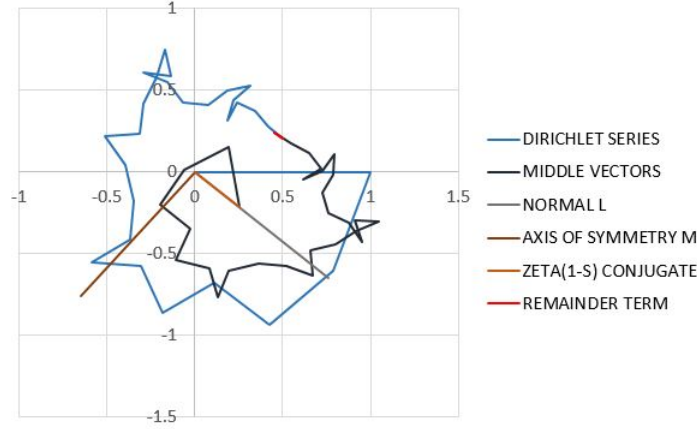


Figure 47: Base point #4525, the vector of values of the Riemann zeta function parallel to the normal to the axis of symmetry, $s = 0.65 + 5006.484i$

While, when $\sigma = 1/2$, in accordance with the mirror symmetry of the vector system of the second approximate equation of the Riemann zeta function when $\sigma = 1/2$, the vector of value of the Riemann zeta function rotates so that it is always located along the normal L to the axis of symmetry of this coordinate system (fig. 38).

According to the position relative to the real axis of the complex plane at the base point when $\sigma \neq 1/2$, the first middle vector Y_1 of the Riemann spiral, when it is below the real axis of the complex plane, rotates towards the first vector X_1 of the Riemann spiral and, conversely, when the first middle vector Y_1 of the Riemann spiral is above the real axis of the complex plane, it rotates away from the first vector X_1 of the Riemann spiral.

If the first middle vector Y_1 of the Riemann spiral at the base point when $\sigma \neq 1/2$ rotates towards the first vector X_1 of the Riemann spiral, then, in accordance with the conformal symmetry of the vector system of the second approximate equation of the Riemann zeta function when $\sigma \neq 1/2$, until the rotation of the first middle vector Y_1 of the Riemann spiral is completed, it will take a special position when the axis of symmetry M of this vector system passes through both the zero of the complex plane and the end of the first middle vector Y_1 of the Riemann spiral.

Conversely, if the first middle vector Y_1 of the Riemann spiral at the base point when $\sigma \neq 1/2$ rotates away from the first vector X_1 of the Riemann spiral, from the beginning of the rotation of the first middle vector Y_1 of the Riemann spiral, it already occupied a special position when the axis of symmetry M of this vector system is passed through both the zero of the complex plane and the end of the first middle vector Y_1 of the Riemann spiral.

This special position of the first middle vector Y_1 of the Riemann spiral corresponds to the special position of the vector of value of the Riemann zeta function when it locates along to the axis of symmetry M (fig. 44, 45) of the vector system of the second approximate equation of the Riemann zeta function.

According to the rules of summation of vectors in this special position of the first middle vector Y_1 of the Riemann spiral, the projection of the vector system of the second approximate equation of the Riemann zeta function on the normal L to the axis of symmetry of this vector system is equal to zero, hence

$$\zeta(s)_L = 0; \quad (122)$$

By increasing the imaginary part of a complex number, the first middle vector Y_1 of the Riemann spiral will move to another special position when the normal L to the axis of symmetry of the vector system of the second approximate equation of the Riemann zeta function passes through both the zero of the complex plane and the end of the first middle vector Y_1 of the Riemann spiral at that moment it rotated by an angle $\pi/2$ from the first special position in the moving coordinate system formed by the normal L to the axis of symmetry and the axis of symmetry M of this vector system.

Second special position of the first middle vector Y_1 of the Riemann spiral corresponds to the special position of the vector of value of the Riemann zeta function when it locates along the normal L to the axis of symmetry (fig. 46, 47) of the vector system of the second approximate equation of the Riemann zeta function.

According to the rules of summation of vectors in this special position of the first middle vector Y_1 of the Riemann spiral, the projection of the vector system of the second approximate equation of the Riemann zeta function on the axis of symmetry M of this vector system is equal to zero, hence

$$\zeta(s)_M = 0; \quad (123)$$

Thus, when we performed an additional analysis of the vector system of the second approximate equation of the Riemann zeta function in accordance with the identified ratio of the arguments (121) and monotonic increase of the angle of twist of vectors we found that each base point corresponds to *two special positions* of the first middle vector Y_1 of the Riemann spiral, in which when $\sigma \neq 1/2$ the projections of the vector system of the second approximate equation of the Riemann zeta function on the normal L to the axis of symmetry and on the axis of symmetry M of this vector system *alternately* take a value of zero and when $\sigma = 1/2$ one of which corresponds to the non-trivial zero of the Riemann zeta function.

Now we need to make sure that the modulus of the Riemann zeta function cannot take a value of zero except for the special position of the first middle vector Y_1 of the Riemann spiral when $\sigma = 1/2$.

We will analyzing the projections of the vector system of the second approximate equation of the Riemann zeta function on the normal L to the axis of symmetry and on the axis of symmetry M of this vector system starting from the boundary of the critical strip, where the Riemann zeta function has no non-trivial zeros, i.e. for values $\sigma = 0$ and $\sigma = 1$.

Construct the graphs of the projections of the vector system of the second approximate equation of the Riemann zeta function on the normal L to the axis of symmetry and on the axis of symmetry M of this vector system when $\zeta(1+it)_L = 0$, in accordance with the ratio of the arguments (121) of the vectors of values of the Riemann zeta function, when values of the complex variable symmetric about the critical line, we obtain another equality $\zeta(0+it)_L = 0$ (fig. 48).

Analysis of the projections of the vector system of the second approximate equation of the Riemann zeta function on the normal L to the axis of symmetry and on the axis of symmetry M of this vector system shows that in the interval A_k of the imaginary part of a complex number from $t_1: \zeta(1+it_1)_L = 0$ to $t_2: \zeta(1/2+it_2)_L = 0$, any value of t corresponds to a value $0 < \sigma < 1: \zeta(\sigma+it)_L = 0$.

In other words, in the interval A_k for each value of the imaginary part of a complex number, the graph of the function $\zeta(\sigma+it)_L = 0$ crosses the abscissa axis twice for the symmetric values $\sigma+it$ and $1-\sigma+it$ until when $\sigma = 1/2$ it reaches a value of the non-trivial zero of the Riemann zeta function.

While the graph of the function $\zeta(\sigma+it)_M = 0$ at any value t of the imaginary part of a complex number from the interval A_k crosses the abscissa axis only once, at the point $\sigma = 1/2$ (fig. 49).

Now we construct the graphs of the projections of the vector system of the second approximate equation of the Riemann zeta function on the normal L to the axis of symmetry and on the axis of symmetry M of this vector system when $\zeta(1+it)_M = 0$, in accordance with the ratio of the arguments (121) of the vectors of value of the Riemann zeta function, when values of the complex variable symmetric about the critical line, we obtain another equality $\zeta(0+it)_M = 0$ (fig. 51).

Analysis of the projections of the vector system of the second approximate equation of the Riemann zeta function on the normal L to the axis of symmetry and on the axis of symmetry M of this vector system shows that in the interval

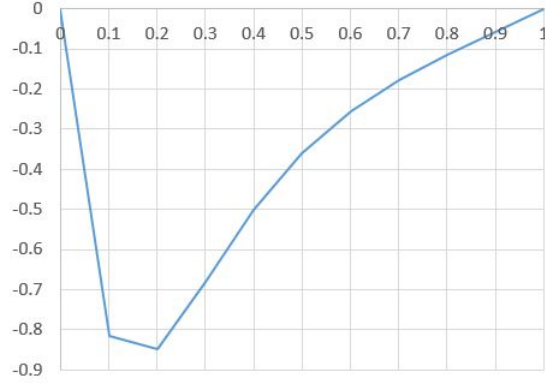


Figure 48: Base point #4525, projection of the vector system on the normal L to the axis of symmetry when $\zeta(1 + 5006, 09072i)_L = 0$

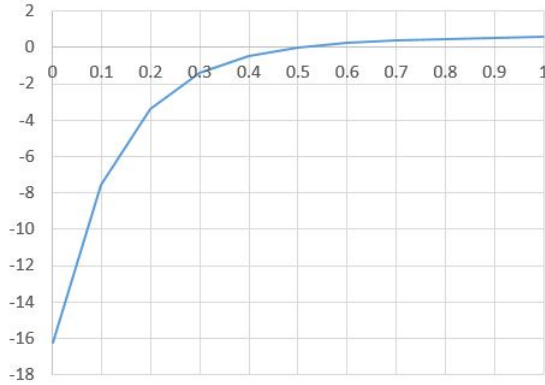


Figure 49: Base point #4525, projection of the vector system on the axis of symmetry M when $\zeta(1+5006, 09072i)_L = 0$

C_k of the imaginary part of a complex number from t'_1 : $\zeta(1 + it'_1)_M = 0$ to t'_2 : $\zeta(1/2 + it'_2)_M = 0$, any value of t' corresponds to a value $0 < \sigma < 1$: $\zeta(\sigma + it')_M = 0$.

In other words, in the interval C_k for each value of the imaginary part of a complex number, the graph of the function $\zeta(\sigma + it')_M = 0$ crosses the abscissa axis three times for the symmetric values $\sigma + it'$, $1 - \sigma + it'$ and at the point $\sigma = 1/2$.

While the graph of the function $\zeta(\sigma + it')_L = 0$ at any value t' of the imaginary part of a complex number from the interval C_k never crosses the abscissa axis (fig. 50).

Therefore, in the interval C_k for any value of the imaginary part of a complex number and any value of the real part of a complex number $0 < \sigma < 1$, the Riemann zeta function has no non-trivial zeros.

Analysis of the projections of the vector system of the second approximate equation of the Riemann zeta function on the normal L to the axis of symmetry and on the axis of symmetry M of this vector system in the interval of B_k between intervals A_k and C_k and in the interval D_k between intervals C_k and A_{k+1} shows that the projection at any value of the imaginary part of a complex number and any value of the real part of a complex number when $0 < \sigma < 1$ is not equal to zero, therefore, in the interval of B_k and D_k the Riemann zeta function has no non-trivial zeros.

It should be noted that the sign of the projection of the vector system on the axis of symmetry M of the vector system of the second approximate equation of the Riemann zeta function changes at each interval C_k , i.e. it depends on the number of the base point (fig. 66).

While the sign of the projection of the vector system on the normal L to the axis of symmetry of the vector system of the second approximate equation of the Riemann zeta function depends on the location of the first middle vector Y_1 of the Riemann spiral at the base point (fig. 66), i.e. it changes at each interval A_k .

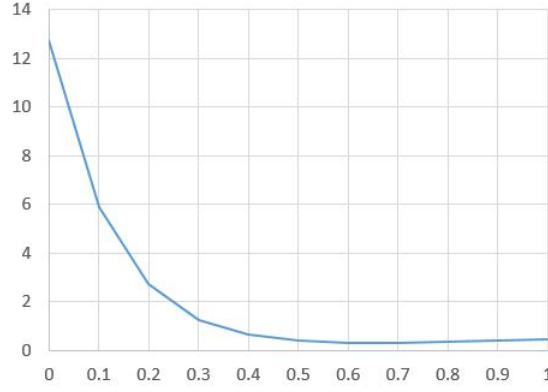


Figure 50: Base point #4525, projection of the vector system on the normal L to the axis of symmetry when $\zeta(1 + 5006, 4559i)_M = 0$

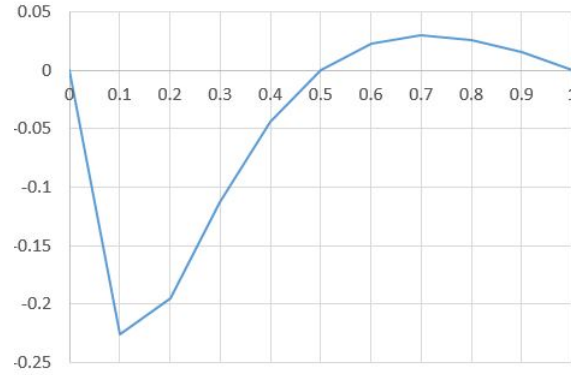


Figure 51: Base point #4525, projection of the vector system on the axis of symmetry M when $\zeta(1 + 5006, 4559i)_M = 0$

Thus, when we performed an additional analysis of the vector system of the second approximate equation of the Riemann zeta function we found that each base point corresponds to *four intervals* in which the projections of the vector system of the second approximate equation of the Riemann zeta function on the normal L to the axis of symmetry and on the axis of symmetry M of this vector system take certain values and only in one interval when $\sigma = 1/2$ they can be zero at the same time (fig. 52 and 53), in this moment the Riemann zeta function takes a value of non-trivial zero.

Now that we know all possible variants of the ratio of the projection of vectors system of the second approximate equation of the Riemann zeta function on normal L to the axis of symmetry and on the axis of symmetry M of this vector system we found out *what and why* can be these projections for any value of the real part of a complex number in the critical strip, and on the boundary of the critical strip, i.e. for values $\sigma = 0$ and $\sigma = 1$, where the Riemann zeta function has no non-trivial zeros, as it proved Adamar and vallée Poussin.

We have found out how these projections change when the imaginary part of the complex number changes and how these changes are related to the number of the base point and the position of the first middle vector Y_1 of the Riemann spiral at the base point, we have to answer two questions:

- 1) Why should these projections have such ratios for any base point?
- 2) Why can't there be any other reason for the modulus of the Riemann zeta function to go to zero when $\sigma \neq 1/2$?

The first question has already been answered in the analysis of the projections of the vector system on the normal L to the axis of symmetry and on the axis of symmetry M of the vector system of the second approximate equation of the Riemann zeta function:

- 1) The vector system of the second approximate equation of the Riemann zeta function rotates when the imaginary part of the complex number changes, which we can confirm this by the equation of the axis of symmetry (74) of this vector system;

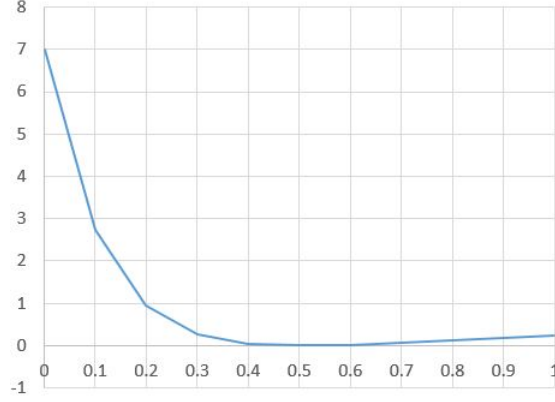


Figure 52: Base point #4525, projection of the vector system on the normal L to the axis of symmetry when $\zeta(1/2 + 5006, 208381106i)_L = 0$

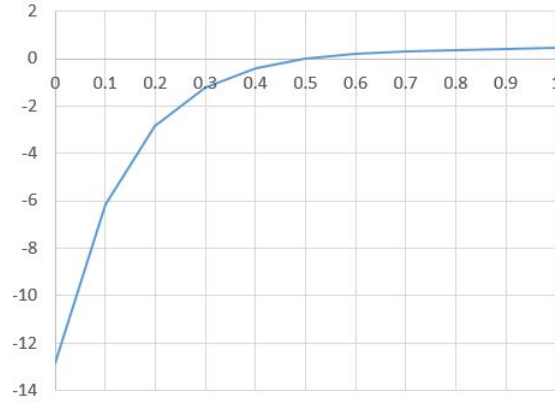


Figure 53: Base point #4525, projection of the vector system on the axis of symmetry M when $\zeta(1/2 + 5006, 208381106i)_L = 0$

- 2) The vector system periodically passes the base points, where it is convenient to fix its special properties;
- 3) The special properties of the vector system are determined by the position of the first middle vector Y_1 of the Riemann spiral at the base point relative to the real axis of the complex plane and the axes of the moving coordinate system formed by the normal L to the axis of symmetry and the axis of symmetry M of the vector system of the second approximate equation of the Riemann zeta function;
- 4) The arguments of $\zeta(s)$ and $\overline{\zeta(1-s)}$ have axial symmetry around the normal L to the axis of symmetry of the vector system of the second approximate equation of the Riemann zeta function;
- 5) The vectors of value of $\zeta(s)$ and $\overline{\zeta(1-s)}$ rotate in different directions at the same speed in the moving coordinate system formed by the normal L to the axis of symmetry and the axis of symmetry M of the vector system of the second approximate equation of the Riemann zeta function;
- 6) Projections of the vector system of the second approximate equation of the Riemann zeta function on the normal L to the axis of symmetry and on the axis of symmetry M of this vector system are determined by the vectors of value of $\zeta(s)$ and $\overline{\zeta(1-s)}$.

Thus, the projections of the vector system of the second approximate equation of the Riemann zeta function on the normal L to the axis of symmetry and on the axis of symmetry M of this vector system have periodic properties (which we described earlier) with relation to the base points, so these properties of the projections of the vector system must be observed at any base point, and therefore for all values of the complex variable, where this vector system determines a value of the Riemann zeta function, i.e., on the entire complex plane except the real axis, where, as is known, the Riemann zeta function has only trivial zeros.

To answer the second question, why there can be no other reason for the modulus of the Riemann zeta function to zero when $\sigma \neq 1/2$, it is necessary to consider possible variants of such a zero transformation, for example:

- 1) The interval A_k , where $\zeta(s)_L = 0$, intersects with the interval C_k , where $\zeta(s)_M = 0$, for any value of a complex variable when $\sigma \neq 1/2$;
- 2) The condition $\zeta(s)_L = 0$ and $\zeta(s)_M = 0$ is satisfied in the interval B_k or D_k , where $\zeta(s)_L \neq 0$ and $\zeta(s)_M \neq 0$, for any value of the complex variable in the critical strip.

It is obvious that the module $\zeta(s)$ can not arbitrarily be reduced to zero because this would require that the zero was reduced module of all vectors X_n and Y_n of the Riemann spiral, which contradicts (71, 72).

Somebody can think of other reasons why the modulus of the Riemann zeta function can transform to zero when $\sigma \neq 1/2$, we hope that upon careful examination they will all be refuted, because the identified properties of the projections of the vector system of the second approximate equation of the Riemann zeta function on the normal L to the axis of symmetry and on the axis of symmetry M of this system show the direction of confirmation why the Riemann zeta function may not have non-trivial zeros when $\sigma \neq 1/2$.

Now we consider another method of confirmation the Riemann hypothesis, based on the properties of the vector system of the second approximate equation of the Riemann zeta function.

We need to find out in which cases the invariants L_1 and L_2 (91) of this vector system and the vector of the remainder term R of the second approximate equation of the Riemann zeta function can form a triangle (92).

Consider the invariants L_1 and L_2 at the special points of the first middle vector Y_1 of the Riemann spiral, when the axis of symmetry M of the vector system of the second approximate equation of the Riemann zeta function passes through both the zero of the complex plane and the end of the first middle vector Y_1 of the Riemann spiral (fig. 54), and when the normal L to the axis of symmetry of the vector system of the second approximate equation of the Riemann zeta function passes through both the zero of the complex plane and the end of the first middle vector Y_1 of the Riemann spiral (fig. 55).

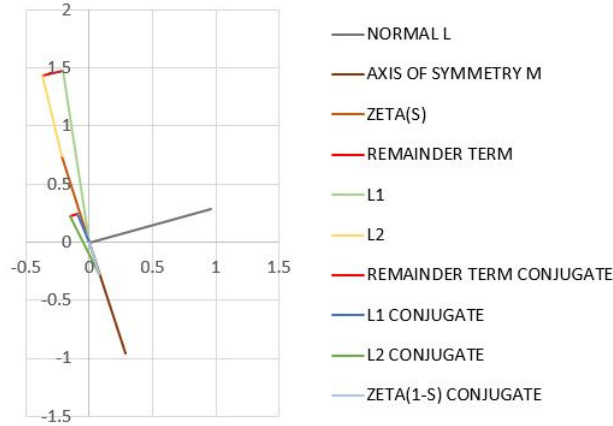


Figure 54: Base point #4525, the vector of values of the Riemann zeta function parallel to the axis of symmetry, $s = 0.35 + 5006.186i$ and $s = 0.65 + 5006.186i$

In all other cases, in accordance with the continuity of values of the Riemann zeta function, the invariants L_1 and L_2 will occupy different intermediate positions (fig. 56).

When the normal L to the axis of symmetry of the vector system of the second approximate equation of the Riemann zeta function passes through both the zero of the complex plane and the end of the first middle vector Y_1 of the Riemann spiral (fig. 57) invariants L_1 and L_2 can occupy a position close to the trapezoid, but in any case, obviously, can not form a triangle.

It is obvious that the invariants L_1 and L_2 can occupy the position closest to the triangle only when the axis of symmetry M of the vector system of the second approximate equation of the Riemann zeta function passes through both the zero of the complex plane and the end of the first middle vector Y_1 of the Riemann spiral (fig. 54), so we will perform further analysis of the invariants L_1 and L_2 in this special position of the first middle vector Y_1 of the Riemann spiral.

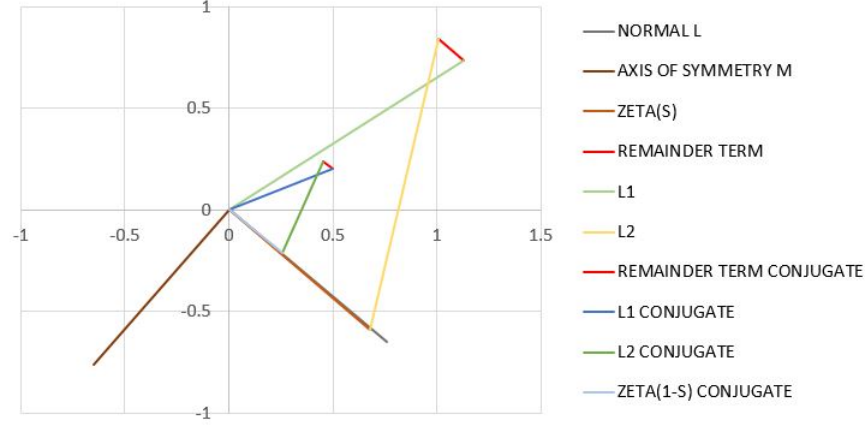


Figure 55: Base point #4525, the vector of values of the Riemann zeta function parallel to the normal to the axis of symmetry, $s = 0.35 + 5006.484i$ and $s = 0.65 + 5006.484i$

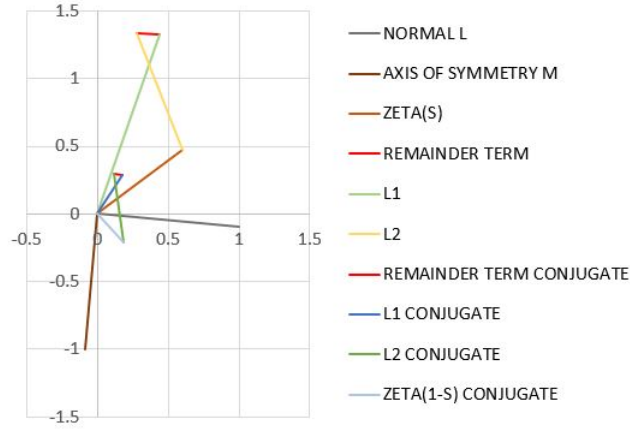


Figure 56: Base point #4525, intermediate position of the vector of values of the Riemann zeta function, $s = 0.35 + 5006.186i$ and $s = 0.65 + 5006.186i$

It should be noted that in this position of the axis of symmetry M of the vector system of the second approximate equation of the Riemann zeta function when $\sigma = 1/2$ in accordance with the mirror symmetry, this vector system forms a closed polyline, and therefore the Riemann zeta function takes a value of non-trivial zero (fig. 58).

In the ordinate of the non-trivial zero of the Riemann zeta function, the projection modulus of the invariant L_1 on the axis of symmetry M of the vector system of the second approximate equation of the Riemann zeta function increases when σ decreases and, conversely, it decreases when σ increases.

The projection of the invariant L_2 on the axis of symmetry M of the vector system of the second approximate equation of the Riemann zeta function changes according to the sign of the projection of its gradient on the axis of symmetry M :

$$grad_M L_2 = \sum_{n=1}^m \left(\frac{\partial Y_n}{\partial \sigma} \right)_M; \quad (124)$$

If the sign of the projection of the invariant L_2 on the axis of symmetry M of the vector system of the second approximate equation of the Riemann zeta function is equal to the sign of the projection of its gradient on the axis of symmetry M , then the projection of the invariant L_2 on the axis of symmetry M increases when σ increases (fig. 59) respectively while σ decreases it decreases also (fig. 60) and, conversely, if the sign of the projection of the invariant L_2 on the axis of symmetry M is not equal to the sign of the projection of its gradient on the axis of symmetry M , then when σ increases the projection of the invariant L_2 on the axis of symmetry M decreases (fig. 61) respectively while σ decreases it increases (fig. 62).

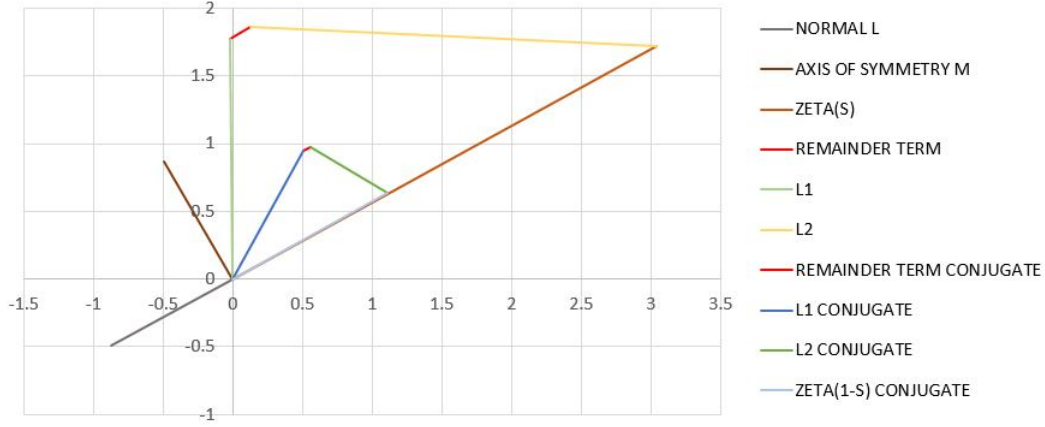


Figure 57: Base point #4520, the vector of values of the Riemann zeta function parallel to the normal to the axis of symmetry, $s = 0.35 + 5001.415i$ and $s = 0.65 + 5001.415i$

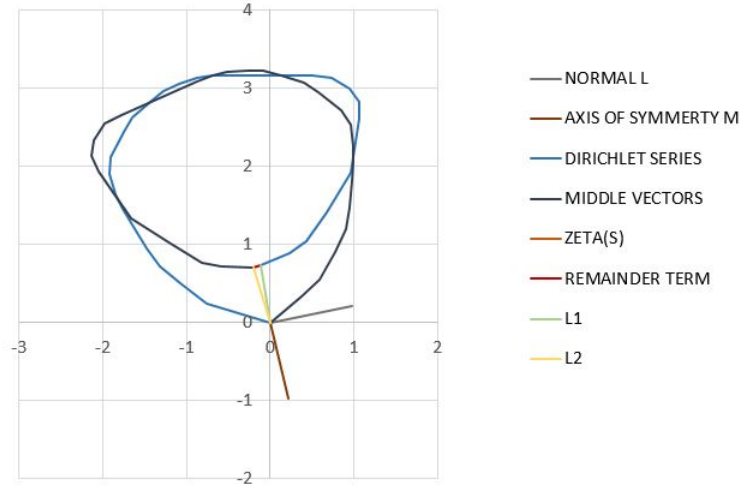


Figure 58: Base point #4525, non-trivial zero of the Riemann zeta function, $s = 0.5 + 5006.208381106i$

The sign of the projection of the gradient of the invariant L_2 on the axis of symmetry M depends on the distribution of angles and modulus of the middle vectors, which becomes obvious if we arrange the middle vectors in increasing order of their angles (fig. 58).

Researches show that when $\sigma \neq 1/2$ at the point when $\zeta(s)_M = 0$ the sign of the projection of the gradient of the invariant L_2 on the axis of symmetry M is kept.

Now, when we consider the invariants L_1 and L_2 at the point where the axis of symmetry M of the vector system of the second approximate equation of the Riemann zeta function passes through both the zero of the complex plane and the end of the first middle vector Y_1 of the Riemann spiral (fig. 54), it is sufficient to consider the sum of projections of vectors L_1 , L_2 and R on the axis of symmetry M , because at this point the sum of projections of vectors L_1 , L_2 and R on the normal L to the axis of symmetry is equal to zero.

Consider separately the sum of projections of invariants L_1 and L_2 on the axis of symmetry M of the vector system of the second approximate equation of the Riemann zeta function:

$$\Delta L = \sum_{n=1}^m (X_n(s))_M + \sum_{n=1}^m (Y_n(s))_M; \quad (125)$$

and the projection of vector R of the remainder term of the second approximate equation of the Riemann zeta function:

$$\Delta R = R \sin(\Delta\varphi_R); \quad (126)$$

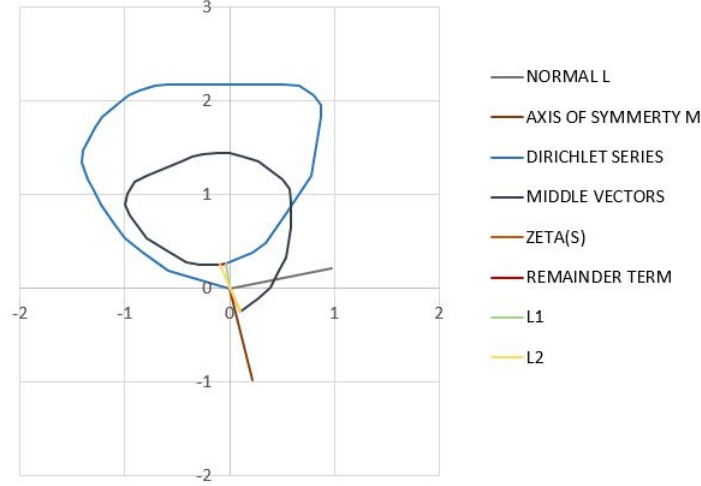


Figure 59: Base point #4525, the ordinate of the non-trivial zero of the Riemann zeta function, positive gradient, $s = 0.65 + 5006.208381106i$

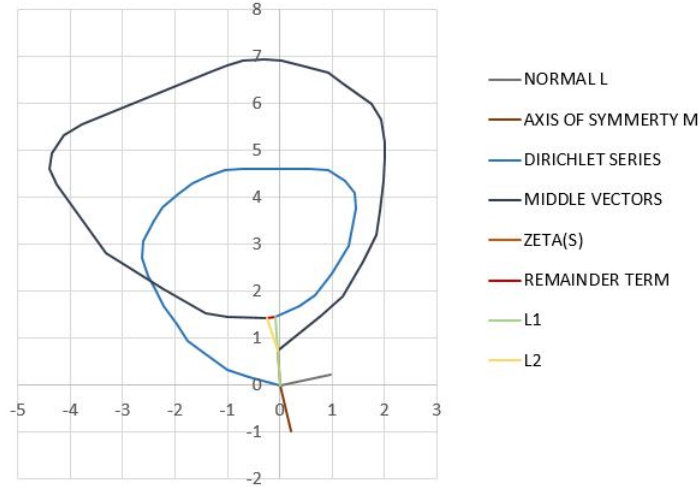


Figure 60: Base point #4525, the ordinate of the non-trivial zero of the Riemann zeta function, positive gradient, $s = 0.35 + 5006.208381106i$

where $\Delta\varphi_R$ is the deviation of the vector of the remainder term R of the second approximate equation of the Riemann zeta function from the normal L to the axis of symmetry of the vector system of the second approximate equation of the Riemann zeta function.

Then the vector condition (92) of the non-trivial zero of the Riemann zeta function can be rewritten as follows:

$$|\Delta L| = |\Delta R|; \quad (127)$$

We already know that in accordance with the mirror symmetry of the vector system of the second approximate equation of the Riemann zeta function when $\sigma = 1/2$ at the point when the axis of symmetry M of this vector system passes through both the zero of the complex plane and the end of the first middle vector Y_1 of the Riemann spiral (fig. 58), the Riemann zeta function takes a value of non-trivial zero.

Thus $\Delta L = 0$ and $\Delta R = 0$.

When $\sigma \neq 1/2$, the mirror symmetry of the vector system of the second approximate equation of the Riemann zeta function is broken, in other words, $\Delta L \neq 0$ and $\Delta R \neq 0$, hence the change in ΔL , if the Riemann zeta function can take a value of non-trivial zero, must be compensated by the change in ΔR .

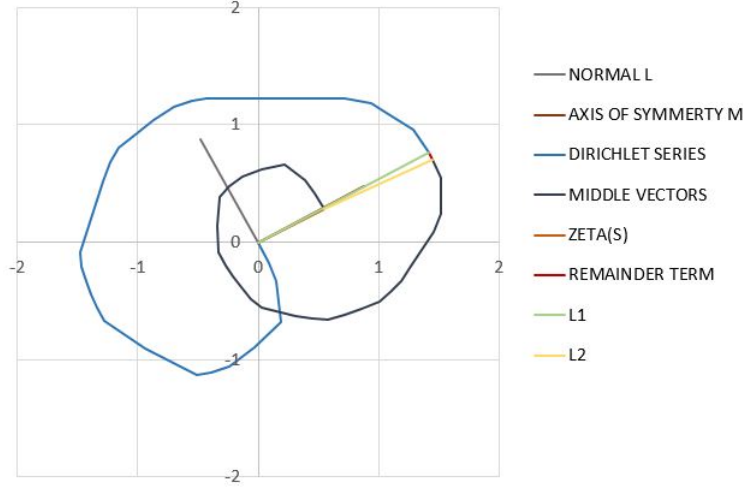


Figure 61: Base point #4521, the ordinate of the non-trivial zero of the Riemann zeta function, negative gradient, $s = 0.65 + 5001.889773627i$

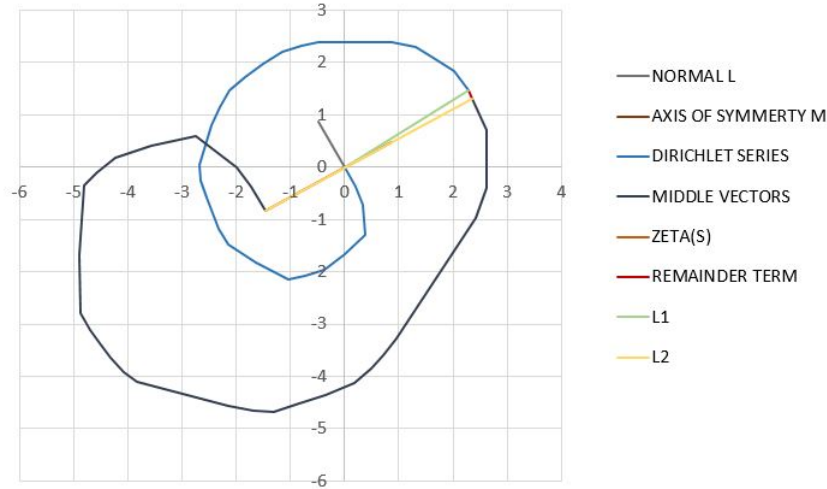


Figure 62: Base point #4521, the ordinate of the non-trivial zero of the Riemann zeta function, negative gradient, $s = 0.35 + 5001.889773627i$

Consider the dependence of the sum of projections of the invariants L_1 and L_2 (fig. 63) and the projection of the vector R of the remainder term (fig. 64) on the axis of symmetry M of the vector system of the second approximate equation of the Riemann zeta function from the real part of a complex number at the point when the axis of symmetry M of this vector system passes through both the zero of the complex plane and the end of the first middle vector Y_1 of the Riemann spiral.

It is obvious that these functions are equal only at the point $\sigma = 1/2$, i.e. on the critical line.

Consider the *boundary function* that separates values ΔL and ΔR (fig. 65), at the point where the axis of symmetry M of the vector system of the second approximate equation of the Riemann zeta function passes through both the zero of the complex plane and the end of the first middle vector Y_1 of the Riemann spiral:

$$F(s) = A \left(\frac{\sum_{n=1}^m |Y_n(s)|}{\sum_{n=1}^m |X_n(s)|} - 1 \right); \quad (128)$$

where A is some constant greater than zero.

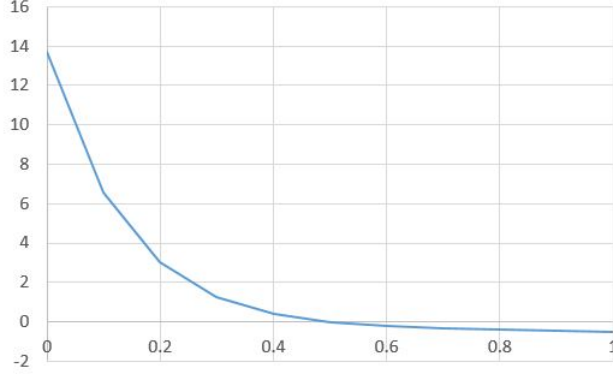


Figure 63: Base point #4525, sum of projections of invariants L_1 and L_2 , ordinate $\zeta(0.35 + 5006.186i)_L = 0$

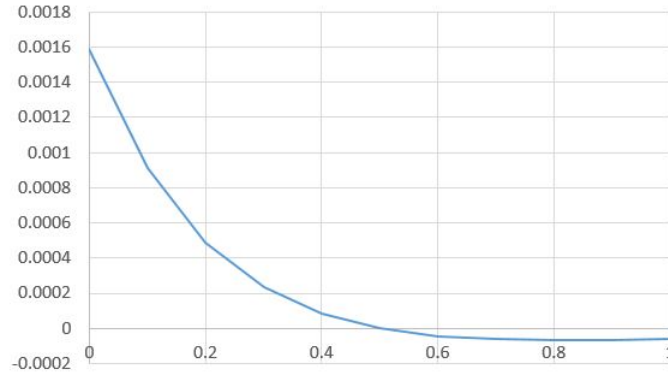


Figure 64: Base point #4525, projection of the remainder term R , ordinate $\zeta(0.35 + 5006.186i)_L = 0$

It is obvious that the sum of projections of invariants L_1 and L_2 (fig. 63) on the axis of symmetry M of the vector system of the second approximate equation of the Riemann zeta function when $\sigma = 0$ is determined by a value of the projection $\zeta(0 + it)_M$ (fig. 66), because in this case, $|\Delta L| \gg |\Delta R|$ (fig. 64), therefore, the sum of projections of invariants L_1 and L_2 on the axis of symmetry M at all points except $\sigma = 1/2$ modulo more than values of the boundary function, while values the projection of the vector R of the remainder term on the axis of symmetry M of the vector system of the second approximate equation of the Riemann zeta function in all points except $\sigma = 1/2$ modulo smaller than values of the boundary functions.

Now we need to find out the dependence of the angle of deviation $\Delta\varphi_R$ of vector remainder member of the second approximate equation of the Riemann zeta function from normal L to the axis of symmetry of the vector system of the second approximate equation of the Riemann zeta function, because a value of this angle determines a value of ΔR .

Although that Riemann recorded the remainder term (75) of the second approximate equation of the Riemann zeta function explicitly, Riemann and other authors use the argument of the remainder term only for the particular case of (82) when $\sigma = 1/2$, so we use the explicit expression for the CHI functions (66) and will calculate the argument of the remainder term using the exact values of the Riemann zeta function [22]:

$$\Delta\varphi_R = \frac{1}{2} \text{Arg}(\chi(s)) - \text{Arg}(R(s)) = \frac{1}{2} \arccos\left(\frac{\text{Re}(\chi(s))}{|\chi(s)|}\right) - \arccos\left(\frac{\text{Re}(R(s))}{|R(s)|}\right); \quad (129)$$

where

$$R(s) = \zeta(s) - \sum_{n=1}^m X_n(s) - \sum_{n=1}^m Y_n(s); \quad (130)$$

$$|R(s)| = \sqrt{\text{Re}(R(s))^2 + \text{Im}(R(s))^2}; \quad (131)$$

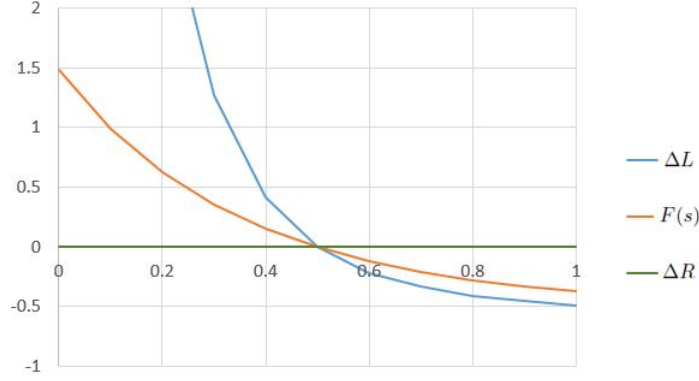


Figure 65: Base point #4525, boundary function $F(s)$, ordinate $\zeta(0.35 + 5006.186i)_L = 0$, $A = 0.5$

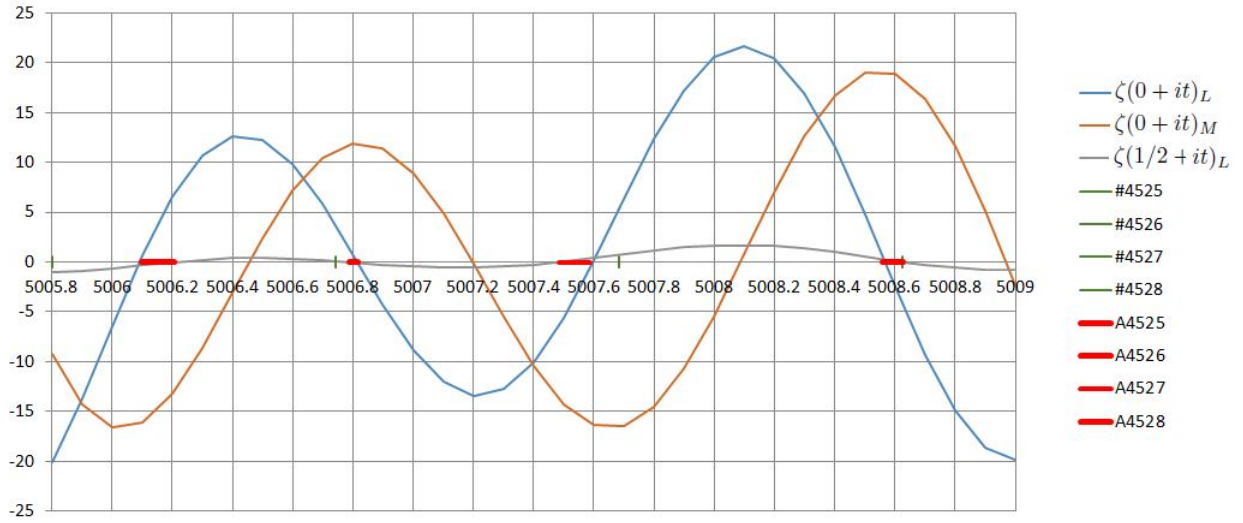


Figure 66: Graphics of projections of the Riemann zeta function

The calculations show a linear relationship (fig. 67) of the angle of deviation $\Delta\varphi_R$ of the vector of the remainder term of the second approximate equation of the Riemann zeta function from normal L to the axis of symmetry of this vector system from the real part of a complex number.

This dependence is confirmed for any values of the imaginary part of a complex number, since it is determined by the form of the polyline formed by the vector system of the second approximate equation of the Riemann zeta function, for symmetric values $\sigma + it$ (fig. 41) and $1 - \sigma + it$ (fig. 42).

It can be shown that these polylines are mirror congruent, hence all the angles of these polylines are mirror congruent, including the arguments of the remainder terms.

The angle of deviation $\Delta\varphi_R$ of the vector of the remainder term of the second approximate equation of the Riemann zeta function from normal L to the axis of symmetry of the vector system of the second approximate equation dzeta-functions of Riemann has a periodic dependence (fig. 68) from the imaginary part of a complex number, with a period equal to an interval (73), where fractional part of the expression $\sqrt{t/2\pi}$, which varies from 0 to 1 (fig. 69), has the periodic dependence also.

The angle of deviation $\Delta\varphi_R$ of the vector of the remainder term of the second approximate equation of the Riemann zeta function from normal L to the axis of symmetry of this vector system has the maximum value at the boundaries of the intervals (73), and the absolute value of the maximum variance asymptotically decreases (fig. 70) with the growth of the imaginary part of a complex number, which corresponds to the evaluation of the remainder term of the gamma

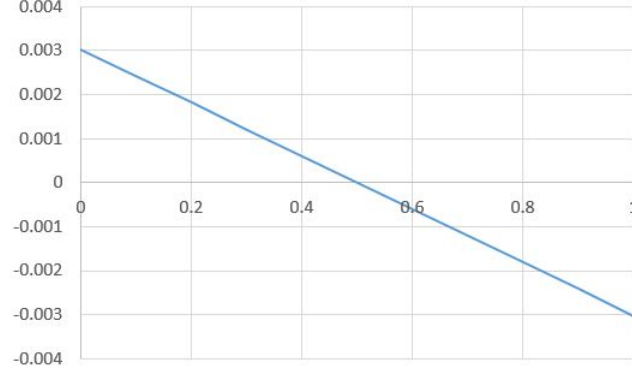


Figure 67: Base point #4525, the deviation angle of vector $\Delta\varphi_R$ of remainder term, rad, ordinate $\zeta(0.35 + 5006.186i)_L = 0$

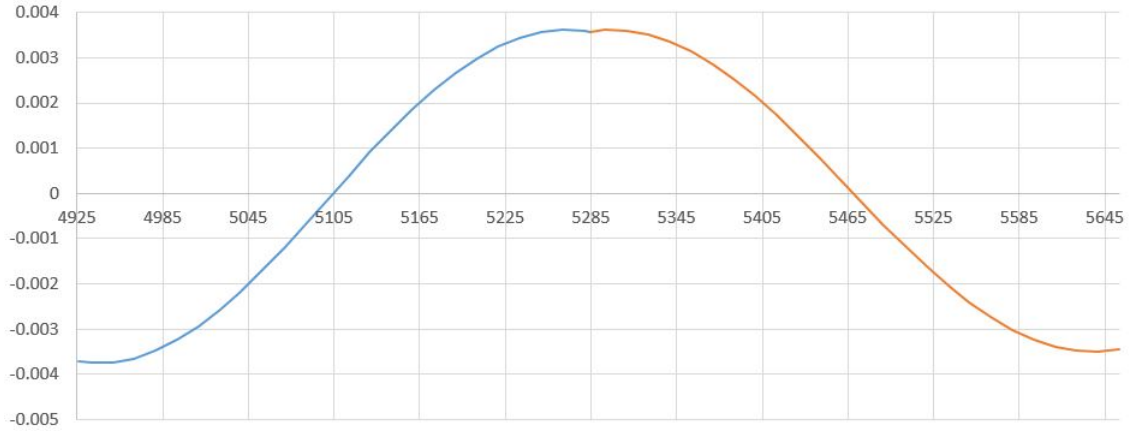


Figure 68: The deviation angle of vector $\Delta\varphi_R$ of remainder term, rad (from the imaginary part of a complex number)

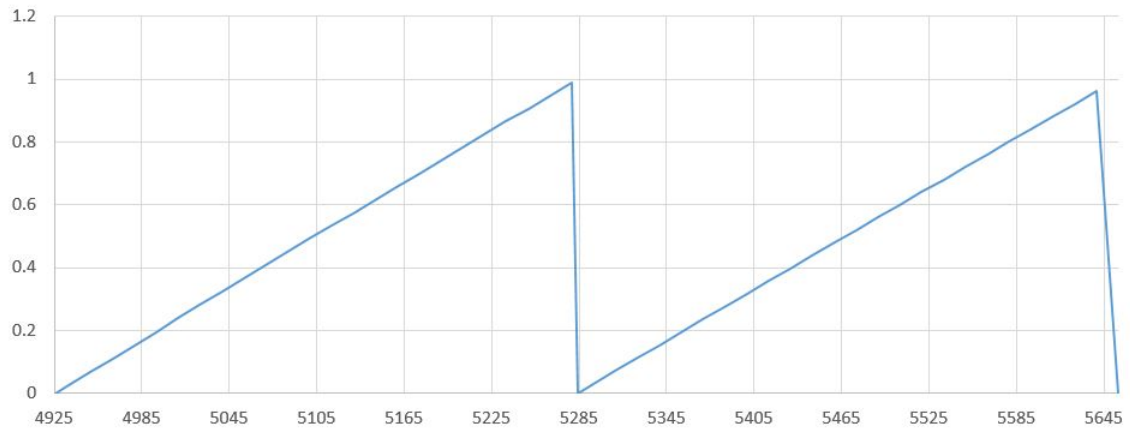


Figure 69: Fractional part of $\sqrt{t/2\pi}$ (from imaginary part of complex number)

function:

$$\mu(s) \rightarrow 0, t \rightarrow \infty; \quad (132)$$

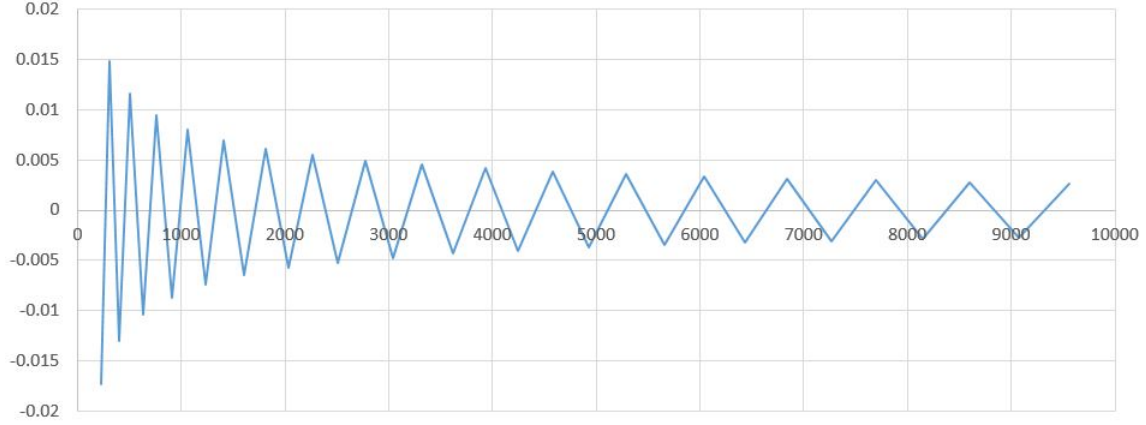


Figure 70: The maximum derivation angle of the vector $\Delta\varphi_R$ of the remainder term, rad (from the imaginary part of a complex number)

Thus, at the point where the axis of symmetry M of the vector system of the second approximate equation of the Riemann zeta function passes through both the zero of the complex plane and the end of the first middle vector Y_1 of the Riemann spiral, the condition (127) can be true only when $\sigma = 1/2$, since $\sigma \neq 1/2$ $|\Delta L| > |\Delta R|$ on any interval (73).

Somebody can think of different options, why expression (128) cannot be *bounding function*, but we hope that they will all be refuted.

4 Summary

Was Riemann going to speak at the Berlin Academy of Sciences on the occasion of his election as a corresponding member to present a proof of the asymptotic law of the distribution of prime numbers?

Only Riemann himself could have answered this question, but we are inclined to assume that he did not intend to.

Neither before nor after (Riemann died seven years later) he did not return to the subject publicly.

Riemann did not publish any paper in progress, so the paper on the analysis of the formula, which is now called the Riemann-Siegel formula was published by Siegel based on Riemann's notes, but this paper is rather a development of the analytical analysis of the Riemann zeta function, rather than a proof of the asymptotic distribution law of prime numbers.

The speech was rather about the analytical function of the complex variable.

Riemann showed how bypassing the difficult arguments about the convergence of the series, which defines the function, we can get its analytical continuation using the residue theorem.

Riemann also used a feature of a function of a complex variable for which zeros are its singular points, which carry basic information about the function.

It was in connection with this feature of the complex variable function that the Riemann hypothesis appeared - the hypothesis of the distribution of zeros of the Riemann zeta function.

Strange is also the absence of any mention of the representation of complex numbers by points on the plane, although Riemann in his report uses the rotation of the zeta function by the angle $Arg(\chi(s))/2$, which is certainly an operation on complex numbers as points on the plane.

Such relation to complex numbers seems even more strange in light of the fact that Riemann was a student of Gauss, who was one of the first to introduce the representation of complex numbers by points on the plane.

In other words, we tend to assume that the zeta function was chosen to show how we can solve the problem by methods of functions of a complex variable, Riemann is not important the problem itself, it is important approach and methods that gives the theory of functions of a complex variable as the apotheosis of the theory of analytic functions.

Although that a theorem of the distribution of prime numbers is proved analytically, i.e. using the analytical Riemann zeta function, later it was found a proof that uses the functions of a real variable, i.e. an elementary proof.

Thus, the role of the Riemann zeta function has shifted towards regularization, the so-called methods of generalized summation of divergent series.

The Riemann hypothesis seems to belong to such problems, since the generalized Riemann hypothesis deals with an entire class of Dirichlet L-functions.

Zeta function regularization is also used in physics, particularly in quantum field theory.

We prefer to conclude that the main role of the Riemann zeta function is in the understanding of generalized methods for summing asymptotic divergent series and as a consequence of constructing an analytic continuation of the functions of a complex variable.

Based on that on numerous forums „seriously“ is discussed infinite sum of natural numbers:

$$1 + 2 + 3 + \dots = -\frac{1}{12}; \quad (133)$$

only a few understand the essence of the generalized summation or regularization of divergent series.

Here mathematics encounters philosophy, namely with *the law of unity of opposites*.

The essence of generalized summation is *regularization* (that is why the second name of the method is regularization) - it means that a divergent series cannot exist without its *opposite* - convergent series.

In other words, there is only *one series*, but it converges in one region and diverges in another.

The most natural such series is the Dirichlet series:

$$\sum_{n=1}^{\infty} \frac{1}{n^s}; \quad (134)$$

which in the real form was researched by Euler (he first raised the question of the need for the concept of generalized summation), and in the complex form it was considered by Riemann.

Riemann left the question of generalized summation, skillfully replacing the divergent Dirichlet series by already regularized integral of gamma functions of a complex variable:

$$\Gamma(z) = \frac{1}{e^{i2\pi z} - 1} \int_L t^{z-1} e^{-t} dt; \quad (135)$$

The essence of unity „summation“ of an infinite series is in the definition of „sum“ this series in the region where this series converges and in the region where *the same* series diverges.

The misconception begins in the definition of *infinite sum*. In the case of a convergent series, it only seems to us that we can find the „sum“ of this series. In fact, we find *limit of partial sums* because in accordance with the convergence of the series, such a limit exists (by definition).

Euler first formulated the need for a different concept of the word „sum“ in the application to the divergent series (or rather to the series in the region where it diverges), he explained this by the practical need to attach some value divergent series.

We now know that this value is found as *limit of generalized partial sums* of an infinite series.

And the main condition that is imposed on the method of obtaining generalized partial sums (except that there must be a limit) is *regularity*, i.e. the limit of generalized partial sums in the region where the series converges must be equal to the limit of partial sums of this series.

This understanding, as Hardy observed, came only with the development of the theory of the function of a complex variable, namely the notion of *analytic continuation*, which is closely linked to the infinite series that defines the analytic function, and is also closely linked to the fact that this infinite series converges in one region and diverges in another.

An analytic continuation of a function of a complex variable, if it is possible, is unique and this fact (which has a rigorous proof) is possible only if there exists a limit of generalized partial sums of an infinite series by which the analytic function is defined, in the region where this series diverges.

In the theory of generalized summation of divergent series, it is also rigorously proved that if the limit of generalized partial sums exists for two different regularization methods (obtaining generalized partial sums), then it has the same value.

It is this correspondence of different methods of obtaining generalized partial sums and analytic continuation of the function of a complex variable that Hardy had in mind.

The Dirichlet series $\sum_{n=1}^{\infty} \frac{1}{n^s}$ in complex form defines the Riemann zeta function.

As is known, this series diverges in the critical strip, where the Riemann zeta function has non-trivial zeros.

Hence all non-trivial zeros of the Riemann zeta function are *limit* of generalized partial sums of the Dirichlet series, while the trivial zeros of the Riemann zeta function define odd Bernoulli numbers, which are all zero.

In the Riemann zeta function theory to regularize the Dirichlet series the Euler-MacLaren formula¹⁰ is traditionally used, as we mentioned earlier, this formula is used if the partial sums of a divergent series are suitable for calculating the generalized sum of that divergent series.

The Euler-MacLaren generalized summation formula allows us to move from an infinite sum to an improper integral, i.e. to the limit of generalized partial sums of the Dirichlet series.

The geometric analysis of partial sums of the Dirichlet series, which defines the Riemann zeta function, allowed us to make an important conclusion that a generalized summation of infinite series is possible if this series diverges asymptotically.

And then we get into the essence of the definition of analytic functions through *asymptotic* infinite series, and a value of the function equal to a value of the asymptote in any case or when the series asymptotically converge or when a series diverges asymptotically, while in order to find the limit of this asymptote when the series converges, use partial sums of this series and when the series diverges, to find the limit of the asymptote, we must use the regular generalized partial sum.

And then we can obtain an analytic continuation of the function given by the *asymptotic infinite series*.

Therefore, the result obtained at the very beginning of the research, namely the use of an alternative method of generalized summation of Cesaro, which was obtained geometrically, is as important as the description of the various options to confirm the Riemann hypothesis.

5 Conclusion

We believe that the method of geometric analysis of Dirichlet series, based on the representation of complex numbers by points on the plane, will complement the set of tools of analytical number theory.

The method described in this paper allows us to get into the essence of the function of a complex variable, to identify regularities that explain any value of this function (including in the region where the series that define this function diverges) and most importantly it gives *an idea of the exact value of zero* as the sum of vectors that form a closed polyline.

After going through the analysis of the vector system of the second approximate equation of the Riemann zeta function, we can formulate the results of the second method of confirmation the Riemann hypothesis without using this vector system, since we only needed it to find the key points that indicate that the Riemann zeta function *cannot have non-trivial zeros in the critical strip, except for the critical line*.

Obviously we can move from the fixed coordinate system formed by the axes $x = \text{Re}(s)$ and $y = \text{Im}(s)$, to the moving coordinate system formed by axes L with angle $\varphi_L = \text{Arg}(\chi(s))/2$ and by axes M with angle $\varphi_M = (\text{Arg}(\chi(s)) + \pi)/2$ passing through the zero of the complex plane.

Then from the functional equation of the Riemann zeta function:

$$\zeta(s) = \chi(s)\zeta(1-s); \quad (136)$$

and equality arguments of functions:

$$\text{Arg}(\zeta(1-s)) = -\text{Arg}(\zeta(\overline{1-s})); \quad (137)$$

using the arithmetic of the arguments of complex numbers, when we rotate the vector of a value of Riemann zeta function by the angle $\text{Arg}(\chi(s))/2$ in the negative direction, we obtain:

$$\text{Arg}(\zeta(s)) - \frac{\text{Arg}(\chi(s))}{2} = -(\text{Arg}(\zeta(\overline{1-s})) - \frac{\text{Arg}(\chi(s))}{2}); \quad (138)$$

¹⁰unfortunately, the fact that the Euler-McLaren summation formula is used for the Riemann zeta function as a method of generalized summation of divergent series is not mentioned in all textbooks.

Consequently, in the moving coordinate system formed by the axes L and M , the angles of the vectors of value of $\zeta(s)$ and $\zeta(\overline{1-s})$ are symmetric about the axis L , thus, in accordance with the symmetry of the angles, the vector of value of $\hat{\zeta}(s) = \zeta(1/2 + it)$ is always directed along the axis L .

In other words, in the moving coordinate system formed by the axes L and M , the vector of value of $\hat{\zeta}(s) = \zeta(1/2 + it)$ remains fixed and only changes its modulus and sign, while the vectors of value of $\zeta(s)$ and $\zeta(\overline{1-s})$ when $\sigma \neq 1/2$ rotate in this moving coordinate system in different directions with the same speed.

Therefore:

a) the projection $\hat{\zeta}(s)_M = \zeta(1/2 + it)_M$ is always zero;

b) the projections $\zeta(s)_L$ and $\zeta(\overline{1-s})_L$ are periodically equal to zero when the vectors of value of $\zeta(s)$ and $\zeta(\overline{1-s})$ both locate along the axis M they have opposite directions and at this point the projections $\zeta(s)_M$ and $\zeta(\overline{1-s})_M$ are not equal to zero, because $\zeta(s)_L$ is an odd harmonic function, and $\zeta(s)_M$ is an even harmonic function that conjugate to $\zeta(s)_L$;

c) the projections $\zeta(s)_M$ and $\zeta(\overline{1-s})_M$ are periodically equal to zero when the vectors of value of $\zeta(s)$ and $\zeta(\overline{1-s})$ both locate along the axis L while they have the same direction and at this point the projections $\zeta(s)_L$ and $\zeta(\overline{1-s})_L$ are not equal to zero, since $\zeta(s)_L$ is an odd harmonic function, and $\zeta(s)_M$ is an even harmonic function that conjugate to $\zeta(s)_L$;

So only $\hat{\zeta}(s)_M$ and $\hat{\zeta}(s)_L$ can be equal to zero at the same time, because $\hat{\zeta}(s)_L = \zeta(1/2 + it)_L$ is an odd harmonic function, and $\hat{\zeta}(s)_M = \zeta(1/2 + it)_M$ is a harmonic function *identically equal to zero* (fig. 71).

Therefore, when $\sigma \neq 1/2$, the Riemann zeta function cannot be zero, because when $\sigma \neq 1/2$, the projections $\zeta(s)_L$ and $\zeta(s)_M$ cannot be equal to zero at the same time (fig. 72).

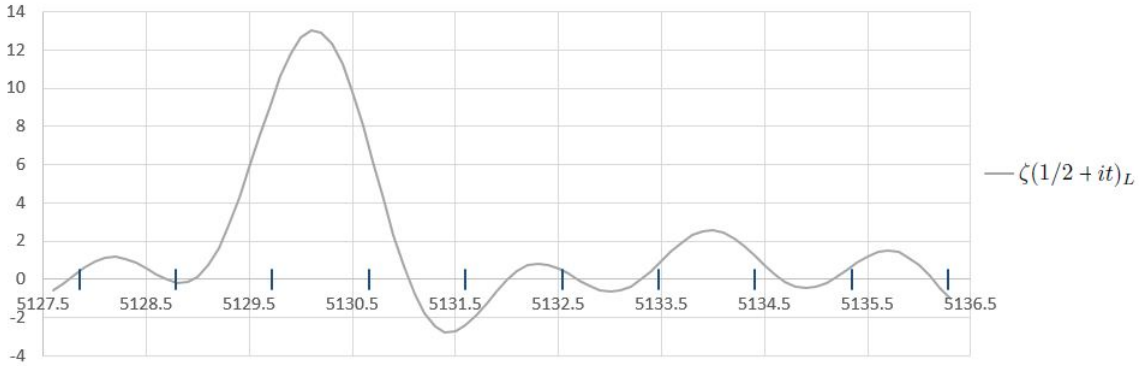


Figure 71: Graphics of projections of the Riemann zeta function, $\sigma = 1/2$

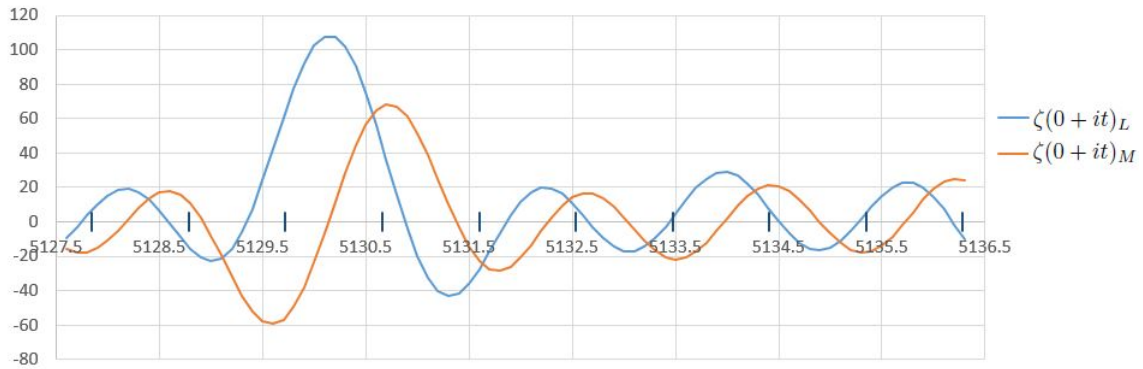


Figure 72: Graphics of projections of the Riemann zeta function, $\sigma = 0$

There may be a Lemma on conjugate harmonic functions identically nonzero, but we have not found it, just like the Lemma on the symmetric polygon we proved earlier (Lemma 3).

Therefore, to confirm our conclusions, we are forced to return to the vector system of the second approximate equation of the Riemann zeta function.

Vertical marks on the graphs (fig. 71 and 72) is *the base point*, corresponding to solution of the equation:

$$\text{Arg}(\chi(\frac{1}{2} + it_k)) = (2k - 1)\pi; \quad (139)$$

Using the mirror symmetry property of the vector system of the second approximate equation of the Riemann zeta function when $\sigma = 1/2$, we previously defined two types of base points:

a_1 - if the first middle vector of the Riemann spiral at the base point is above or along the real axis of the complex plane (the second position corresponds to the non-trivial zero of the Riemann zeta function at the base point is a likely event), in this case the non-trivial zero of the Riemann zeta function that corresponds to this base point is located between this and the previous base point;

a_2 - if the first middle vector of the Riemann spiral at the base point is below the real axis of the complex plane, then the non-trivial zero of the Riemann zeta function that corresponds to this base point is located between this and the next base point;

as well as four types of intervals between base points of different types:

$A_1 = a_1a_1$ and $A_2 = a_2a_2$ - intervals of this kind contain one non-trivial zero of the Riemann zeta function;

$B = a_2a_1$ - interval of this kind contains two non-trivial zeros of the zeta function of Riemann;

$C = a_1a_2$ - interval of this kind does not contain any non-trivial zero of the Riemann zeta function.

We also found that there cannot be the following combinations of intervals:

A_1A_2, A_2A_1, BB and CC ;

Hence we have *a fixed set* of combinations of intervals:

$A_1A_1 = a_1a_1a_1, A_1C = a_1a_1a_2, CB = a_1a_2a_1, CA_2 = a_1a_2a_2, BA_1 = a_2a_1a_1, BC = a_2a_1a_2, A_2B = a_2a_2a_1, A_2A_2 = a_2a_2a_2$;

It is obvious that the sequence of base points which are represented in the graphs (fig. 71 and 72), contains all the possible combinations of intervals:

$a_2a_2a_2a_1a_1a_1a_2a_2a_2 = A_2A_2BA_1A_1BCBA_2$;

In accordance with the properties of the vector system of the second approximate equation of the Riemann zeta function, we can determine the sign of the function $\zeta(\sigma + it)_L$ and the sign of its first derivative at each base point.

This requires:

- 1) determine the type of base point by the position of the first middle vector Riemann spiral relative to the real axis of the complex plane at the base point;
- 2) determine the direction of the normal L to the axis of symmetry of the vector system of the second approximate equation of the Riemann zeta function at the base point;

Then

A) If the first middle vector Riemann spiral is below the real axis of the complex plane, the function $\zeta(\sigma + it)_L$ will have the sign opposite to the direction of the normal L to the axis of symmetry;

B) If the first middle vector of the Riemann spiral is above the real axis of the complex plane, the function $\zeta(\sigma + it)_L$ will have a sign corresponding to the direction of the normal L to the axis of symmetry;

C) The sign of the first derivative of the function $\zeta(\sigma + it)_L$ always has a sign corresponding to the direction of the normal L to the axis of symmetry;

These rules are executed for any combination of intervals from *a fixed set*, so they are executed for any combination of intervals that can occur.

In the moving coordinate system formed by axes L and M when $\sigma \neq 1/2$, the vector of values of the Riemann zeta function must rotate on the angle $\pi/2$ from the position corresponding to $\zeta(\sigma + it)_L = 0$ to the position corresponding

to $\zeta(\sigma + it)_M = 0$ as well as from the position corresponding to $\zeta(\sigma + it)_M = 0$ to position corresponding to $\zeta(\sigma + it)_L = 0$, hence *all the zeros of the function $\zeta(\sigma + it)_M$ when $\sigma \neq 1/2$, lie between the zeros of the function $\zeta(\sigma + it)_L$.*

Corollary 1. The function $\zeta(1/2 + it)_L$ has an infinite number of zeros (this statement corresponds to Hardy's theorem [2] on an infinite number of non-trivial zeros of the Riemann zeta function on the critical line).

Corollary 2. The number of non-trivial zeros of the Riemann zeta function on the critical line corresponds to the number of base points:

$$N_0(T) = \left\lceil \left| \frac{T}{2\pi} \left(\log \frac{T}{2\pi} - 1 \right) - \frac{1}{8} + \frac{2\mu(T) - \alpha_2}{2\pi} \right| \right\rceil + 2; \quad (140)$$

where $\mu(T)$ is the remainder term of the gamma function (63) when $\sigma = 1/2$;

α_2 argument of the CHI function at the second base point.

Corollary 3. The function $\zeta(\sigma + it)_L$ when $\sigma \neq 1/2$ has an infinite number of zeros.

Corollary 4. The function $\zeta(\sigma + it)_M$ when $\sigma \neq 1/2$ has an infinite number of zeros.

Corollary 5. Zeros of function $\zeta(\sigma + it)_L$ and functions $\zeta(\sigma + it)_M$ when $\sigma \neq 1/2$ are not the same, because all zeros of function $\zeta(\sigma + it)_M$ when $\sigma \neq 1/2$ lie between zeros of function $\zeta(\sigma + it)_L$.

Based on the obtained results, we believe that the methods of confirmation of the Riemann hypothesis based on the properties of the vector system of the second approximate equation of the Riemann zeta function will soon lead to its proof.

6 Gratitudes

Special thanks to Professor July Dubensky, who allowed to speak at the seminar and instilled confidence in the continuation of the research. Colleagues and friends who listened to the first results and supported throughout the research. My wife, who helped to prepare the presentation at the seminar, supported and believed in success.

The organizers of the conference of Chebyshev collection in Tula, inclusion in the list of participants of this conference allowed to prepare the first version of the paper, but a exclusion from the list of participants mobilized and allowed to obtain new important results of the research.

References

- [1] J. P. Gram. Note sur les zeros de la fonction de Riemann. Acta Mathematica, (27):289– 304, 1903.
- [2] Hardy, G.H. (1914). “Sur les zeros de la fonction $\zeta(s)$ ”. Comp. Rend. Acad. Sci. (158): 1012—1014.
- [3] Hardy, G. H. and J. E. Littlewood, 1921, The Zeros of Riemann's Zeta Function on the Critical Line. Mathematische Zeitschrift
- [4] J. E. Littlewood, On the zeros of the Riemann zeta-function, Proc. Camb. Phil. Soc. 22 (1924), 295-318.
- [5] Siegel K., 1932, On Riemann's Nachlass for Analytic Number Theory, Translated by Eric Barkan and David Sklar, Available at: <https://arxiv.org/pdf/1810.05198>
- [6] G.H. Hardy, 1949, Divergent series, Oxford At The Clarendon Press, Available at: <https://archive.org/details/DivergentSeries>
- [7] N. Levinson, More than one third of zeros of Riemann's zeta-function are on $\sigma = 1/2$, Adv. Math. 13 (1974), 383-436.
- [8] W. Gabcke, Neue Herleitung und explicite Restabschätzung der Riemann-Siegel-Formel, Ph.D. Dissertation, Gottingen, 1979.
- [9] Titchmarsh, E.C. (1988) The Theory of the Riemann Zeta Function. Oxford University Press, Oxford.
- [10] J. B. Conrey, More than two fifths of the zeros of the Riemann zeta function are on the critical line, J. reine angew. Math. 399(1989), 1-26.
- [11] Euler, 2000, Foundations of Differential Calculus, translated by J.D. Blanton, Available at: <https://link.springer.com/content/pdf/bfm%3A978-0-387-22645-3%2F1.pdf>

- [12] Xavier Gourdon, The 10^{13} first zeros of the Riemann Zeta function, and zeros computation at very large height (2004)
- [13] Carl Erickson, A Geometric Perspective on the Riemann Zeta Function's Partial Sums, Stanford Undergraduate Research Journal, Available at: http://www.stanford.edu/group/journal/cgi-bin/wordpress/wp-content/uploads/2012/09/Erickson_NatSci_2005.pdf
- [14] <https://mathoverflow.net/questions/34699/approaches-to-riemann-hypothesis-using-methods-outside-number-theory>
- [15] H. M. Bui, Brian Conrey, Matthew P. Young, 2011, More than 41% of the zeros of the zeta function are on the critical line, Available at: <https://arxiv.org/pdf/1002.4127.pdf>
- [16] S. Feng, Zeros of the Riemann zeta function on the critical line, <http://arxiv.org/abs/1003.0059>.
- [17] T. S. Trudgian, A modest improvement on the function $S(T)$, 2012, Mathematics of Computation, vol. 81, no. 278, pp. 1053-1061, Available at: <https://arxiv.org/abs/1010.4596>
- [18] Raymond Manzoni, Simpler zeta zeros Available at: <https://math.stackexchange.com/questions/805396/simpler-zeta-zeros/815480#815480>
- [19] <https://aimath.org/wp-content/uploads/bristol-2018-slides/Sarnak-talk.pdf>
- [20] N. Preobrazhenskaya, S. Preobragenskii, 100% of the zeros of the Riemann zeta-function are on the critical line, <https://arxiv.org/abs/1805.07741>
- [21] <http://empslocal.ex.ac.uk/people/staff/mrwatkin/zeta/RHproofs.htm>
- [22] http://upbyte.net/news/vychislenie_dzeta_funkcii_rimana/2015-07-20-703